A mathematical optimal control based approach to pharmacological modulation with regulatory networks and external stimuli

(Titel der Dissertation)

Dissertation zur Erlangung des

naturwissenschaftlichen Doktorgrades

der Julius-Maximilians-Universität Würzburg

vorgelegt von

Tim Breitenbach
(Vor- und Familienname)

Bad Brückenau
(Geburtsort)

Würzburg, 2018

Eingereicht am: ……..……..

Mitglieder der Promotionskommission:

Vorsitzender: ……..

Gutachter: Thomas Dandekar

Gutachter: Roy Gross

Tag des Promotionskolloquiums: ……..…

Doktorurkunde ausgehändigt am: …….……

A mathematical optimal control based approach to pharmacological modulation with regulatory networks and external stimuli

Tim Breitenbach

Danksagung

Ich möchte mich an dieser Stelle für die Unterstützung bedanken, die ich während der Entstehung dieser Arbeit erfahren durfte und mir eine große Hilfe war.

Ein herzliches Dankeschön an Thomas. Durch seine Offenheit für neue Ansätze, seine Geduld und Beharrlichkeit, vor allem in der Anfangsphase unserer Zusammenarbeit, hat er mir den Zugang zur Forschung verschafft, deren Resultate zu dieser Arbeit geführt haben.

Vielen Dank für das Verständnis meiner Freunde dafür, dass ich auf meinem Weg manchmal ein Stück alleine gehen wollte um diese Arbeit voranzubringen.

Dankeschön auch für die Unterstützung durch viele hilfsbereite Menschen in meinem Umfeld. Vor allem möchte ich meinen Eltern dafür danken, dass sie mir durch ihren unermüdlichen Einsatz immer den Rücken frei halten, sodass ich mich mit ganzer Kraft der Entwicklung meiner Fähigkeiten widmen kann.

Contents

Zusammenfassung

In dieser Arbeit werden Modelle für molekulare Netzwerke bestehend aus gewöhnlichen Differentialgleichungen durch Terme erweitert, die die Wechselwirkung zwischen dem entsprechenden molekularen Netzwerk und der Umgebung berücksichtigen, in die das molekulare Netzwerk eingebettet ist. Diese Terme modellieren die Effekte von externen Stimuli auf das molekulare Netzwerk. Die Nutzbarkeit dieser Erweiterung wird mit einem Modell der circadianen Uhr demonstriert, das mit gewissen Termen erweitert wird und Daten von mehreren verschiedenen Experimenten zugleich reproduziert.

Sobald das Modell einschließlich der externen Stimuli aufgestellt ist, wird eine Grundstruktur entwickelt um externe Stimuli zu berechnen, die einen gewünschten vordefinierte Effekt auf das molekulare Netzwerk haben. Zu diesem Zweck wird die Aufgabe, geeignete externe Stimuli zu finden, als ein mathematisches optimales Steuerungsproblem formuliert, für welches, um es zu lösen, viele mathematische Methoden zur Verfügung stehen. Verschiedene Methoden werden diskutiert und ausgearbeitet um eine Lösung für das entsprechende optimale Steuerungsproblem zu berechnen. Auf die Anwendung dieser Grundstruktur pharmakologische Interventionspunkte oder effektive Wirkstoffkombinationen zu finden, wird hingewiesen und diese diskutiert. Weiterhin wird diese Grundstruktur in Bezug zu existierenden Netzwerkanalysewerkzeugen gesetzt und ihre Kombination für die Netzwerkanalyse diskutiert um zweckbestimmte externe Stimuli zu finden.

Die gesamte Grundstruktur wird mit biologischen Beispielen verifiziert, indem man die berechneten Ergebnisse mit Daten aus der Literatur vergleicht. Zu diesem Zweck wird die Blutplättchenaggregation untersucht basierend auf einem entsprechenden genregulatorischen Netzwerk und damit assoziierte Rezeptoren werden detektiert. Weiterhin wird ein Wechsel von einem T-Helfer Zelltyp in einen anderen in einer Tumorumgebung analysiert, wobei fehlende Agenzien berechnet werden um den entsprechenden Wechsel in vitro zu induzieren. Als nächstes wird ein genregulatorisches Netzwerk eines Myokardiozyten untersucht, wobei gezeigt wird wie die präsentierte Grundstruktur genutzt werden kann um verschiedene Behandlungsstrategien in Bezug auf ihre nutzbringenden Wirkungen und Nebenwirkungen quantitativ zu vergleichen. Darüber hinaus wird ein konstitutiv aktivierter Signalweg, der deshalb unerwünschte Effekte verursacht, modelliert und Interventionspunkte mit entsprechenden Behandlungsstrategien werden bestimmt, die das genregulatorische Netzwerk wieder von einem pathologischen Expressionsmuster zu einem physiologischen steuern.

Part I

Introduction, basic concepts and methods

Summary

In this work models for molecular networks consisting of ordinary differential equations are extended by terms that include the interaction of the corresponding molecular network with the environment that the molecular network is embedded in. These terms model the effects of the external stimuli on the molecular network. The usability of this extension is demonstrated with a model of a circadian clock that is extended with certain terms and reproduces data from several experiments at the same time.

Once the model including external stimuli is set up, a framework is developed in order to calculate external stimuli that have a predefined desired effect on the molecular network. For this purpose the task of finding appropriate external stimuli is formulated as a mathematical optimal control problem for which in order to solve it a lot of mathematical methods are available. Several methods are discussed and worked out in order to calculate a solution for the corresponding optimal control problem. The application of the framework to find pharmacological intervention points or effective drug combinations is pointed out and discussed. Furthermore the framework is related to existing network analysis tools and their combination for network analysis in order to find dedicated external stimuli is discussed.

The total framework is verified with biological examples by comparing the calculated results with data from literature. For this purpose platelet aggregation is investigated based on a corresponding gene regulatory network and associated receptors are detected. Furthermore a transition from one to another type of T-helper cell is analyzed in a tumor setting where missing agents are calculated to induce the corresponding switch in vitro. Next a gene regulatory network of a myocardiocyte is investigated where it is shown how the presented framework can be used to compare different treatment strategies with respect to their beneficial effects and side effects quantitatively. Moreover a constitutively activated signaling pathway, which thus causes maleficent effects, is modeled and intervention points with corresponding treatment strategies are determined that steer the gene regulatory network from a pathological expression pattern to physiological one again.

Chapter 1

Introduction

Biological research consists of collecting data by performing experiments and interpreting the corresponding data in order to identify the relevant causes of the observed outcomes. These insights into the study object and into the connections of the underlying mechanisms are summarized in a model that includes all the relevant information about a study object. This process is called modeling. For the purpose of further developing and improving a model of a study object hypotheses are generated based on the existing model and tested with further experiments. Specifically the hypotheses are set up and tested with respect to their ability to explain the connection of data of a corresponding experiment or to predict its outcome. For this task mathematical structures are a useful tool as they allow to formulate hypotheses as exactly as we like both qualitatively and quantitatively and thus to test the hypotheses very accurately and obtain detailed models. This works by the virtue of mapping the underlying mechanisms of a study object to appropriate mathematical structures. Once this assignment has taken place the resulting mathematical object can be processed with a suitable mathematical formalism where the results are now a matter of the logical structure of the mathematical object. The results of the corresponding mathematical operations represent the hypotheses for the experiment that one deals with.

In our case we consider molecular networks, especially the interplay of mutual activation and inhibition of their molecular agents. These interactions of the single agents of a network with the others are modeled with ordinary differential equations (ODEs). These equations describe the temporal change of a quantity depending on the status of the other agents in the network. Thus they are an ideal choice to describe that the mechanism of the change of the status of each network's agent is determined by the current status of the network, that means the status of the agents of the network.

Once the regulatory mechanisms of the agents of a molecular network are modeled by ODEs, this approach also allows to include the interaction of this molecular network with its environment that it is embedded in and the external influences. Examples for such external influences, called external stimuli, are besides chemical substances like small molecules or proteins, physical external stimuli like temperature [57], mechanical stress [15, 56, 34] or gravity [55]. These external stimuli can be effectively modeled by modifying the equations of the molecular network by terms that include the effects of these external stimuli. That means they influence the temporal change of certain agents of the molecular network beyond the influence that comes from the other agents of the molecular network. In this way we only include the essential information with respect to the interaction of the molecular network with its environment. The external stimuli also serve to create interfaces between the part of the experiment that is of special interest and its environment with which the molecular network interacts as an open system. An example can be different cell types communicating with each other. Each cell type is modeled with a specific molecular network where the secretion from one cell serves as an external stimulus for another cell type like T-cells that change the expression pattern of other immune cells by interferon [28].

The effect of external stimuli on the network can have two basic effects depending on the intrinsic features of the molecular network. The changes of the network caused by the external stimuli remain although the external stimuli have already decayed or the changes only last as long as the external stimuli are present. That is illustrated with different biological cases in the following. For the case that

the changes of the molecular network caused by the external stimuli remain although the external stimuli have already decayed is for example the differentiation of stem cells. By applying chemical agents, which are the mentioned external stimuli, the stem cells differentiate to different tissues, corresponding to the external stimuli, see for example [47, 31] and do not dedifferentiate if the corresponding chemical agents are washed out. Another issue is that the cells can even be reprogrammed that means that the cell being a certain type of tissue changes its type of tissue, see for example [62] and stably remains in this tissue although the corresponding chemical agents are washed out. A further special case is the switch from a cancer cell to apoptosis [51, 35] where the genetic expression program associated with apoptosis is not left any more, even when the corresponding external stimuli are taken away from the cell, once the effect of the responsible external stimuli have exceeded a certain threshold. However for the second case there are molecular networks where the changes caused by external stimuli just last as long as the corresponding external stimuli are active. When the external stimuli are not present any more, then the system relaxes back to the "ground state", that is the unperturbed status of the molecular network, which it left because of the perturbation by the external stimuli. Examples for such a framework are when a pathogen senses its host by certain chemical agents [12, 19, 23, 54] or other pathogens [58, 38], called quorum sensing. These agents differ in different environments and thus serve as signals or in our framework external stimuli which change the gene expression of a bacterium or pathogen for instance. A further example that also well illustrates the framework of effective modeling is starvation. That means that the lack of nutrients can lead to cell cycle arrest [49] and can change the expression pattern [48, 7]. Thus starvation acts as an external stimulus that is active when nutrients have been consumed and where the expression pattern changes as soon as the external stimulus decays that means nutrients are available again. Other external stimuli of that type are medical treatments where the desired effect declines when the active ingredient is excreted from the body. This means that in this case when the active ingredients decrease the network relaxes back to the pathological state in contrast to the case above where the effect stays although the active ingredients decline. The potential for such a behavior is in the inner structure of the model of the molecular network.

Experiments are not only performed to understand the underlying mechanisms that cause the behavior of a study object as an end in itself but also for the purpose how to manipulate the study object to induce desired effects. A huge research field where this question is often asked is pharmacology. The question is what pharmacological intervention points of a molecular network cause a change from a pathological state to a physiological one. Once the corresponding molecular network is mapped to an appropriate mathematical model, effects of different treatment strategies can be simulated in a computer, called in silico. Moreover there is a systematical way to search for effective intervention points in a molecular network or drug combination for a desired effect to maximize beneficial effects while reducing maleficent side effects at the same time. This means for instance just to perturb the pathologically expressed genes while the physiologically expressed ones are not perturbed.

For this purpose the corresponding task is formulated as a mathematical optimal control problem as follows. The effects of the external stimuli on the network and the interaction of all the agents of the molecular network with each other are covered by a model discussed so far. Subject to this model that determines the behavior of the agents of the network depending on external stimuli, we formulate a functional that has a small value if the state of the molecular network is close to a desired one. Then the question of finding effective intervention points or drug combinations is now formulated as a mathematical issue where a functional is supposed to be minimized subject to that the time curves of the agents of the molecular network are determined by the corresponding model that describes the interplay of the external stimuli and the molecular network. For the task of finding a solution to a mathematical optimal control problem there are a lot of systematical ways and rational methods to calculate one. The advantage of this proposed method is that we can figure out promising treatment strategies in silico and just have to verify that the calculated treatment strategy has the desired effect instead of finding the best candidate by trial and error by different real experiments that might turn out to be time consuming and cumbersome. By this method the information that is already contained in the interaction of the agents of the molecular network with each other and the external stimuli can be better exploited.

In Chapter 2 we motivate and illustrate the basic concepts and ideas behind the presented thesis

in order to give an overview over the used techniques without giving to many mathematical details.

In Chapter 3 we briefly describe the mathematical methods that we use for modeling and for solving the mathematical tasks that come up during this work. Furthermore we name the used hardware and the software environments in which the solution algorithms are implemented for the numerical experiments. Then we explain the procedure of validating the proposed framework.

In Chapter 4 we introduce our special ODE framework that is extended by terms that describe the effect of external stimuli. Specifically in Section 4.1 we introduce an ODE model from [37] that is useful for describing the behavior of molecular networks. The main feature of this model is that effects in the network only become noticeable if specific thresholds of molecular agents are exceeded. In Section 4.2 we extend this model by terms that include the effect of external stimuli and relate these terms to different molecular regulation mechanisms. In Section 4.3 we validate our framework to include the effects of external stimuli with a further biological example that concerns the circadian clock. We use the model presented in [22] that describes circadian rhythms by enzyme kinetics where the concentration of molecular agents oscillates with a 24 hour period. We extend this model by terms including the effect of external stimuli like light and demonstrate that a lot of experimental results concerning the circadian clock can be obtained with this single and small extended model where also species specific differences are apparent in the results. The fact that a lot of experiments can be described with a single model mechanism demonstrates the usability of our proposed framework for modeling biological networks and their interaction with their environment. Furthermore that mechanism models the effects of the external stimuli that allows an effective modeling where only necessary information are considered such that the model stays clear.

In Chapter 5 we discuss a basic mathematical framework for optimal control problems that is used to calculate external stimuli that cause a desired effect on a molecular network. As discussed above external stimuli can have two principal effects on molecular networks. The effect of the perturbation by the external stimuli can last permanently although the external stimuli are not present any more if the ODE model for the corresponding molecular network includes different stable states. In Section 5.1, we develop a mathematical framework that is specific for the task to switch the state of the molecular network between an initial stable state to a desired stable state. Furthermore algorithms are presented that calculate external stimuli for the desired task. In Section 5.2 we show how to modify that framework to obtain methods for the second case, that is to determine external stimuli that keep the molecular network in a desired state where the network relaxes back to the initial state if the external stimuli decline. Also here algorithms are given that calculate corresponding external stimuli. In Section 5.3 we give an overview over existing software solutions for network analysis and explain their limits with respect to the calculation of external stimuli that cause a desired network behavior. However, we point out how the existing software can be bunched together with our approach to generate a network analyzing tool to plan experiments and perform them in silico.

In Chapter 6 we demonstrate how to use the mathematical framework for biological applications and validate our framework with data from biological experiments. In Section 6.1 we use a small T-helper cell network from [37, Figure 5] in order to illustrate the basic use of the mathematical optimal control framework and how to reinterpret the numerical results for biological experiments. In Section 6.2 we investigate the following two molecular networks. Firstly, a gene regulatory network from [39] modeling the aggregation of platelets and secondly, a gene regulatory network of a T-helper cell from [36] modeling the maturation of a naive T-cell to different differentiated T-cell types. In the first case, we would like to trigger irreversible platelet aggregation and, in fact, we identify the two receptors that are associated with irreversible platelet aggregation upon activation by adenosine diphosphate according to [39] with our framework. In the second case for the T-helper cell network we investigate a switch from a Th17 cell to a regulatory T-cell. This switch is reported in the tumor setting [17] where soluble factors of ovarian cancer ascites are able to preform the transdifferentiation from a Th17 cell to a regulatory T-cell. However according to [17] the essential factors are not determined yet by experiments to induce the switch in vitro while we give a promising prediction of factors that are able to switch from a Th17 cell to a regulatory T-cell in accordance to already known contributing factors. In Section 6.3 we deal with a gene regulatory network of a myocardiocyte and show how the presented framework can be used to find and quantitatively compare different treatment strategies with respect

to their beneficial effects and maleficent side effects. Afterwards we model a constitutively activated pathway that results in a pathogenic expression pattern and show how to find treatment strategies that drive the regulatory network towards a physiological expression pattern.

In Chapter 7 we give the basic intention of this work and discuss where our presented framework extends existing tools for biological network analysis in order to allow further theoretical investigations of biological experiments. Additionally we summarize the theoretical results and their validation by comparing them to published results. The discussion is concluded with an outlook how the proposed framework can be extended to a database driven approach where the experimental time curves of molecular agents upon the effect of external stimuli can be exploited.

In the Appendix we show how to characterize stable states in a molecular network. Furthermore we illustrate some important issues solving ODEs numerically and interpreting the corresponding results.

Chapter 2

Illustration of the basic concepts of the thesis

This chapter briefly motivates the main ideas behind the Chapters 4 to 6 where the results of the work are presented including a detailed explanation of the underlying framework. This framework contains mathematical modeling of molecular networks with ordinary differential equations (ODEs) including the effects of external stimuli and the systematical computational investigation of intervention points to achieve desired effects on a molecular network.

A model of a molecular network contains the regulatory connections by which the different agents of a considered experiment are related to each other, see for example Figure 2.0.1 for an illustration of models of molecular networks. The information can be both qualitative and quantitative.

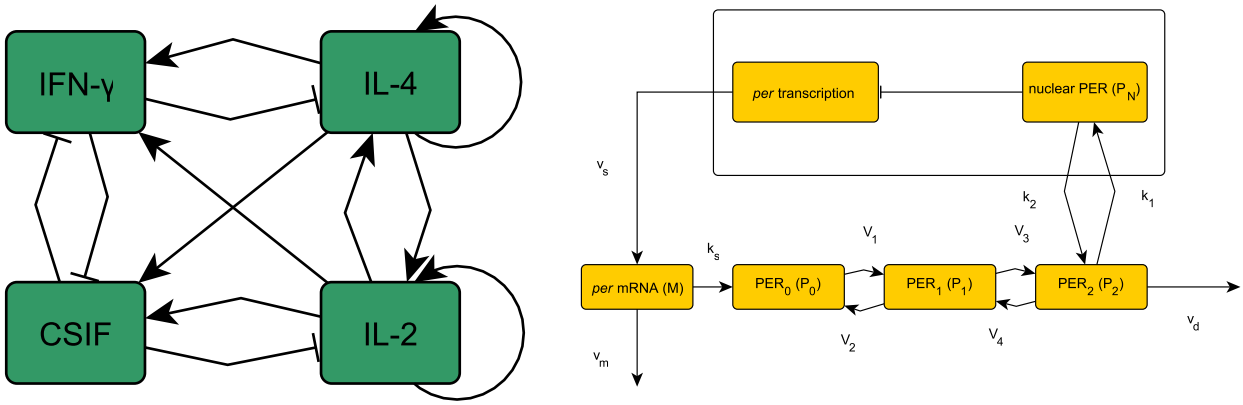

Figure 2.0.1: Representations of molecular networks. Left figure is a simplified T-helper cell network, see Section 6.1 for details. Right figure is the negative feedback loop for the oscillatory *period* gene expression for the circadian rhythm where also the model parameters are incorporated, see Section 4.3 for details. Notice that an arrow is associated with an activating interaction and a t-shape arrow is associated with an inhibiting interaction. The node on the top of an arrow is activated from the one at the bottom and the node on the top of a t-shape arrow is inhibited by the one at the bottom of the t-shape arrow.

First we start explaining illustratively why ODEs are appropriate for modeling molecular networks. These type of equations describe how a quantity alters in time. The change per time of a quantity x_1 is expressed by the derivative of the quantity with respect to time, denoted by $\frac{dx_1}{dt}$ and in general its physical meaning is the one of a rate. On the other hand the mechanism how other agents of the network, for example x_2 and x_3, influence x_1 is described by a functions, for instance $f(x_1, x_2, x_3)$ where the current value of f in this case depends on x_1, x_2 and x_3. Then we have a mathematical model, denoted by $\frac{dx_1}{dt} = f(x_1, x_2, x_3)$, that describes how the quantity x_1 will change per time depending on the current value of the other agents. Analogously for x_2 and x_3. The function f can for example be

given by $x_2 - x_3$, denoted by $f(x_2, x_3) = x_2 - x_3$. That means the rate how the quantity x_1 changes depends only on x_2 and x_3. The quantity x_2 has increasing effects and the quantity x_3 has decreasing effects on the rate $\frac{dx_1}{dt}$ and thus on the current alteration of the quantity x_1. Depending on the sign of $x_2 - x_3$ the quantity x_1 increases, for $x_2 - x_3$ positive, decreases, for $x_2 - x_3$ negative or stays constant if $x_2 - x_3 = 0$. If we give an initial value for x_1, x_2 and x_3 we can calculate the value of each of all three quantities by integrating $\frac{dx_1}{dt} = f(x_1, x_2, x_3)$ on both sides over time starting from the initial time to the final time. This concept of ODEs modeling molecular networks can be illustrated with two genes regulating each other such that a stable expression pattern is obtained. For example if a protein from a corresponding gene 1 enhances the expression of a second gene 2 and in turn the corresponding protein that is synthesized from gene 2 inhibits the expression of gene 1. Then, in this example, we have that the change per time of the protein of gene 1 depends on the current concentration of protein of gene 2 since these proteins inhibit the transcription of mRNA and consequently the rate of synthesis of protein of gene 1 varies depending on the current concentration of protein of gene 2.

Furthermore, let the rate of protein synthesis not only depend on the interaction of the proteins within the network but also on the interplay with external stimuli that come from the environment. For this purpose it is necessary to extend the model by quantities that correspond to the activity of the relevant external stimuli. For example if light or a chemical agent that is sensed by a receptor enhancing gene expression or the digestion of a protein with concentration x_1, then the corresponding equation can be mathematically formulated as $\frac{dx_1}{dt} = f(x_1, x_2, x_3, u_1, u_2)$ where u_1 is associated with the intensity of light and u_2 correlates with the concentration of the chemical agent. For example the function f can be given by $x_2 - x_3 - u_1$ where u_1 has decreasing effects on the rate $\frac{dx_1}{dt}$, denoted by $f(x_2, x_3, u_1) = x_2 - x_3 - u_1$, or the function f can be given by $x_2 - x_3 + u_2$ where u_2 has increasing effects on the rate $\frac{dx_1}{dt}$, denoted by $f(x_2, x_3, u_2) = x_2 - x_3 + u_2$. For mathematical details, especially further examples for f , see Chapter 4.

By these equations the alterations of the quantities x_1, x_2 or x_3 can be described for any time. An important special feature of such equations, which has turned out to be useful for biological modeling, is having solutions that are associated with a stable state or steady state. These states are defined that all rates are zero, that means $\frac{dx_1}{dt} = \frac{dx_2}{dt} = \frac{dx_3}{dt} = 0$. This means that the quantities do not change their values any more and stay constant. A biological example is an expression pattern that is associated with a certain tissue, specifically the differentiation of stem cells into a certain type of tissue. Once the differentiation is finished the cell remains in the corresponding expression pattern if there are no sufficiently strong perturbations. A mathematical example is the following. If we take the system of equations $\frac{dx_1}{dt} = x_2 - x_3 - u_1$, $\frac{dx_2}{dt} = x_3 - x_1$, $\frac{dx_3}{dt} = x_1 - x_2 + u_2$ where we assume u_1 and u_2 to be constant zero functions, $u_1 = u_2 = 0$, that means the system is unperturbed, then we see that there are two different steady states. For $x_1 = x_2 = x_3 = 0$ and for $x_1 = x_2 = x_3 = 1$, we have that the corresponding rates are zero, $\frac{dx_1}{dt} = \frac{dx_2}{dt} = \frac{dx_3}{dt} = 0$. External stimuli, if active, modeled by u_1 and u_2 having values greater than zero, cause changes of the quantities x_1, x_2 and x_3 as the rates are not zero any more according to the equations $\frac{dx_1}{dt} = x_2 - x_3 - u_1$, $\frac{dx_2}{dt} = x_3 - x_1$, $\frac{dx_3}{dt} = x_1 - x_2 + u_2$. If the network is for example initially in the steady state where all the quantities x_1, x_2 and x_3 have the value 0, then a certain combination of active external stimuli u_1 and u_2 might cause a switch from the steady state where we have $x_1 = x_2 = x_3 = 0$ to the steady state $x_1 = x_2 = x_3 = 1$. The biological meaning is for instance that a stable expression pattern of a cell is changed and thus a differentiated stem cell transdifferentiates to another cell type.

In this thesis we propose a general mechanism to include the effects of external stimuli and validate this mechanism by theoretically describing experiments of the circadian clock, see Section 4.3 for details. We show that with this mechanism the circadian clock can be entrained to external phases and induce a phase shift of the circadian clock. Furthermore we investigate our mathematical model under constant light and compare the results with experimental data from the literature. Next we give two different sets of parameters for the model such that we obtain different phase response curves. One curve is typical for flies and one curve is typical for mammalians. Then we demonstrate how to couple different clocks by interpreting the output from one clock as an external stimulus for another clock. We set up a food entrained peripheral clock similar to liver cells that shift their clock according to signals from the brain and food intake. Also we discuss that by coupling several microscopic clocks whose

coupling strength to light slightly differs results in a macroscopic behavior where the total rhythm of all clocks can be stopped by a strong light pulse and then again be restarted by another strong light pulse.

Once a mathematical model with external stimuli is created the mathematical optimal control theory offers a systematical way to calculate a selection of external stimuli that has a desired effect on the network. For this purpose, besides a mathematical model that describes the effect of the external stimuli on the molecular network and the interaction of the molecular agents among each other, the desired effect needs to be formulated in mathematical terms. This can be done as follows. If we consider for example a gene regulatory network, then each gene has a desired expression pattern. However if the actual expression pattern differs in a pathological manner, the difference between the actual value and the desired value is greater than zero. This now paves the way for the mathematical formulation of this problem. If we sum up the square of all differences from each expression level and its desired value, then we have to minimize this functional, called target functional, with the available external stimuli subject to the model describing the interaction of genes and external stimuli. These external stimuli that fulfill the desired task are called solution to the optimal control problem. In order to find external stimuli that cause the smallest target functional value there are several methods provided with this thesis, see Chapter 5 for details.

Solutions to optimal control problems can be determined in several ways. There are so called local optimization methods that, for the calculation, exploit features of an optimal solution that it has to fulfill since it is mostly computationally too expensive to calculate these solutions directly by testing all the possible admissible values for the external stimuli and then choose the combination that caused the smallest target functional value. Such a feature that a solution to an optimal control problem fulfills under certain conditions is that the first derivatives are zero. For example if we consider the function $J_1(x_1) = (x_1 - 0.5)^2$, then the minimum is at $x_1 = 0.5$ where the first derivative $\frac{\partial J}{\partial x_1} = 2(x_1 - 0.5)$ is zero at $x_1 = 0.5$. Another example is the function $J_2(x_1, x_2) = (x_1 - 0.1)^2 + (x_2 - 0.6)^2$ where the minimum is located at $(x_1, x_2) = (0.1, 0.6)$. Also the first derivatives $\frac{\partial J}{\partial x_1} = 2(x_1 - 0.1)$ and $\frac{\partial J}{\partial x_2} = 2(x_2 - 0.1)$ are zero at $(x_1, x_2) = (0.1, 0.6)$. For illustration see Figure 2.0.2. The local optimization methods are combined with global optimization methods that are provided with this work. By an appropriate combination of a representative of each class of methods efficient and tailored calculation methods can be generated to investigate molecular networks with respect to useful intervention points.

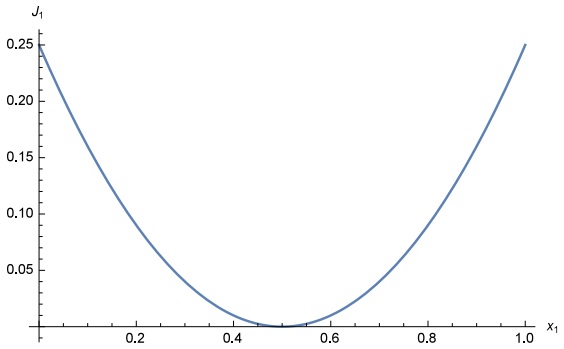

Figure 2.0.2: Illustrations of the function J_1.

Now, we have a framework that first allows us to include the effects of external stimuli into molecular networks and second formulate the experimental question of finding appropriate external stimuli to influence a molecular network in a desired way in mathematical terms. In the next step, we demonstrate that a solution to the resulting mathematical optimal control problem can be reinterpreted in a biological context and thus validate the framework. A detailed discussion of biological applications of the framework including validating results can be found in Chapter 6.

For the first example we use a gene regulatory network that describes the irreversible aggregation of platelets. The irreversible aggregation is associated with a high concentration of integrin. For our calculations we let the corresponding network start with a low concentration of integrin and equip the network at several points with external stimuli. For irreversible platelet aggregation we desire

that the value of integrin is high in the molecular network. The result is that by our calculations we exactly determine two receptors that are associated with irreversible platelet aggregation when they are activated by adenosine diphosphate.

In a second example we consider a gene regulatory network that describes the maturation of T-helper cells from a naive T-cell. We have the situation that the corresponding network starts with initial values that are associated with a Th17 cell type. The task is to find intervention points to transdifferentiate the Th17 cell type to a regulatory T-cell type. This transformation is reported in an ovarian tumor setting where not all the soluble factors are known that are contained in the ascites that mediate the transdifferentiation. We figure out two additional intervention points to the one that is already known from experiments to play a major role in the process of transdifferentiation.

In a third example we consider a gene regulatory network of a myocardiocyte. Also in this setting we demonstrate how promising treatment strategies can be computationally developed and quantitatively compared. For this purpose we can use our target functional where the sum of all squared differences of the actual expression levels and their desired values serves as a measure for the quality of a treatment strategy. The closer each gene expression is to the desired value, the smaller is the target functional value and thus the better the treatment strategy is. Specifically that means that side effects are reduced while beneficial effects are maximized. As our presented framework determines the given external stimuli such that the target functional attains its smallest value possible with the given set of external stimuli, the method is objective in order to compare different treatment strategies. This means that for each strategy different genes in the molecular network are equipped with an external stimulus that can either activate or inhibit the corresponding gene expression.

In a further investigation with the gene regulatory network of the myocardiocyte we show how to model a constitutively activated pathway and how to find a treatment strategy to eliminate the maleficent effects. This also plays a role in oncogenesis, see [14, 20, 29] for instance where the proposed way of modeling constitutive activated pathways might also turn out to be useful. In our case we have a constitutively activated receptor that triggers a hypertrophic stimulus for the myocardiocyte which is associated with maleficent effects. After we have used our framework to figure out the most effective treatment strategy to eliminate the maleficent effects and to intensify the beneficial effects, we compare this strategy to a treatment where only a receptor is activated that is associated with a non-hypertrophic stimulus which has just beneficial effects. In the calculations it turns out that a homo-dimerization of a protein has to be inhibited. Furthermore we investigate to what degree the homo-dimerization has to be inhibited such that the treatment subject to the conditions of the constitutively activated receptor causing a hypertrophic stimulus is still as good as an activation via a receptor that is associated with a non-hypertrophic stimulus where no receptor is constitutively activated. We predict a threshold for the homo-dimerization where no hypertrophic effects occur.

Chapter 3

Materials and methods

In this chapter, we note the methods that are used to generate the results of the thesis. Furthermore required hardware and software packages are named.

The calculations can conveniently be performed on a desktop PC with 16 GB RAM and a processor with 4 kernels with each 3.5 GHz, specifically we used an Intel(R) Core(TM) i5-4690 CPU @ 3.50GHz. For the implementation of the mathematical algorithms Mathworks Matlab is used. For the execution of the provided Matlab Files the Matlab Symbolic math toolbox is required and the parallel computing toolbox is recommended but not necessary. The basic implementations that are used in the next part of the thesis are provided with this work. The codes are commented. The experiments for Section 4.3 are performed with Wolfram Mathematica, version number 10.1.0.0. The corresponding files are also commented and provided with this thesis. No further software solutions are used for the present thesis than the already named ones.

The mathematical methods are the following. The mathematical models are based on ordinary differential equations. These equations are solved with an explicit Euler scheme implemented with Matlab throughout this work except in Section 4.3 where the equations are solved with NDSolve of Mathematica.

There are several implemented methods provided with this thesis in order to solve the resulting optimal control problems. There are heuristic global optimization methods that have been developed during the research for this thesis. Local optimization methods, taken from the literature, are provided with this work. These are first a projected gradient method and second a sequential quadratic Hamiltonian method. Both were implemented for the thesis to have an exactly tailored software solution.

For the validation of the theoretical experiments, we have not performed experiments in vivo or in vitro. We validate our framework indirectly by comparing our results to already published data in the literature. Corresponding references are pointed out at the corresponding site in this thesis.

Part II

Results

Chapter 4

Modeling of biological systems and external stimuli

This section is about modeling biological systems with ordinary differential equations. Specifically, a certain type of ordinary differential equations that is based on [37] is introduced and extended with a mechanism that models the effect of external stimuli. We remark that the considerations of this section also hold for any well posed model of ordinary differential equations. The following two sections are based on [10, Section 2].

4.1 A system of differential equations to model regulatory networks

A biological system for our purposes consists of the interplay of different agents that we are interested in. An agent can be a gene, a RNA or a protein. It is our goal to set up an effective model of just the agents of interest. The agents that we assume to be important for the understanding of the dynamics of the corresponding biological system can interact by activating or inhibiting agents of the network.

For the procedure of our effective modeling with regulatory networks we start with identifying each of the n agents, $n \in \mathbb{N}$, of our biological system that we would like to model with one node $k \in \{1, ..., n\}$ of an interaction graph. Additionally, this interaction graph contains all the information which node regulates which node by either activation or inhibition. Then from this information a system of ordinary differential equations can be set up as proposed in [37, Equation 3] for instance. For each activity level $x_k : \mathbb{R} \to \mathbb{R}$, $k \in \{1, ..., n\}$ of a node k, we have the following equation

$$\frac{dx_k}{dt} = \frac{-\mathrm{e}^{\frac{1}{2}h} + \mathrm{e}^{-h\left(\omega_k - \frac{1}{2}\right)}}{\left(1 - \mathrm{e}^{\frac{1}{2}h}\right)\left(1 + \mathrm{e}^{-h\left(\omega_k - \frac{1}{2}\right)}\right)} - \gamma_k x_k \tag{4.1.1}$$

where

$$\omega_k = \begin{cases} \omega_k^A \omega_k^I & \text{if node } k \text{ has activators and inhibitors} \\ \omega_k^A & \text{if node } k \text{ has only activators} \\ \omega_k^I & \text{if node } k \text{ has only inhibitors} \end{cases}$$

and

$$\omega_k^A = \left(\frac{1 + \sum_{j \in A_k} \alpha_j^k}{\sum_{j \in A_k} \alpha_j^k}\right)\left(\frac{\sum_{j \in A_k} \alpha_j^k x_j}{1 + \sum_{j \in A_k} \alpha_j^k x_j}\right), \qquad \omega_k^I = 1 - \left(\frac{1 + \sum_{j \in I_k} \beta_j^k}{\sum_{j \in I_k} \beta_j^k}\right)\left(\frac{\sum_{j \in I_k} \beta_j^k x_j}{1 + \sum_{j \in I_k} \beta_j^k x_j}\right).$$

Model (4.1.1) describes the time depending changing of the activity level x_k, $k \in \{1, ..., n\}$ from the initial time $t = 0$ to a final time horizon $T > 0$ for a given initial state $x_0 \in \mathbb{R}^n$ with $x(0) = x_0$. The time depending changing $\frac{dx_k}{dt}$ of node k depends on the network dynamics modeled according to the right hand-side of (4.1.1) whose parameters we explain in the following. The activators of node k are elements of the subset $\{x_j |\ j \in A_k \subseteq \{1, ..., n\}\} \subseteq \{x_k |\ k \in \{1, ..., n\}\}$ where A_k contains all the indices of the nodes $\{1, ..., n\}$ which activate node k. The corresponding $\alpha_j^k > 0$ weights the contribution of

the activity level x_j of node j to the total activation of node k. Analogously, the inhibitors of node k are elements of the subset $\{x_j|\ j \in I_k \subseteq \{1,...,n\}\} \subseteq \{x_k|\ k \in \{1,...,n\}\}$ where I_k contains all the indices of the nodes $\{1,...,n\}$ that inhibit node k. The corresponding $\beta_j^k > 0$ weights the contribution of the activity level x_j of node j to the total inhibition of node k. Furthermore, $h > 0$ where h models the cooperativity. If h is large, then the behavior of the equation is close to a switcher while small h are closer to a linear behavior of the activity level with respect to the input activity level. We remark that h for the presented case is equal for all nodes of the network. However it can be extended in that way that h_k differs for each node k if the biological system modeled with (4.1.1) makes it necessary. According to [37], the first term of (4.1.1) is called the activation function or activation term.

The activity level of a node in an experiment is defined by the interaction with other nodes. The activity of a node can be measured by any concentration of a product of transcription or translation such as mRNA or proteins for instance that is in a biologically active form such that it interacts with other agents in the network. If for example node k models a gene, then the activation term models the rate of transcription or translation and the product of this process, either RNA or proteins, can interact with other agents. Consequently if in the model a node stands directly for a protein, then activity of the protein can also mean the concentration of its biological active form.

The second term is called the decay where $\gamma_k > 0$ models the speed of decay of the activity level x_k of node k. As an example the decay can be the digestion of protein by for example ubiquitination. In general the decay is a term that subsumes all the effects that irreversibly transform the agent the node stands for to a biologically inactive form.

Following this consideration we have two possibilities to interpret the activity level x_k of a node k. The first possibility is that the activity level takes values between 0 and 1 where 0 means that the concentration of the biologically active agent that is associated with the node is zero or 1 means that the biologically active agent has the highest concentration that can be measured in the system. The second possibility is that the activity level x_k is the concentration of the agent corresponding to the node k. This is the usual case if the network parameters are fitted to experimental data where concentrations of agents are measured.

If the network is used in the framework of activity, we have that solutions to (4.1.1) only take values between 0 and 1. This can be seen as follows. If the initial value $x_0 \in [0,1]$, then $\omega_k \in [0,1]$ for all $k \in [0,1]$. If $\omega_k \in [0,1]$ for all $k \in \{1,...,n\}$ then the activation term takes only values between 0 and 1. The activation term takes 0 for $\omega_k = 0$. If we factor out a minus sign in the numerator and the denominator of the activation term, then if ω_k increases, the numerator of the activation term increases and the denominator decreases where it takes its maximum value at $\omega_k = 1$ where for the denominator it holds

$$-\left(\mathrm{e}^{\frac{1}{2}h} - 1\right)\left(1 + \mathrm{e}^{-\frac{1}{2}h}\right) = 1 - \mathrm{e}^{\frac{1}{2}h} + \mathrm{e}^{-\frac{1}{2}h} - 1 = -\mathrm{e}^{\frac{1}{2}h} + \mathrm{e}^{-\frac{1}{2}h}.$$

Thus the value of the activation term takes at most 1 and thus the value for x_k growth until, as $\gamma_k = 1$, x_k is at most 1 and thus the two terms of the right hand-side of (4.1.1) cancel out and x_k stays constant. If the decay has a bigger value than the activation term, then the sign of the right hand side is negative and the value of x_k decreases until the decay equals the activation term. The value of x_k cannot go below 0 as the decay scales with x_k. Thus if once $x_k = 0$ the decay is zero and cannot contribute to a further decrease of x_k below zero.

An important property of (4.1.1) is that for certain network configurations there are stable activity levels whose values stay the same for all times after a transient if x_0 is not already such a stable state. Such states are called steady states, see Section 8.1 in the appendix for details. These stable activity levels can also be found in biological systems like a stable expression pattern. We stress that once the system is in a steady state, it cannot switch its current state by itself that means without external stimuli by definition of a steady state.

4.2 The extension of regulatory networks by external stimuli

The application of external stimuli aims at two different kinds of changes of the network's activity pattern. The first one is to drive the network from one steady state to another desired one where

the network again rests although the external stimuli have already decayed. That means that the whole network is driven from one steady state to another because the perturbation of the activity level of certain nodes is such that the steady state, in which the whole network is, is left and is brought sufficiently close to the desired steady state such that the network relaxes into that one. This is one possible way to switch between two different steady states of a network. The second kind of change of the network's activity pattern is to alter the activity levels of certain nodes for the duration of application of the external stimuli where these activity levels relax to the values of the steady state in which the whole network still is after the external stimuli have decayed. That means in this case that there is no switch between two different steady states.

To be able to affect a network by external stimuli, especially activity levels of certain nodes, we have to introduce some mechanism into (4.1.1) which we explain in the following.

Now, we set up a mechanism that includes the effect of external stimuli on the activity level x_k of a node k. For this purpose, we introduce a function $u_j : \mathbb{R} \to [0,1]$ that models the activity level of each external stimulus $j \in \{1,...,m\}$, $m \in \mathbb{N}$. In our model $u_j = 0$ means that the external stimulus is not active. The activity level of the stimulus is supposed to be linearly interpolated to its maximum activity level that is modeled by $u_j = 1$.

For the next step, we have to distinguish two cases. In the first one, the activity level x_k, $k \in \{1,...,n\}$, takes only values between 0 and 1. This is achieved by setting $\gamma_k = 1$ for all $k \in \{1,...,n\}$ as the activation term takes only values between 0 and 1. Then the activity level x_k increase at most until the activation term equals $\gamma_k x_k$ and thus $\frac{dx_k}{dt} = 0$ which means that the node k has reached a steady state. If the initial value x_0 has only values between 0 and 1, then ω_k takes only values between 0 and 1.

An activation of node k by an external stimulus j is modeled by adding $\sigma_{kj} u_j (1 - x_k)$ to the right hand-side of (4.1.1). That means if for the external stimulus $u_j \equiv 0$, then there is no activation of node k by the external stimulus j. If node k has full activity, then the external stimulus has also no effect on the activity level x_k of node k. Analogously, an inhibition of node k by an external stimulus j can be modeled by subtracting $\eta_{kj} u_j x_k$ from the right hand-side of (4.1.1). That means, if for the external stimulus $u_j \equiv 0$, then there is no inhibition of node k by the external stimulus j. If node k has no activity, then the external stimulus j has no effect on the activity level x_k of node k. The parameters $\sigma_{kj} \geq 0$ and $\eta_{kj} \geq 0$ are used to fit the value u_j to experimental activation or inhibition of the modeled external stimulus. The parameters can also be used to weight the contribution of external stimulus j to the activation or inhibition, respectively, of node k where $\sigma_{kj} = 0$ or $\eta_{kj} = 0$ means that external stimulus j does not directly effect node k. Concluding, our first extended model for the activity level x_k of node k is given as in the discussion above but exchanging (4.1.1) by

$$\frac{dx_k}{dt} = \frac{-e^{\frac{1}{2}h} + e^{-h\left(\omega_k - \frac{1}{2}\right)}}{\left(1 - e^{\frac{1}{2}h}\right)\left(1 + e^{-h\left(\omega_k - \frac{1}{2}\right)}\right)} - \gamma_k x_k + \sum_{j=1}^{m} \sigma_{kj} u_j (1 - x_k) - \sum_{j=1}^{m} \eta_{kj} u_j x_k \tag{4.2.1}$$

for $k \in \{1,...,n\}$.

The model (4.2.1) can be extended to external stimuli which act on the activation term in the following way. We model the following situation where a substrate cannot decrease the activity level x_k of a corresponding node k but its activation term. For example, if one blocks areas in the promoter region by oligopeptides such that transcription factors can bind worse to the DNA, then the expression of the corresponding gene product slows down as the activation term is smaller. Such a model can be formulated as follows

$$\frac{dx_k}{dt} = \frac{-e^{\frac{1}{2}h} + e^{-h\left(\omega_k - \frac{1}{2}\right)}}{\left(1 - e^{\frac{1}{2}h}\right)\left(1 + e^{-h\left(\omega_k - \frac{1}{2}\right)}\right)} \left(\prod_{j=1}^{m} (1 - \zeta_{kj} u_j)\right) - \gamma_k x_k + \sum_{j=1}^{m} \sigma_{kj} u_j (1 - x_k) - \sum_{j=1}^{m} \eta_{kj} u_j x_k \tag{4.2.2}$$

for all $k \in \{1,...,n\}$ where $0 \leq \zeta_{kj} \leq 1$. If $\zeta_{kj} = 0$ for all k and j, then model (4.2.2) transforms into (4.2.1). By the coefficients ζ_{kj}, one can adjust how much the external stimulus j affects the activation term of the node k even at full activity of u_j. That means that for $\zeta_{kj} = 0$, the external stimulus j has

no effect on node k. For $\zeta_{kj} = 1$, a fully activated external stimulus j, which corresponds to $u_j = 1$, totally prevents the expression of the product of node k. If $0 < \zeta_{kj} < 1$, then even a fully activated external stimulus j cannot totally prevent the corresponding expression. This captures the nature of an equilibrium reaction as it appears when, for example, transcription factors compete with other substrates in binding to the DNA. Therefore, ζ_{kj} can also be used to fit the effect of u_j to experimental data.

Remark 1. We compare (4.2.1) with (4.2.2) where $\eta_{kj} = 0$ for all $k \in \{1, ..., n\}$ and all $j \in \{1, ..., m\}$ from a numerical point of view to model a decay of an activity level x_k. We have that the numerical treatment of (4.2.2) is easier. The reason for this comes from the fact that for large parameters η_{kj}, $k \in \{1, ..., n\}$, $j \in \{1, ...m\}$ we possibly have to choose small step sizes for the numerical solution to obtain a stable numerical solution procedure, see the considerations for (8.2.4) for details. That is the reason why as long as it is just important that the activity level of the corresponding node decreases when the activity level of an external stimuli increases, we recommend (4.2.2) with $\eta_{kj} = 0$, for all $k \in \{1, ..., n\}$ and $j \in \{1, ...m\}$. This shows that a good model has to contain different issues ranging from capturing all the relevant effects that play a role for the biological system that is to be modeled up to numerical aspects that ensure that the corresponding equations are solvable within a reasonable time.

For the second case where $x_k \geq 0$ and x_k is interpreted as a concentration of an agent, we have the following possibilities to include the effects of external stimuli. The only difference to (4.2.2) is the activation by external stimuli. The terms for inhibition are well defined as they cannot bring the value of x_k below zero as discussed above. However, if we would like to have that if there is already a large value of x_k and thus the external stimuli is supposed to have a lesser effect in this case, then we cannot use the term $(1 - x_k)$ to dampen the effect as there is no sharply defined upper bound for x_k. In this case, we can use a term that decreases when x_k increases. We choose $\mathrm{e}^{-\beta_k x_k}$ with $\beta_k > 0$ for all $k \in \{1, ..., n\}$ where β_k can be fitted to experimental data. Then we obtain from (4.2.2) the following

$$\frac{dx_k}{dt} = \frac{-\mathrm{e}^{\frac{1}{2}h} + \mathrm{e}^{-h\left(\omega_k - \frac{1}{2}\right)}}{\left(1 - \mathrm{e}^{\frac{1}{2}h}\right)\left(1 + \mathrm{e}^{-h\left(\omega_k - \frac{1}{2}\right)}\right)} \left(\prod_{j=1}^{m} (1 - \zeta_{kj} u_j)\right) - \gamma_k x_k + \sum_{j=1}^{m} \sigma_{kj} u_j \mathrm{e}^{-\beta_k x_k} - \sum_{j=1}^{m} \eta_{kj} u_j x_k \tag{4.2.3}$$

for all $k \in \{1, ..., n\}$. If the upper bound for the intended purpose is not that important, we can simplify the term that implements the activation of the external stimuli of (4.2.3) by replacing $\mathrm{e}^{-\beta_k x_k}$ with 1 such that we have

$$\frac{dx_k}{dt} = \frac{-\mathrm{e}^{\frac{1}{2}h} + \mathrm{e}^{-h\left(\omega_k - \frac{1}{2}\right)}}{\left(1 - \mathrm{e}^{\frac{1}{2}h}\right)\left(1 + \mathrm{e}^{-h\left(\omega_k - \frac{1}{2}\right)}\right)} \left(\prod_{j=1}^{m} (1 - \zeta_{kj} u_j)\right) - \gamma_k x_k + \sum_{j=1}^{m} \sigma_{kj} u_j - \sum_{j=1}^{m} \eta_{kj} u_j x_k \tag{4.2.4}$$

for all $k \in \{1, ..., n\}$. This can be used to have an easy possibility to just increase the activity level by the action of an external stimulus.

Remark 2. Notice that in the case of $u_j = 0$ for all $j \in \{1, ..., m\}$ our extended Equations (4.2.1), (4.2.2), (4.2.3) and (4.2.4) transform into (4.1.1) which is the unperturbed network. That especially means that the values of the steady states and other model parameters of (4.1.1) of a regulatory network are independent of the external stimuli. Thus these steady states and model parameters are a priori given or computable, respectively, without knowing what external stimuli might effect the regulatory network. This is reasonable because if for instance the steady states of regulatory network model all the genetic programs which a cell can perform, then these programs are an intrinsic property of this cell independent of possible external stimuli which ever can exist. However, an external stimuli might cause a change from one genetic program to another if applied. In our framework, the cell or the system modeled with a regulatory network, respectively, is considered as an open system, that means an independent system which is able to interact with its environment via the effects of external stimuli.

Next, we illustrate how these external stimuli u_j, $j \in \{1, ..., m\}$ can be realized in a real experiment. In general, we say that the activity level of a node is high if the product which corresponds to the node

has a high concentration and is low if the corresponding product's concentration is low. An example is the expression of a protein of a gene. If the concentration of the protein is high, then we say that the corresponding gene is at a high activity level and analogously reverse.

That means, that activation of a node by the term $\sum_{j=1}^{m} \sigma_{kj} u_j (1 - x_k)$, $\sum_{j=1}^{m} \sigma_{kj} u_j \mathrm{e}^{-\beta_k x_k}$ or $\sum_{j=1}^{m} \sigma_{kj} u_j$ is every operation on the node which increases the concentration of the product associated with a certain node. Therefore, increasing the activity level can be done by adding the product of the corresponding node to the system with which it influences other nodes, like RNA or protein. This simulates a higher activity level of the corresponding node. Another effect which increases the activity of the node is adding a substrate to the system which improves transcription or translation. Imaginable is the activation of an enhancer region close to a promoter associated with a node. We emphasize that these effects are not like a knock in of a gene as this operation changes the topology of the network which means that nodes or edges are added to the network's graph.

The inhibition of a node by the term $\sum_{j=1}^{m} \eta_{kj} u_j x_k$ means that the concentration of the product associated with that node is decreased, like an additional decay. This can be done, for example, by antibodies which bind to the product, digestion of the product by enzymes or any other modification, like post transcriptional or post translational modifications, at the product which inhibits its intended function in the system and thus converts the product into a biologically inactive form. Then the concentration of the biologically active product decreases and this is considered as a decay of the activity level of the corresponding node. The inhibition by the term $\prod_{j=1}^{m} (1 - \zeta_{kj} u_j)$ is associated with decreasing the activation term which can be the inhibition of transcription or translation factors like a competitive binding to the DNA binding zone of a promoter. The presented inhibition mechanisms are associated with a so called knock down. Analogously to a knock in, a knock out changes the topology of the network as well and corresponds to the deletion of a node or an edge from the network. This operation is not modeled by the action of the external stimuli within the framework proposed in this work.

Besides drugs or some other chemicals acting as external stimuli, there are further external stimuli like physical signals. Our presented framework provides the possibility to effectively model the effects of these external stimuli on certain nodes. For example light or mechanical stress, which is detected by receptors and is converted into activation or inhibition of a node. For example, DNA damage caused for example by X-rays activates p53 [32] that can be associated with a node in a network or temperature sensed by RNA thermometers can chance expression patterns [57]. This can be modeled within our framework by covering the effects of these external stimuli by the functions u_j, $j \in \{1, ..., m\}$ that activate or inactivate the corresponding nodes. We remark that this is a very effective modeling as we just consider the essential effects of the interactions within a real system that we model.

In order to compare the results from these models with results from an experiment in detail, one has to check if the behavior of the real network is the same like the one of the model network when applying an external stimulus as far as the nodes' activity is concerned. Furthermore, one can check if an external stimulus has the same effect on a node's activity like used in the model in order to adjust the coefficients σ_{kj}, η_{kj} and ζ_{kj}. In this way, the coupling strength of an external stimulus can be taken into account. For example, if an inhibiting external stimulus j supposed to cause a knock down of node k cannot force a node's activity level below a certain level although fully applied, then one can adjust the corresponding coefficient η_{kj} or ζ_{kj} until the model has the same behavior. Analogously, if an external stimulus cannot steer a node's activity level to its full amplitude or not above a certain value although fully applied, then one can adjust the corresponding coefficient σ_{kj} or β_k until the model shows the same behavior like the real system. One should also check if the external stimulus like a certain molecular agent used to put the external stimulus from the model into effect has an exclusive effect on the corresponding node in the real system or if the utilized agent has a multi target effect on several nodes at once in the real system. If the utilized external stimulus has multi target effects on several nodes, then such an external stimulus j can be considered with the model above in that way that the coefficients ζ_{kj}, σ_{kj} or η_{kj} are greater than zero for more than just one k. Then the external stimulus j appears in more then one equation meaning that it has an effect on the corresponding nodes.

4.3 External stimuli and a circadian clock model

This section is based on [9] and is intended to demonstrate that the framework that includes external stimuli into a model of ordinary differential equations in an effective way reproduces experimental data and thus validates this mechanism of the regulatory networks introduced in Section 4.2. By effective we mean that we only include the essential effects of the external stimuli to certain agents oft the network. In order to show the functionality of our framework we chose a model for the circadian clock which describes oscillations of molecular agents. Circadian clocks are daily time-keeping mechanisms that help organisms to anticipate the usual 24 hour fluctuations on earth. The rhythms generated by circadian clocks are of endogenous nature and persist even in the absence of environmental cues with a species-specific period that usually deviates from 24 hours. They are synchronized, which means entrained to the 24 hour rhythm on earth by several environmental cues, called Zeitgebers, of which light has the largest impact. According to [40], circadian clocks have the following well defined properties. First they entrain to Zeitgeber cycles with a limited range of entrainment, second they can follow phase shifts of Zeitgeber cycles, but they need a certain number of transient cycles until they have established their previous phase to the Zeitgeber cycle. Third they can be phase shifted by light-pulses in a time-dependent manner that is characterized in a phase-response curve and fourth they run freely under constant conditions with a species-specific period, which is light-dependent. Constant light either lengthens or shortens the free-running period and constant light of high intensity dampens the clock and finally leads to arrhythmicity.

Specifically we use the model from [22] which is based on enzyme kinetics that is modeled by ordinary differential equation. This system of ordinary differential equations provides a limit cycle and thus can be used to model endogenous oscillation of proteins in a cell, which is associated with endogenous clocks. Furthermore the model describes the oscillations of the *Drosophila* period protein (PER) and its multiple phosphorylation. A schematic of the network and a detailed description is given in Figure 4.3.1 and the corresponding system of ordinary differential equations is given by

$$\frac{d}{dt}M = v_s \frac{K_1^n}{K_I^n + P_N^n} - v_m \frac{M}{K_m + M} \tag{4.3.1}$$

$$\frac{d}{dt}P_0 = k_s M - V_1 \frac{P_0}{K_1 + P_0} + V_2 \frac{P_1}{K_2 + P_1} \tag{4.3.2}$$

$$\frac{d}{dt}P_1 = V_1 \frac{P_0}{K_1 + P_0} - V_2 \frac{P_1}{K_2 + P_1} - V_3 \frac{P_1}{K_3 + P_1} + V_4 \frac{P_2}{K_4 + P_2} \tag{4.3.3}$$

$$\frac{d}{dt}P_2 = V_3 \frac{P_1}{K_3 + P_1} - V_4 \frac{P_2}{K_4 + P_2} - k_1 P_2 + k_2 P_N - v_d \frac{P_2}{K_d + P_2} \tag{4.3.4}$$

$$\frac{d}{dt}P_N = k_1 P_2 - k_2 P_N \tag{4.3.5}$$

where M is the concentration of *per* mRNA in the cytosol, P_0 is the concentration of unphosphorylated, P_1 is the concentration of monophosphorylated, P_2 is the concentration of biphosphorylated PER protein and P_N is the concentration of the biphosphorylated PER protein in the nucleus. Concentrations are defined with respect to the total cell volume.

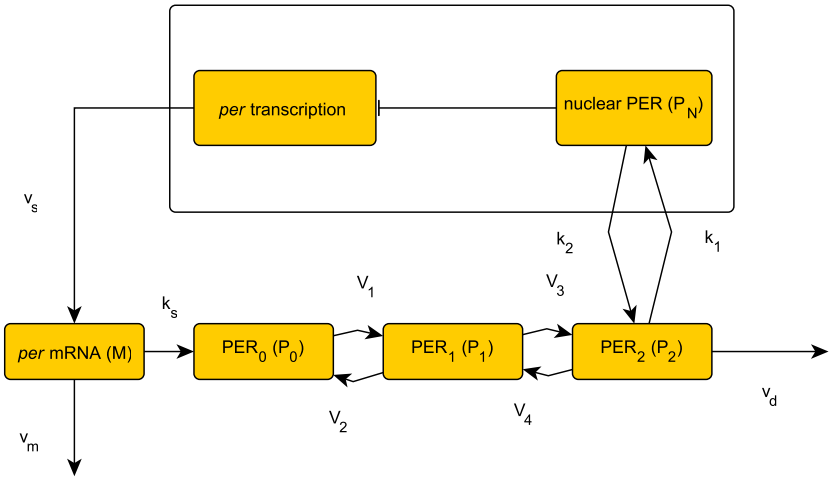

Figure 4.3.1: Model for circadian PER oscillations, see [22]. Scheme of the model for circadian oscillations in PER and *per* mRNA. The corresponding system of equations is given by (4.3.1) to (4.3.5). The *per* mRNA (M) is transcribed in the nucleus and exported to the cytosol, where it accumulates at a maximum rate v_s; at the same time it is degraded by an enzyme of maximum rate v_m and Michaelis constant K_m. The rate of translation of the PER protein is assumed to be proportional to M and is characterized by a first-order rate constant k_s. The parameters V_i and K_i, $i = 1, 2, 3, 4$, denote the maximum rate and Michaelis constant of the kinase(s) and phosphatase(s) involved in the reversible phosphorylation of P_0 into P_1 and P_1 into P_2 of the PER protein, respectively. The fully phosphorylated form (P_2) is degraded by an enzyme of maximum rate v_d and Michaelis constant K_d and imported into the nucleus at a rate characterized by the first-order rate constant k_1. Export of the nuclear, biphosphorylated form of PER (P_N) into the cytosol is characterized by the first-order rate constant k_2. The negative feedback exerted by nuclear PER protein on *per* transcription is described by an equation of the Hill type, in which n denotes the degree of cooperativity and K_I the threshold constant for inhibition.

Also in the work of [22], the model used in the present work is validated with experimental results. For our calculations we use the following values for the parameters which can be found in [22, Figure 2]. We have $v_s = 0.76\frac{\mu\text{M}}{h}$, $v_m = 0.65\frac{\mu\text{M}}{h}$, $K_m = 0.5\mu\text{M}$, $k_s = 0.38\frac{1}{h}$, $v_d = 0.95\frac{\mu\text{M}}{h}$, $k_1 = 1.9\frac{1}{h}$, $k_2 = 1.3\frac{1}{h}$, $K_I = 1\mu\text{M}$, $K_d = 0.2\mu\text{M}$, $n = 4$, $K_1 = K_2 = K_3 = K_4 = 2\mu\text{M}$, $V_1 = 3.2\frac{\mu\text{M}}{h}$, $V_2 = 1.58\frac{\mu\text{M}}{h}$, $V_3 = 5\frac{\mu\text{M}}{h}$, $V_4 = 2.5\frac{\mu\text{M}}{h}$ with the initial values $M(0) = 0.5$, $P_0(0) = 0.5$, $P_1(0) = 0.5$, $P_2(0) = 0.6$, $P_N(0) = 1.5$. We always calculate the model from time $t = 0$ to a final time. The calculations in this work are performed with Wolfram Mathematica. In Figure 4.3.2, we have a plot of the model where we see an almost 24 hours rhythm analogous to [22, Figure 2].

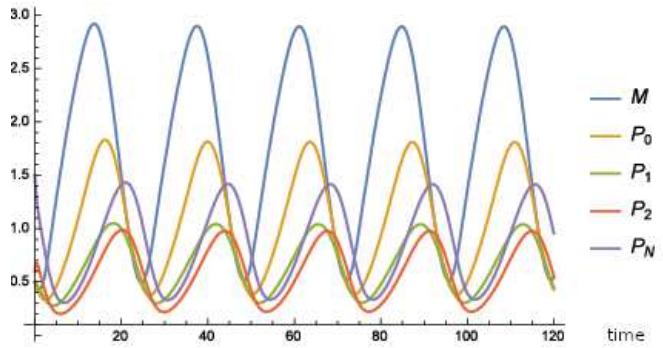

Figure 4.3.2: A plot of the model (4.3.1) to (4.3.5) with the parameters $v_s = 0.76\frac{\mu\text{M}}{h}$, $v_m = 0.65\frac{\mu\text{M}}{h}$, $K_m = 0.5\mu\text{M}$, $k_s = 0.38\frac{1}{h}$, $v_d = 0.95\frac{\mu\text{M}}{h}$, $k_1 = 1.9\frac{1}{h}$, $k_2 = 1.3\frac{1}{h}$, $K_I = 1\mu\text{M}$, $K_d = 0.2\mu\text{M}$, $n = 4$, $K_1 = K_2 = K_3 = K_4 = 2\mu\text{M}$, $V_1 = 3.2\frac{\mu\text{M}}{h}$, $V_2 = 1.58\frac{\mu\text{M}}{h}$, $V_3 = 5\frac{\mu\text{M}}{h}$, $V_4 = 2.5\frac{\mu\text{M}}{h}$ with the initial values $M(0) = 0.5$, $P_0(0) = 0.5$, $P_1(0) = 0.5$, $P_2(0) = 0.6$, $P_N(0) = 1.5$. The time is plotted on the abscissa and the corresponding concentration with respect to the whole cell volume is plotted on the ordinate.

Entrainment to light-dark cycles

Now, we extend the model of [22] by a mechanism that allows to include the effect external stimuli. In the following experiment we would like to have that an external stimulus influences the circadian clock such that it synchronizes to the rhythm of the external time phase. Such an external stimulus is for example light, see [25] or any other substance that influences the concentration of an agent of the model (4.3.1) to (4.3.5). In our first experiment, we synchronize the phase of the endogenous clock to the phase of an external Zeitgeber. We start our discussion by assuming that the external stimulus leads to a further decay of *per* mRNA (M) in order to compare these results to different molecular mechanisms like a degradation of PER protein which is considered later. We model the further decay of *per* mRNA by

$$\frac{d}{dt}M = v_s\frac{K_1^n}{K_1^n + P_N^n} - v_m\frac{M}{K_m + M} - \varkappa uM \tag{4.3.6}$$

instead of (4.3.1). The term $-uM$ models the effect that if the external stimulus is strong and M is large, then the decay of M is strong, that means a lot of *per* mRNA is degraded and if the external stimulus is weak and M is small, then there is almost no additional decay of M. The constant $\varkappa$ is a coupling constant that weights the contribution of the term $-uM$ to the time variation of M. For our experiment, we use $\varkappa = 0.05$.

Our first experiment is as follows. We assume that light is our external stimulus and causes an increased degradation of *per* mRNA and the light intensity oscillates with a period of 24 hours according to

$$u(t) \coloneqq \cos\left(2\pi\frac{t}{24} + \varphi\right) + 1 \tag{4.3.7}$$

where φ is the time shift of external and internal time of the cell. We start with $\varphi = 0$. Then, the external stimulus has the same phase as the endogenous time of the cell, see Figure 4.3.3 and the curves almost look like the unperturbed ones from Figure 4.3.2. That means that our framework is in accordance with the model proposed in [22]. Furthermore, we see that the period stays the same and is not changed by the mechanism that includes the effect of the external stimulus. Representing the proteins, we present only a detailed plot of M in Figure 4.3.3b as the other plots look similar. This is done throughout this section.

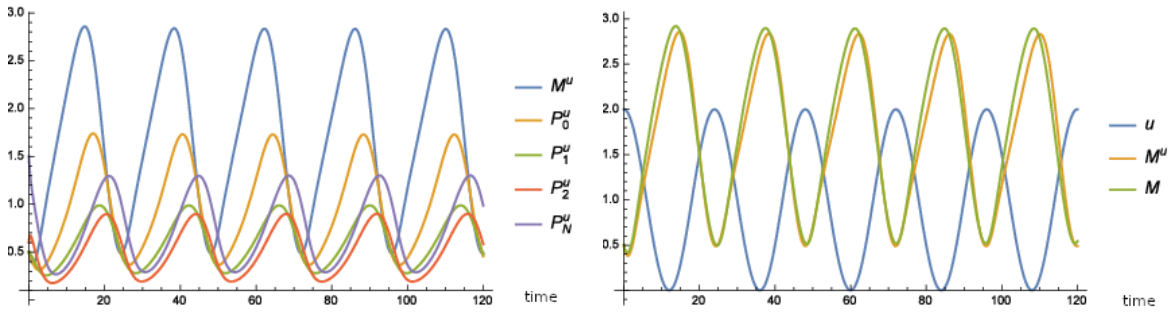

(a) Time curves where the superscript u indicates that these time curves belong to the solution to the extended model consisting of (4.3.6) and (4.3.2) to (4.3.5) with (4.3.7) for $\varphi = 0$ and $\varkappa = 0.05$.

(b) Time curve of the external stimulus u defined in (4.3.7), of M calculated from the model (4.3.1) to (4.3.5) and of M^u calculated from (4.3.6) and (4.3.2) to (4.3.5) with (4.3.7) for $\varphi = 0$ and $\varkappa = 0.05$.

Figure 4.3.3: The model (4.3.6) and (4.3.2) to (4.3.5) does not differ from the original model (4.3.1) to (4.3.5) if the molecular clock is in the phase of the external Zeitgeber. The time is plotted on the abscissa and the corresponding concentration with respect to the whole cell volume is plotted on the ordinate.

If the external time is shifted compared to the endogenous time of the cell by for example $\varphi = \pi$, then we see in Figure 4.3.4 that the endogenous time is shifted by approximately 12 hours after a transient of about 48 hours. The external stimulus synchronizes the endogenous time with the external time such that the phase of the cell's endogenous time is again in sync with the phase of the external time. We remark that the period of about 24 hours is unperturbed after the transient.

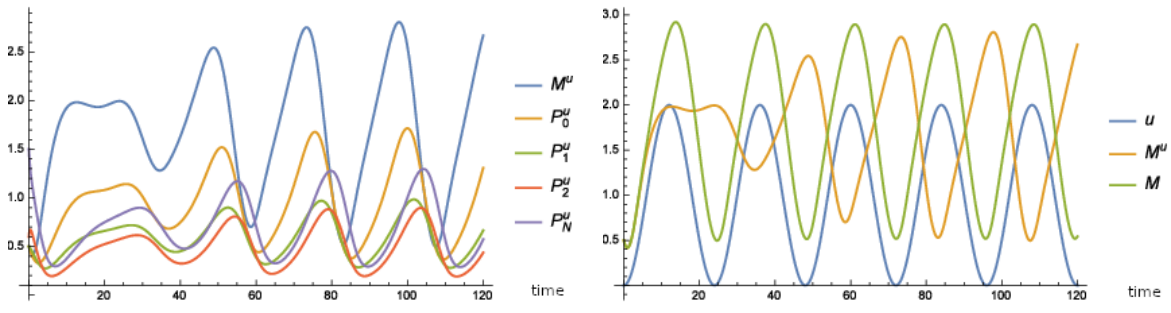

(a) Time curves where the superscript u indicates that these time curves belong to the solution to the extended model consisting of (4.3.6) and (4.3.2) to (4.3.5) with (4.3.7) for $\varphi = \pi$and $\varkappa = 0.05$.

(b) Time curve of the external stimulus u defined in (4.3.7), of M calculated from the model (4.3.1) to (4.3.5) and of M^u calculated from (4.3.6) and (4.3.2) to (4.3.5) with (4.3.7) for $\varphi = \pi$ and $\varkappa = 0.05$.

Figure 4.3.4: The external stimulus induces a shift of the molecular clock's phase of 12 hours. The time is plotted on the abscissa and the corresponding concentration with respect to the whole cell volume is plotted on the ordinate.

For illustration, we have the figures analogous to the results above for $\varphi = \frac{\pi}{2}$ and have a shift of about 6 hours after a transient, see Figure 4.3.5.

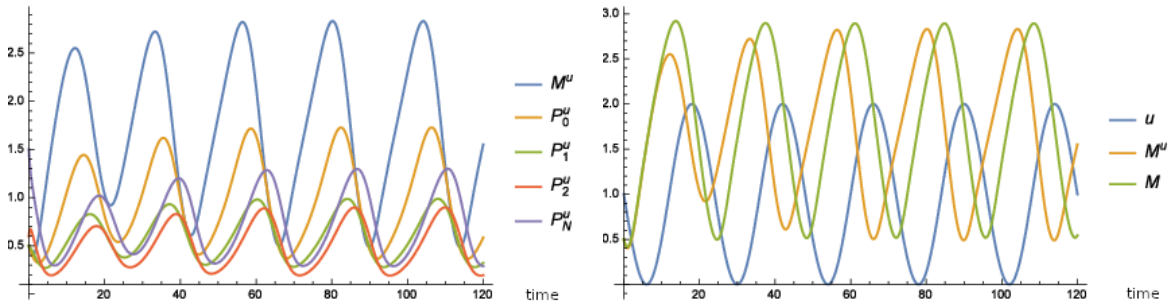

(a) Time curves where the superscript u indicates that these time curves belong to the solution to the extended model consisting of (4.3.6) and (4.3.2) to (4.3.5) with (4.3.7) for $\varphi = \frac{\pi}{2}$ and $\varkappa = 0.05$.

(b) Time curve of the external stimulus u defined in (4.3.7), of M calculated from the model (4.3.1) to (4.3.5) and of M^u calculated from (4.3.6) and (4.3.2) to (4.3.5) with (4.3.7) for $\varphi = \frac{\pi}{2}$ and $\varkappa = 0.05$.

Figure 4.3.5: The external stimulus induces a shift of the molecular clock's phase of about 6 hours. The time is plotted on the abscissa and the corresponding concentration with respect to the whole cell volume is plotted on the ordinate.

Phase shifts by a strong stimulus

In the next experiment, we show that we can restart the endogenous clock with a strong knock down of the *per* mRNA (M) modeled by

$$u(t) := \begin{cases} 5 & \text{if } 0 \leq t \leq t_s \\ 0 & \text{else} \end{cases} \tag{4.3.8}$$

where $t_s > 0$.

In Figure 4.3.6, we depict the results. We have that as soon as the external stimulus u stops, then the oscillation starts again with a shift of the endogenous time's phase.

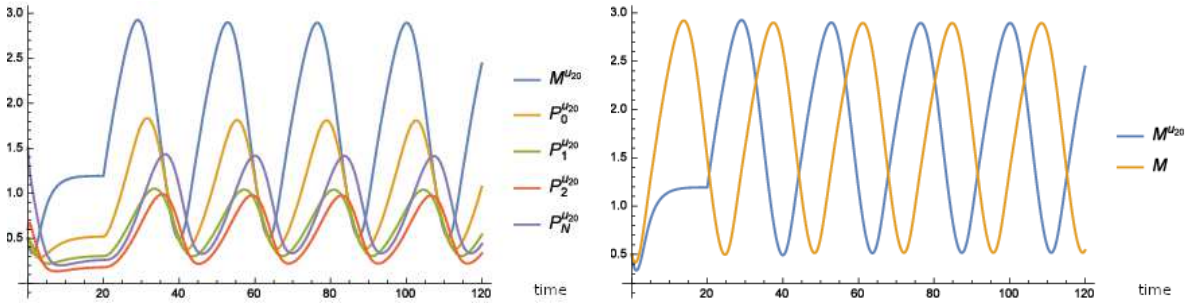

(a) Time curves of all molecular agents where the superscript u_{20} indicates that these time curves belong to the solution to the extended model consisting of (4.3.6) and (4.3.2) to (4.3.5) for (4.3.8) with $t_s = 20$ and $\varkappa = 0.05$.

(b) Time curve of M calculated from the model (4.3.1) to (4.3.5) and of $M^{u_{20}}$ calculated from (4.3.6) and (4.3.2) to (4.3.5) for (4.3.8) with $t_s = 20$ and $\varkappa = 0.05$.

Figure 4.3.6: The external stimulus stops the oscillations which restart after the external stimulus has decayed. The time is plotted on the abscissa and the corresponding concentration with respect to the whole cell volume is plotted on the ordinate.

In Figure 4.3.7, we see that if the knock down of the mRNA takes longer, then the beginning of the oscillation is retarded and thus the shift of the endogenous time's phase is greater. In this way, by knocking down the *per* mRNA we can restart the endogenous time whenever we desire.

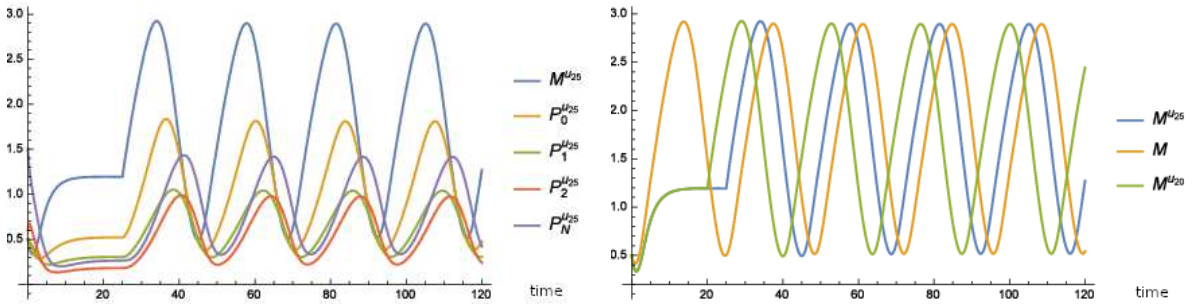

(a) Time curves where the superscript u_{25} indicates that these time curves belong to the solution to the extended model consisting of (4.3.6) and (4.3.2) to (4.3.5) for (4.3.8) with $t_s = 25$ and $\varkappa = 0.05$.

(b) Time curve of M calculated from the model (4.3.1) to (4.3.5), of M^{u25} calculated from (4.3.6) and (4.3.2) to (4.3.5) for (4.3.8) with $t_s = 25$, $\varkappa = 0.05$ and of M^{u20} calculated from (4.3.6) and (4.3.2) to (4.3.5) for (4.3.8) with $t_s = 20$ and $\varkappa = 0.05$.

Figure 4.3.7: Depending on the point of time when the external stimulus decays, we obtain a different shift of the molecular clock's phase. The time is plotted on the abscissa and the corresponding concentration with respect to the whole cell volume is plotted on the ordinate.

Next, we show that analogous results can be obtained with different models. If we model inhibition of the transcription of the *per* gene by

$$\frac{d}{dt}M = v_s \frac{K_1^n}{K_1^n + P_N^n}(1-u) - v_m \frac{M}{K_m + M} \tag{4.3.9}$$

instead of (4.3.1) while the remaining equations are given as in (4.3.2) to (4.3.5) with

$$u(t) := \begin{cases} 1 & \text{if } 0 \le t \le t_s \\ 0 & \text{else} \end{cases}, \tag{4.3.10}$$

$t_s = 20$, then we can recognize a shift of the phase similar to the one in Figure 4.3.8.

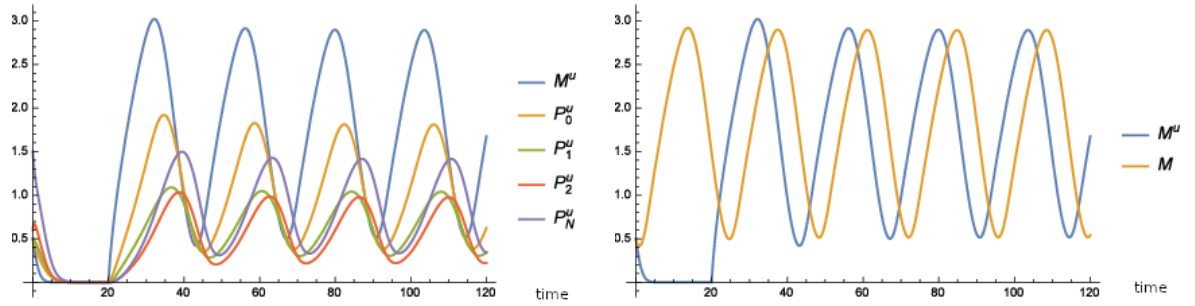

(a) Time curves where the superscript u indicates that these time curves belong to the solution to the extended model consisting of (4.3.9) and (4.3.2) to (4.3.5) for (4.3.10) with $t_s = 20$.

(b) Time curve of M calculated from the model (4.3.1) to (4.3.5) and of M^u calculated from (4.3.9) and (4.3.2) to (4.3.5) for (4.3.10) with $t_s = 20$.

Figure 4.3.8: Inhibiting the transcription of *per* gene restarts the molecular clock as soon as the inhibition stops. The time is plotted on the abscissa and the corresponding concentration with respect to the whole cell volume is plotted on the ordinate.

The inhibition of the translation of the *per* mRNA can be modeled by

$$\frac{d}{dt}P_0 = k_s M(1-u) - V_1 \frac{P_0}{K_1 + P_0} + V_2 \frac{P_1}{K_2 + P_1} \tag{4.3.11}$$

instead of (4.3.2) in the system of equations (4.3.1) to (4.3.5). In Figure 4.3.9, we see the results. These results where the concentration of PER protein goes to zero and starts oscillating again when the translation of PER starts again can also be seen experimentally in [61, Figure 3]. In this experiment

cells are exposed to cycloheximide which inhibits the protein synthesis at the ribosomes. Then the oscillations of PER protein decay in all cells and when the cycloheximide is washed out the oscillations start again such that all the cells then have the same phase of their endogenous clock. Furthermore in Figure 4.3.9, we see that the concentration of mRNA increases as there is no protein inhibiting the transcription of the *per* mRNA.

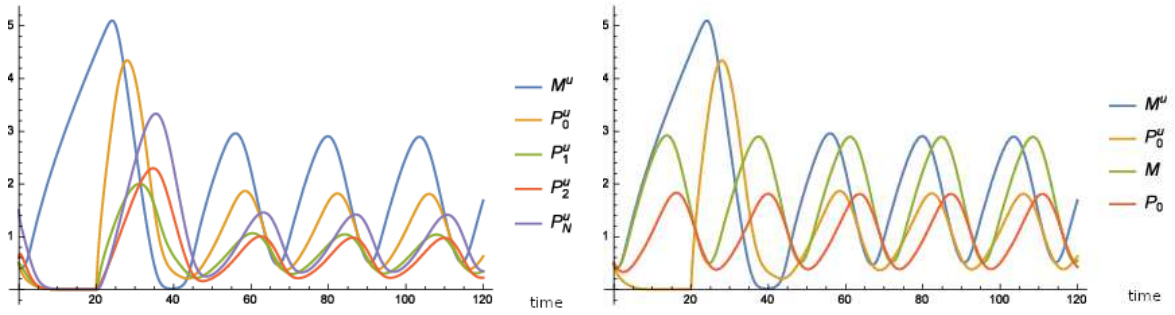

(a) Time curves where the superscript u indicates that these time curves belong to the solution to the extended model consisting of (4.3.1) to (4.3.5) where (4.3.2) is replaced by (4.3.11) for (4.3.10) with $t_s = 20$.

(b) Time curve of M and P_0 calculated from the model (4.3.1) to (4.3.5) and of M^u and P_0^u calculated from (4.3.1) to (4.3.5) where (4.3.2) is replaced by (4.3.11) for (4.3.10) with $t_s = 20$.

Figure 4.3.9: Inhibiting the translation of *per* mRNA restarts the molecular clock as soon as the inhibition stops. The time is plotted on the abscissa and the corresponding concentration with respect to the whole cell volume is plotted on the ordinate.

For the same model as in the last experiment but with the external stimulus

$$u(t) := \frac{1}{4}\left(\cos\left(2\pi\frac{t}{24} + \varphi\right) + 1\right) \tag{4.3.12}$$

with $\varphi = \pi$, we have an analogous result as for the first experiment for (4.3.6) and (4.3.2) to (4.3.5) with (4.3.7) that is depicted in Figure 4.3.4. We can compare these results by looking at Figure 4.3.10 where the synchronization of the endogenous time with the external time for a shift of 12 hours is shown for the model consisting of (4.3.1) to (4.3.5) where (4.3.2) is replaced by (4.3.11) for (4.3.12) wit $\varphi = \pi$.

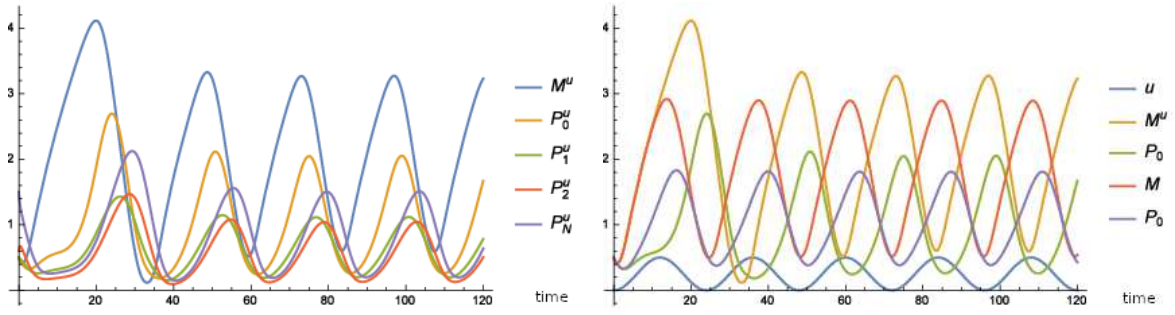

(a) Time curves where the superscript u indicates that these time curves belong to the solution to the extended model consisting of (4.3.1) to (4.3.5) where (4.3.2) is replaced by (4.3.11) for (4.3.12) with $\varphi = \pi$.

(b) Time curve of the external stimulus u defined in (4.3.12), of M and P_0 calculated from the model (4.3.1) to (4.3.5) and of M^u and P_0^u calculated from (4.3.1) to (4.3.5) where (4.3.2) is replaced by (4.3.11) for (4.3.12) with $\varphi = \pi$.

Figure 4.3.10: Inhibiting the translation of the *per* mRNA with an external stimulus with a period of 24 hours according to (4.3.12) shifts the phase of the molecular clock. The time is plotted on the abscissa and the corresponding concentration with respect to the whole cell volume is plotted on the ordinate.

Fly and mammalian models

Next, we set up two models, one specific for flies and one specific for mammalians. We have a degradation of the PER protein caused by the external stimulus modeled with

$$\frac{d}{dt}P_0 = k_s M - V_1 \frac{P_0}{K_1 + P_0} + V_2 \frac{P_1}{K_2 + P_1} - \mu u P_0 \tag{4.3.13}$$

where $\mu > 0$. We take our minimal model (4.3.1) to (4.3.5) where (4.3.2) is exchanged by (4.3.13) for flies. We show that, analogously to Figure 4.3.10, the unperturbed rhythm is shifted by about 12 hours if we apply (4.3.12) with $\varphi = \pi$, see Figure 4.3.11.

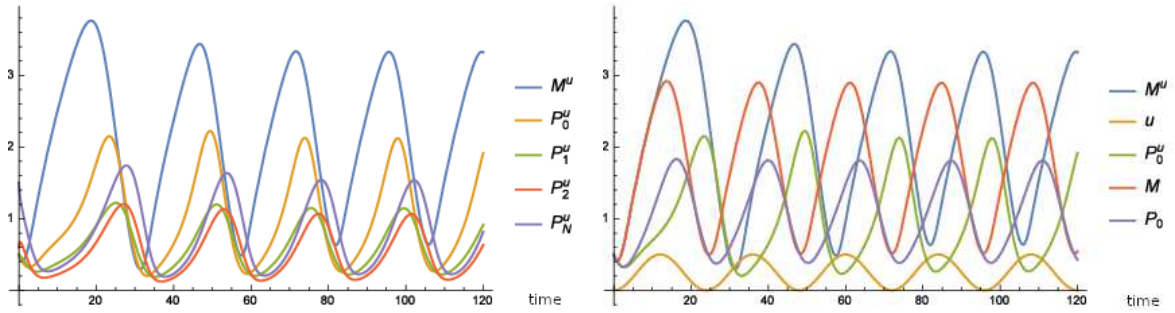

(a) Time curves where the superscript u indicates that these time curves belong to the solution to the extended model consisting of (4.3.1) to (4.3.5) where (4.3.2) is replaced by (4.3.13) for (4.3.12) with $\varphi = \pi$ and $\mu = 1$.

(b) Time curve of the external stimulus u defined in (4.3.12), of M and P_0 calculated from the model (4.3.1) to (4.3.5) where (4.3.2) is to (4.3.5) and of M^u and P_0^u calculated from (4.3.1) to (4.3.5) where (4.3.2) is replaced by (4.3.13) for (4.3.12) with $\varphi = \pi$ and $\mu = 1$.

Figure 4.3.11: A further anti phase degradation of PER protein shifts the phase of the molecular clock. The time is plotted on the abscissa and the corresponding concentration with respect to the whole cell volume is plotted on the ordinate.

In mammals we have that light induces *per* transcription. This can be modeled by the following equations where we replace (4.3.1) by

$$\frac{d}{dt}M = v_s \frac{K_1^n}{K_1^n + P_N^n} - v_m \frac{M}{K_m + M} + \gamma u \exp\left(-\varrho M\right) \tag{4.3.14}$$

while we still use (4.3.2) to (4.3.5) with $\gamma, \varrho > 0$. The term $\exp\left(-\varrho M\right)$ models the fact that if there is a lot of *per* mRNA, then a light stimulus is supposed to be not that effective as it is when there is almost no *per* mRNA. In this section we use $\varrho = 1$.

Range of entrainment

In the next experiment we show the entrainment to different periods. For this purpose we choose the external stimulus

$$u_{T_p}(t) := 0.06 \cdot \left(\cos\left(2\pi \frac{t}{T_p}\right) + 1\right) \tag{4.3.15}$$

whose period can be set to any period T_p where $T_p > 0$. The periods are determined by the peaks of the simulated oscillating concentrations of the *per* mRNA detected with the FindArgMax function of Mathematica in the range $t \in [170, 220]$ hours to exclude effects from the transient. We start with the model (4.3.1) to (4.3.5) where (4.3.2) is exchanged by (4.3.13) with $\mu = 2$. We call this model the **fly model**. We obtain a period of 27.8 hours for $T_p = 29$, a period of 27.7 hours for $T_p = 28$, a period of 26.9 hours for $T_p = 27$, a period of 26.0 hours for $T_p = 26$, a period of 25.0 hours for $T_p = 25$, a period of 24.0 hours for $T_p = 24$, a period of 23.0 hours for $T_p = 23$, a period of 22.0 hours for $T_p = 22$, a period of 21.0 hours for $T_p = 21$, a period of 19.9 hours for $T_p = 20$, a period of 20.3 hours for $T_p = 19$ and a period of 20.0 hours for $T_p = 18$. The values are plotted in Figure 4.3.12a.

Now, we use the model (4.3.14) instead of (4.3.1) and still use (4.3.2) to (4.3.5) with $\gamma = 2.5$. We call this model the **mammalian model**. The parameters have different values to adapt each model

to obtain a more or less realistic range of entrainment to the external period. We obtain a period of 23.8 hours for $T_p = 26$, a period of 24.3 hours for $T_p = 25$, a period of 23.6 hours for $T_p = 24$, a period of 22.6 hours for $T_p = 23$, a period of 23.8 hours for $T_p = 22$ and a period of 22.0 hours for $T_p = 21$. The values are plotted in Figure 4.3.12b.

In both cases we have a limited range of entrainment, whereby the latter is much larger in flies (8 hours, Figure 4.3.12a) than in mammals (2 hours, Figure 4.3.12b). This effect of a limited range of entrainment is reported, for example, in [4, Figure 2].

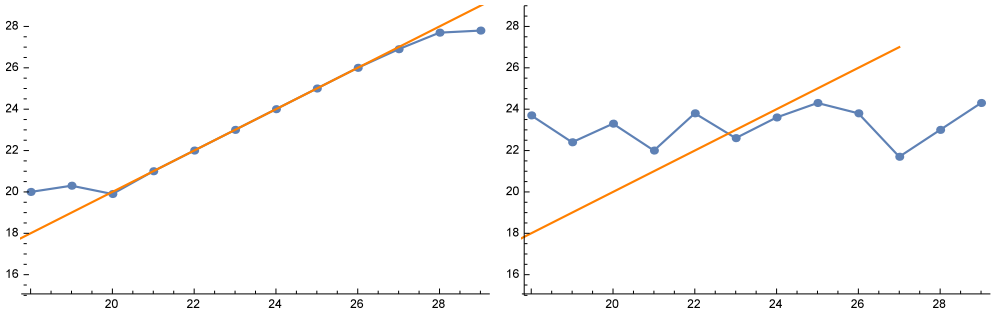

(a) (b)

Figure 4.3.12: On the abscissa the period T_p of the external Zeitgeber is plotted and on the ordinate the entrained period of the endogenous clock is plotted. The orange line is the ideal entrainment where the period of the external Zeitgeber is exactly adopted. (a) Data points for the blue graph: $(18, 20.0)$, $(19, 20.3)$, $(20, 19.9)$, $(21, 21.0)$, $(22, 22.0)$, $(23, 23.0)$, $(24, 24.0)$, $(25, 25.0)$, $(26, 26.0)$, $(27, 26.9)$, $(28, 27.7)$, $(29, 27.8)$. (b) Data points for the blue graph: $(18, 23.7)$, $(19, 22.4)$, $(20, 23.3)$, $(21, 22.0)$, $(22, 23.8)$, $(23, 22.6)$, $(24, 23.6)$, $(25, 24.3)$, $(26, 23.8)$, $(27, 21.7)$, $(28, 23.0)$, $(29, 24.3)$.

In the next experiment, we that the entrained period is constant for the range of entrainment after a transient show for the mammalian model, while the periods outside the range of entrainment are only constant for a certain range followed by a range where the period changes, see Figure 4.3.13. These ranges follow each other and thus oscillate.This effect is known as relative coordination, see [43] for example. The periods are determined as follows. With the Mathematica function FindArgMax, we subtract the time of the peak of the mRNA M in the interval $[190 + T_n, 210 + T_n]$ from the time of the peak of the mRNA M in the interval $[167 + T_n, 180 + T_n]$ where $T_n := 24n$, $n \geq 0$. The time is given in hours. We choose $n \in \{1, ..., 15\}$ which means that we determine the entrained period at each day. In Figure 4.3.14 we plot the corresponding time curves of M where we also see corresponding effects for the amplitude, that means constant amplitudes for the range of entrainment and oscillating amplitudes outside the range of entrainment. From these time curves the data for Figure 4.3.13 is generated.

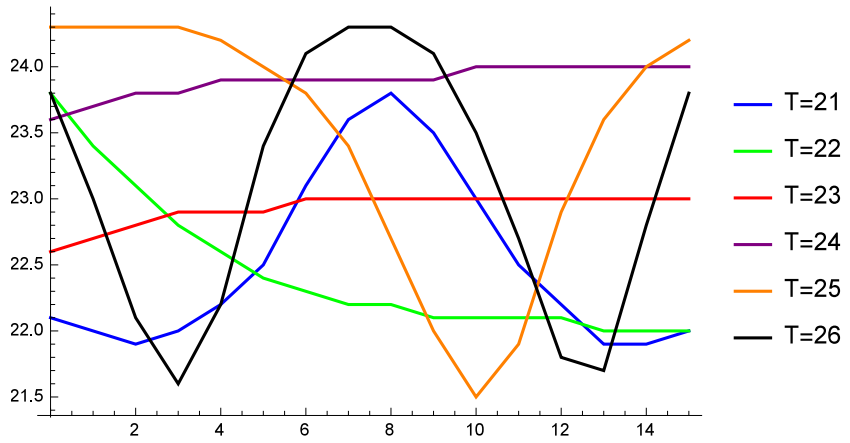

Figure 4.3.13: Period oscillations for different periods of the external Zeitgeber for the mammalian model. The entrained periods are constant after a transient for the range of entrainment and oscillate outside the range of entrainment. On the abscissa the day n is plotted and on the ordinate the entrained period is plotted. The data points are as follows. For $T = 21$: $(0, 22.1)$, $(1, 22.0)$, $(2, 21.9)$, $(3, 22.0)$,$(4, 22.2)$, $(5, 22.5)$, $(6, 23.1)$, $(7, 23.6)$, $(8, 23.8)$,$(9, 23.5)$,$(10, 23.0)$,$(11, 22.5)$,$(12, 22.2)$,$(13, 21.9)$, $(14, 21.9)$, $(15, 22.0)$. For $T = 22$: $(0, 23.8)$, $(1, 23.4)$,$(2, 23.1)$, $(3, 22.8)$, $(4, 22.6)$,$(5, 22.4)$, $(6, 22.3)$, $(7, 22.2)$, $(8, 22.2)$, $(9, 22.1)$,$(10, 22.1)$, $(11, 22.1)$,$(12, 22.1)$, $(13, 22.0)$, $(14, 22.0)$, $(15, 22.0)$. For $T = 23$: $(0, 22.6)$,$(1, 22.7)$, $(2, 22.8)$, $(3, 22.9)$, $(4, 22.9)$, $(5, 22.9)$, $(6, 23.0)$, $(7, 23.0)$, $(8, 23.0)$, $(9, 23.0)$, $(10, 23.0)$, $(11, 23.0)$, $(12, 23.0)$, $(13, 23.0)$, $(14, 23.0)$, $(15, 23.0)$. For $T = 24$: $(0, 23.6)$, $(1, 23.7)$, $(2, 23.8)$, $(3, 23.8)$, $(4, 23.9)$, $(5, 23.9)$, $(6, 23.9)$, $(7, 23.9)$,$(8, 23.9)$, $(9, 23.9)$, $(10, 24.0)$, $(11, 24.0)$, $(12, 24.0)$, $(13, 24.0)$, $(14, 24.0)$,$(15, 24.0)$. For $T = 25$: $(0, 24.3)$,$(1, 24.3)$, $(2, 24.3)$, $(3, 24.3)$, $(4, 24.2)$, $(5, 24.0)$, $(6, 23.8)$, $(7, 23.4)$, $(8, 22.7)$, $(9, 22.0)$,$(10, 21.5)$, $(11, 21.9)$, $(12, 22.9)$, $(13, 23.6)$, $(14, 24.0)$, $(15, 24.2)$. For $T = 26$: $(0, 23.8)$, $(1, 23.0)$, $(2, 22.1)$, $(3, 21.6)$, $(4, 22.2)$, $(5, 23.4)$, $(6, 24.1)$, $(7, 24.3)$, $(8, 24.3)$, $(9, 24.1)$, $(10, 23.5)$, $(11, 22.7)$, $(12, 21.8)$, $(13, 21.7)$, $(14, 22.8)$, $(15, 23.8)$.

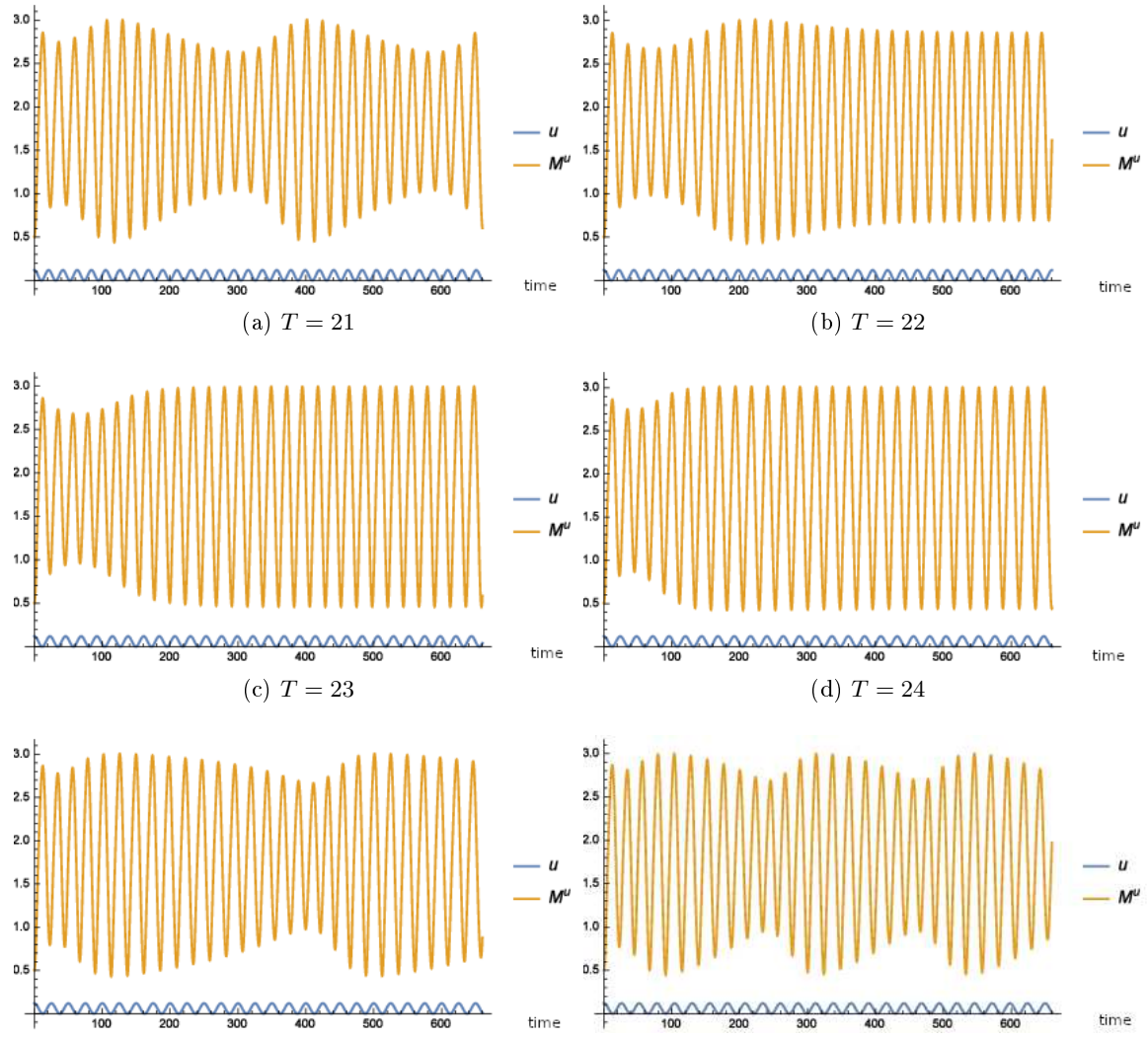

(a) $T = 21$ (b) $T = 22$

(c) $T = 23$ (d) $T = 24$

(e) $T = 25$ (f) $T = 26$

Figure 4.3.14: Time curves of M for the mammalian model for different periods of the external Zeitgeber. We see a constant behavior of the amplitude for the external periods that are within the range of entrainment and an oscillation of the amplitude for the periods of the external Zeitgeber that do not belong to the range of entrainment. The time is plotted in hours on the abscissa and the corresponding concentration with respect to the whole cell volume is plotted on the ordinate.

Constant light

We choose a constant external stimulus modeled by

$$u_c(t) = c \tag{4.3.16}$$

that causes a degradation of P_0 or a further transcription of M. We determine the periods by detecting the peaks of the simulated oscillating concentrations of the *per* mRNA with the FindArgMax function of Mathematica in the range $t \in [80, 120]$ hours.

We start with the fly model with $\mu = 1$ and, by increasing the intensity of the external stimulus, we first obtain a shortening of the period and from a turning point an elongation of the period until we have no oscillation any more which we call arrhythmic behavior. See Figure 4.3.15 for a strong intensity where the oscillations fade until there is no rhythm any more and see Figure 4.3.16 for a weak intensity of the external stimulus where the amplitude of the oscillations is damped compared with the unperturbed oscillations. In detail, we have (in hours) a period of 23.7 for $c = 0$, a period of 23.5 for $c = 0.1$, a period of 23.4 for $c = 0.2$, a period of 23.7 for $c = 0.3$, a period of 24.5 for $c = 0.4$, a period of 25.4 for $c = 0.5$, a period of 26.4 for $c = 0.6$, a period of 27.4 for $c = 0.7$, a period of 28.5

for $c = 0.8$, a period of 29.6 for $c = 0.9$ and from $c = 1$ the oscillations are that weak that we call this state arrhythmic.

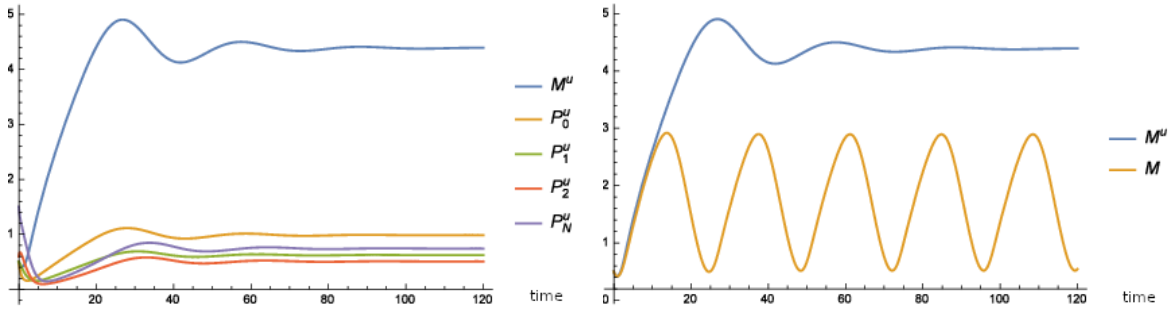

(a) Time curves where the superscript u indicates that these time curves belong to the solution to the extended model consisting of (4.3.1) to (4.3.5) where (4.3.2) is replaced by (4.3.13) for (4.3.16) with $\mu = 1$ and $c = 1$.

(b) Time curve of M calculated from the model (4.3.1) to (4.3.5) and of M^u calculated from (4.3.1) to (4.3.5) where (4.3.2) is replaced by (4.3.13) for (4.3.16) with $\mu = 1$ and $c = 1$.

Figure 4.3.15: A strong permanent external stimulus causes arrhythmic behavior as the oscillations are dampened off. The time is plotted in hours on the abscissa and the corresponding concentration with respect to the whole cell volume is plotted on the ordinate.

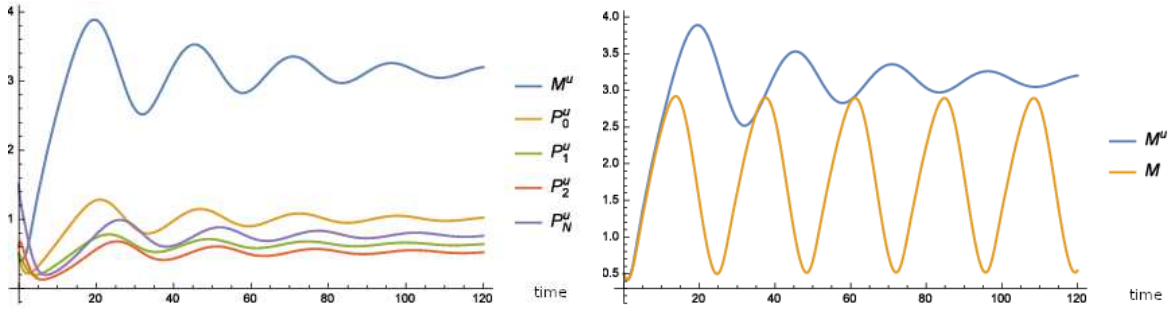

(a) Time curves where the superscript u indicates that these time curves belong to the solution to the extended model consisting of (4.3.1) to (4.3.5) where (4.3.2) is replaced by (4.3.13) for (4.3.16) with $\mu = 1$ and $c = 0.5$.

(b) Time curve of M calculated from the model (4.3.1) to (4.3.5) and of M^u calculated from (4.3.1) to (4.3.5) where (4.3.2) is replaced by (4.3.13) for (4.3.16) with $\mu = 1$ and $c = 0.5$.

Figure 4.3.16: A weak permanent external stimulus causes dampening of the amplitude of the oscillations, however they are still visible. The time is plotted in hours on the abscissa and the corresponding concentration with respect to the whole cell volume is plotted on the ordinate.

Now, we investigate the mammalian model for $\gamma = 2$. This causes that the model also shows arrhythmic behavior for $c = 1$. We remark that μ and γ are chosen such that the arrhythmic behavior always occurs for $c = 1$. As these constants are multiplied with the external stimulus u, we could also take the values for μ and γ from the experiment about the range of entrainment which would cause that the arrhythmic behavior for the fly model and the mammalian model would appear for different c.

We have that the period for the mammalian model becomes shorter until $c = 0.4$ and then the period becomes longer until the stimulus is so strong that no oscillation is detectable any more. The figures in this experiment look similar to the ones from the last experiment. In detail, we have (in hours) a period of 23.7 for $c = 0$, a period of 22.8 for $c = 0.1$, a period of 22.2 for $c = 0.2$, a period of 21.7 for $c = 0.3$, a period of 21.5 for $c = 0.4$, a period of 21.5 for $c = 0.5$, a period of 21.8 for $c = 0.6$, a period of 22.3 for $c = 0.7$, a period of 22.9 for $c = 0.8$ and a period of 23.7 for $c = 0.9$. From $c = 1$ the oscillations are that week that we call this state arrhythmic.

From our experiments, we conclude that for a small range a weak illuminance causes a shortening of the period in the fly model while there is a huge range where a permanent external stimulus lengthens the period. In the mammalian model, there is also a turning point in the illuminance where the period

is lengthened by a permanent external stimulus and this point comes later than in the fly model, see Figure 4.3.17. Furthermore, we conclude that the question if the period is shortened or lengthened by a permanent external stimulus can depend on the model (fly or mammalian) and the corresponding parameters. These differences cause different positions of the turning points when the model changes its behavior from shortening the period to lengthening it or influence the slope from one data point to the next one, see Figure 4.3.17. Moreover we have to consider that if the turning point is not in the range in what we perform our measurements, then we just find a monotone behavior of the period. We remark that measurements are mostly just in a short range of natural illuminance which is maximum about 100000 lux. Therefore if the measurement is orders of magnitudes below this natural daylight illuminance then it may happen that one discovers just the shortening of the period. If the illuminance is too strong and the model has just a short range at the beginning where the period is shortened (fly model), then one also just experiences the lengthening of the period. In [3, Figure 2], we see the dependence of the period under constant light for different species. We stress that most curves there are polygon-like which is in accordance to our experiments considering just the data points. Furthermore almost all curves (except one as far as we can recognize) either first fall and then rise (nocturnal birds) or only rise which is also in accordance to our numerical experiment assuming that in these cases the range where the period is shortened is small or the measurement takes place above the mentioned turning point.

Furthermore, considering [30, Table III] and our model, we have that different organisms or mutants have different ranges of intensity where a constant stimulus causes shortening or lengthening of the period of the endogenous clock. Thus if a period increases or decreases if the organism or mutant is exposed first to constant light and then constant darkness or the other way round, depends on if the intensity of the constant light is in the range where the corresponding graph is below the endogenous period or above. Then when the molecular clock takes its free running period, it shortens or lengthens depending on its period in constant light. We stress that especially with mutants the corresponding turning point might be at a intensity being so high that an external stimulus cannot be applied without causing damage to the considered organism in order to see both behaviors of the period, that means shortening and lengthening.

We remark that if we would like to do this experiment for different orders of magnitude for the illuminance, we can replace u by $\ln(1+u)$, for instance, fitting the corresponding parameter μ or γ.

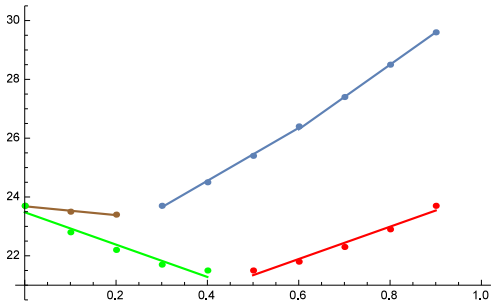

Figure 4.3.17: On the abscissa we have the illuminance c and on the ordinate we have the period length. The data points are from the fly and the mammalian model under constant stimulus, see text above. The brown and blue line is from the fly model and the green and red one is from the mammalian model.

Phase response curves

Now we show that in our model it is essential when a short pulse of light is given with respect to the phase of the oscillation of the endogenous clock in order to cause a shift of the phase of the endogenous clock. We start with the fly model. If we give the light pulse when the concentration of PER protein is high, then we restart the circadian clock, see Figure 4.3.18 and shift it by about eight hours. If we give the light pulse when the concentration of PER protein is low, then the clock is hardly effected, see Figure 4.3.19. We remark that we obtain similar figures for the mammalian model. We have a shift of the clock if the concentration of *per* mRNA is low and almost no effect if the concentration of

per mRNA is high. The one hour light pulse with which we perturb the endogenous clock is given as follows

$$u_{t_0,c}(t) := \begin{cases} c & \text{if } t \in [t_0, t_0+1] \\ 0 & \text{else} \end{cases} \tag{4.3.17}$$

where $c > 0$ and $t_0 \geq 0$.

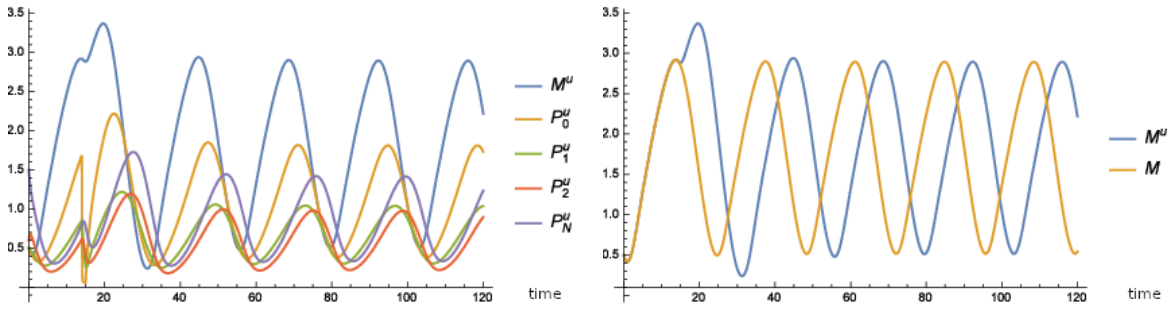

(a) Time curves where the superscript u indicates that these time curves belong to the solution to the extended model consisting of (4.3.1) to (4.3.5) where (4.3.2) is replaced by (4.3.13) with $\mu = 1$ for (4.3.17) with $t_0 = 14$ and $c = 20$.

(b) Time curve of M calculated from the model (4.3.1) to (4.3.5) and of M^u calculated from (4.3.1) to (4.3.5) where (4.3.2) is replaced by (4.3.13) with $\mu = 1$ for (4.3.17) with $t_0 = 14$ and $c = 20$.

Figure 4.3.18: A one hour light pulse causing a degradation of PER protein at a high concentration of PER protein induces a phase shift of the PER oscillation. The time is plotted in hours on the abscissa and the corresponding concentration with respect to the whole cell volume is plotted on the ordinate.

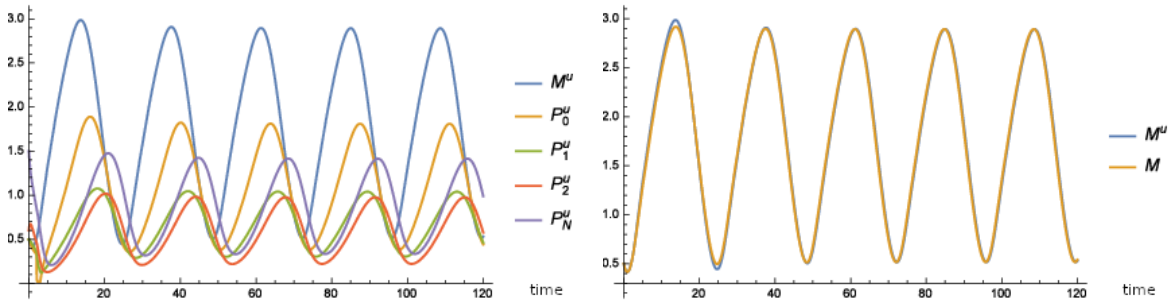

(a) Time curves where the superscript u indicates that these time curves belong to the solution to the extended model consisting of (4.3.1) to (4.3.5) where (4.3.2) is replaced by (4.3.13) with $\mu = 1$ for (4.3.17) with $t_0 = 2$ and $c = 20$.

(b) Time curve of M calculated from the model (4.3.1) to (4.3.5) and of M^u calculated from (4.3.1) to (4.3.5) where (4.3.2) is replaced by (4.3.13) with $\mu = 1$ for (4.3.17) with $t_0 = 2$ and $c = 20$.

Figure 4.3.19: A one hour light pulse does not shift the phase of the molecular clock if the pulse is given when the concentration of PER protein is low. The time is plotted in hours on the abscissa and the corresponding concentration with respect to the whole cell volume is plotted on the ordinate.

In Figure 4.3.20, we see the phase response curves for both models where we choose (4.3.17) with $c = 1$ and correspondingly $\mu = 2$ and $\gamma = 2.5$. The difference of the phase is given in hours where we subtract the time of the peak of the concentration of *per* mRNA from the perturbed model between $t = 85$ and $t = 95$ from the time of the peak of the concentration of *per* mRNA from the unperturbed model (4.3.1) to (4.3.5) between $t = 80$ and $t = 90$. The maximum of concentration is detected by the Mathematica function FindArgMax. Phase response curves are known from experiments and given for example in [46, 42, 45]. Furthermore, the peak of the concentration of *per* mRNA is about 5 hours ahead of the maximum concentration of P_0, see Figure 4.3.2 for instance. Therefore, in the case of the mammalian model we shift t_0 by 5 hours such that we are in the same phase with the fly model in order to compare both phase response curves more easily in one figure. We remark that our theoretical phase response curves have the same qualitative course as experimental curves and even the order of magnitude of the shift fits well to experimental data.

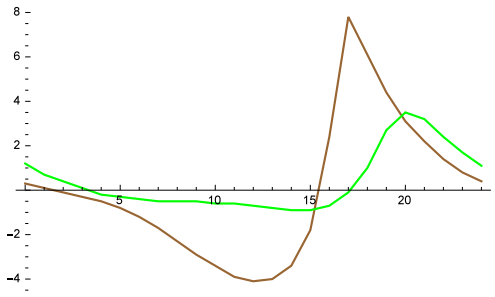

Figure 4.3.20: On the abscissa we have the time t_0 when the external stimulus (4.3.17) for $c = 1$ is given. The model parameters are given as follows $\mu = 2$ and $\gamma = 2.5$. The duration of the external stimulus is one hour. On the ordinate we have the time difference of the maximum peak of M and M^u, that means $\arg\max_{t\in[80,90]} M - \arg\max_{t\in[80,90]} M^u$ where M is calculated from the unperturbed model (4.3.1) to (4.3.5) and M^u once from the fly model, brown curve, and once from the mammalian model, green curve.

Central and peripheral oscillators

In the next experiment, we show that several oscillators can be coupled by our external stimuli framework as follows to further illustrate its range of applicability. A first oscillator reacts to external stimuli in the way as discussed above in this section. A second oscillator receives a signal from the first oscillator that correlates to an agent involved in the first oscillator and thus this signal acts as the "external stimulus" for the second oscillator.

A biological application, which concerns the endogenous clock, of coupled oscillators is the signaling from the suprachiasmatic nucleus (SCN) to the peripheral tissue to synchronize the peripheral clocks [24]. The SCN is a part of the brain of mammals that controls the circadian clock and can be considered as a master clock that entrains the body clocks in peripheral tissue. Our model in this example is as follows. The SCN is the first oscillator and its external stimulus is light, the external stimulus for the peripheral clock, which is the second oscillator, can be hormones, neuronal activity or body temperature. If one of these signals correlates with the occurrence of *per* mRNA or of the (phosphorylated) PER protein, we can couple these two oscillators for example as follows.

We take the basic equations (4.3.1) to (4.3.5), where the first oscillator is sensitive to an external stimulus, that means (4.3.2) is replaced by (4.3.13). The second oscillator with its corresponding agents $\tilde{M}$, $\tilde{P}_0$, $\tilde{P}_1$, $\tilde{P}_2$ and $\tilde{P}_N$ is also modeled by analogous equations as (4.3.1) to (4.3.5) and is coupled to the first by replacing also (4.3.2) by

$$\frac{d}{dt}\tilde{P}_0 = k_s\tilde{M} - V_1\frac{\tilde{P}_0}{K_1+\tilde{P}_0} + V_2\frac{\tilde{P}_1}{K_2+\tilde{P}_1} - \tilde{\mu}\tilde{P}_0P_0 \tag{4.3.18}$$

with $\tilde{\mu} > 0$. That means there is a degradation of $\tilde{P}_0$ if the concentration of P_0 and $\tilde{P}_0$ is high at the same time. The concentration of P_0 is transmitted by for example some signaling pathway to the second oscillator. More specific, the degradation of $\tilde{P}_0$ correlates to a high concentration of P_0 and $\tilde{P}_0$ at the same time. In Figure 4.3.21, we see that the second oscillator is synchronized to a phase shift of π compared to the first one after the transient.

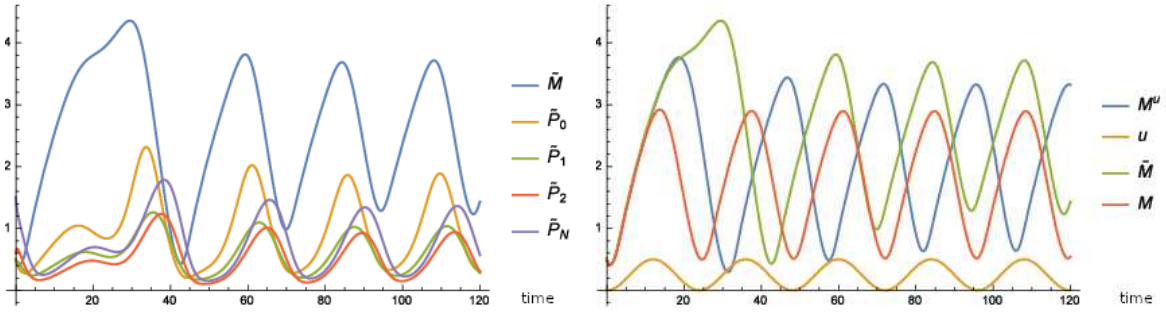

(a) Time curves of the second oscillator where the agents $\tilde{M}$, $\tilde{P}_0$, $\tilde{P}_1$, $\tilde{P}_2$ and $\tilde{P}_N$ fulfill analog equations corresponding to (4.3.1) to (4.3.5) where (4.3.2) is replaced by (4.3.18) and $\tilde{\mu} = 0.5$.

(b) Time curve of the external stimulus u defined in (4.3.12), of M calculated from the model (4.3.1) to (4.3.5), of $\tilde{M}$ calculated by an analogous model like (4.3.1) to (4.3.5) where (4.3.2) is replaced by (4.3.18) with $\tilde{\mu} = 0.5$ and of M^u calculated from (4.3.1) to (4.3.5) where (4.3.2) is replaced by (4.3.13) with $\mu = 1$ for (4.3.12).

Figure 4.3.21: A peripheral oscillator coupled with a phase shift of π to the molecular clock. The time is plotted in hours on the abscissa and the corresponding concentration with respect to the whole cell volume is plotted on the ordinate.

A synchronization which no phase shift can be achieved by the following model

$$\frac{d}{dt}\tilde{P}_0 = k_s\tilde{M} - V_1\frac{\tilde{P}_0}{K_1 + \tilde{P}_0} + V_2\frac{\tilde{P}_1}{K_2 + \tilde{P}_1} - \tilde{\mu}\tilde{P}_0\exp\left(-\beta P_0\right) \tag{4.3.19}$$

where $\beta > 0$. Here, in this model, a higher concentration of P_0 causes a lesser degradation of $\tilde{P}_0$, where the concentration of P_0 is transmitted by some signaling pathway to the second oscillator for example. More specific, a lesser degradation of $\tilde{P}_0$ correlates to a higher concentration of P_0. In Figure 4.3.22, we see the synchronization of both oscillators with a shift of 0 after the transient.

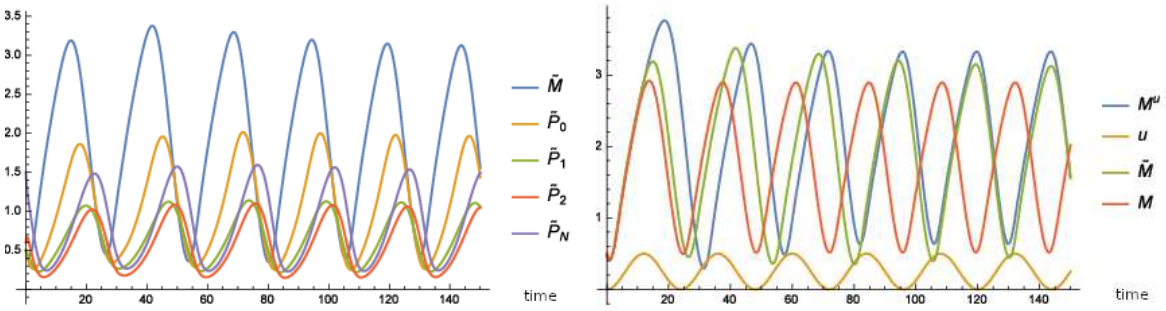

(a) Time curves of the second oscillator where the agents $\tilde{M}$, $\tilde{P}_0$, $\tilde{P}_1$, $\tilde{P}_2$ and $\tilde{P}_N$ fulfill analog equations corresponding to (4.3.1) to (4.3.5) where (4.3.2) is replaced by (4.3.19) with $\tilde{\mu} = 0.5$, $\beta = 2$.

(b) Time curve of the external stimulus u defined in (4.3.12), of M calculated from the model (4.3.1) to (4.3.5), of $\tilde{M}$ calculated by an analogous model like (4.3.1) to (4.3.5) where (4.3.2) is replaced by (4.3.19) with $\tilde{\mu} = 0.5$, $\beta = 2$ and of M^u calculated from (4.3.1) to (4.3.5) where (4.3.2) is replaced by (4.3.13) with $\mu = 1$ for (4.3.12).

Figure 4.3.22: A peripheral oscillator coupled in phase to the molecular clock. The time is plotted in hours on the abscissa and the corresponding concentration with respect to the whole cell volume is plotted on the ordinate.

If we take the model of two coupled oscillators mentioned above and replace (4.3.18) by

$$\frac{d}{dt}\tilde{P}_0^p = k_s\tilde{M} - V_1\frac{\tilde{P}_0^p}{K_1 + \tilde{P}_0^p} + V_2\frac{\tilde{P}_1^p}{K_2 + \tilde{P}_1^p} - \mu^P\tilde{P}_0^p P_2, \tag{4.3.20}$$

where the additional decay of $\tilde{P}_0^p$ depends on the product of $\tilde{P}_0^p$ and P_2 instead of $\tilde{P}_0$ and P_0 as in (4.3.18), then we can see in Figure 4.3.23 that the shift of P_2 compared to P_0 provides a system of

two coupled oscillators where the shift of phase can have more values than just inphase courses, i.e. a phase shift of 0, see Figure 4.3.22 or anti phase courses, i.e. a phase shift of π, see Figure 4.3.21. By this mechanism of coupling different oscillators, nature might create peripheral endogenous clocks which have peaks of the concentrations of certain quantities with any fixed shift of phase to the SCN that appears advantageous.

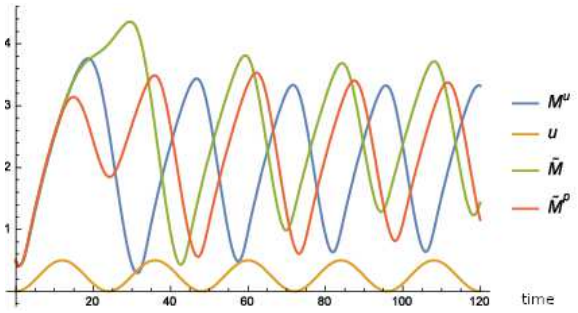

Figure 4.3.23: Time curve of the external stimulus u defined in (4.3.12) where M^u and $\tilde{M}$ are calculated as in Figure 4.3.21. The quantity $\tilde{M}^p$ is calculated by an analogous model as $\tilde{M}$ where (4.3.18) is replaced by (4.3.20) with $\mu^P = 0.5$. After the transient, we have a shift of about 12.7 hours between M^u and $\tilde{M}$ and of about 15.8 hours between M^u and $\tilde{M}^p$. The time is plotted in hours on the abscissa and the corresponding concentration with respect to the whole cell volume is plotted on the ordinate.

Food entrained peripheral clocks

Now, we illustrate the discussion above with the following example. The SCN synchronizes the phase of liver cells to its phase where food intake for example can cause a further shift of the phase of the liver cells' clocks for instance. For the experimental evidence see, [16] or [24]. We choose the model that is used for the experiment depicted in Figure 4.3.22. Furthermore, we equip (4.3.19) with an additional term that models the stimulus that is caused by the food intake as follows

$$\frac{d}{dt}\tilde{P}_0 = k_s\tilde{M} - V_1\frac{\tilde{P}_0}{K_1+\tilde{P}_0} + V_2\frac{\tilde{P}_1}{K_2+\tilde{P}_1} - \tilde{\mu}\tilde{P}_0\exp\left(-\beta P_0\right) - \nu\tilde{u}\tilde{P}_0 \tag{4.3.21}$$

with $\nu > 0$ where the external stimulus is given by

$$\tilde{u}\left(t\right) := \begin{cases} \frac{1}{4}\left(\cos\left(2\pi\frac{t}{24}+\tilde{\varphi}\right)+1\right) & \text{if } t \leq \tilde{t} \\ u\left(t\right) & \text{else} \end{cases} \tag{4.3.22}$$

with $u\left(t\right)$ defined (4.3.12) and $\tilde{t} > 0$. Equation (4.3.21) induces a degradation of $\tilde{P}_0$ by the term $-\nu\tilde{u}\tilde{P}_0$. More specific, the model considers the case that food intake correlates with a degradation of $\tilde{P}_0$. We choose the external stimulus u such that it is inphase with the SCN, that means $\varphi = 0$ in (4.3.12) which models day light. Now we choose $\tilde{\varphi} = \pi$ as food intake is supposed to happen at night instead of the day which corresponds to $\tilde{\varphi} = 0$. That means that until $\tilde{t}$ food intake happens at night and after $\tilde{t}$ food intake is at day time.

In Figure 4.3.24 we only depict the time curves for *per* mRNA to keep the figure clear for $\tilde{t} = 160$. We see that the phase of the peripheral clock ($\tilde{M}$) is shifted by about 6 hours after the transient compared to the phase of the central clock (M^u). When the food intake takes place again at day time as in Figure 4.3.24 after $t = 160$, i.e. there is no shift between u and $\tilde{u}$, then the peripheral clock is synchronized with the SCN again after a transient of about 1 day.

The behavior of the peripheral oscillator can be interpreted as follows. All the external stimuli or signal inputs, respectively, are integrated by the peripheral clock and based on that input information and the weight of the corresponding input information the cell makes a decision when the best time is to be active to do its intended task in the organism. Reacting on different external stimuli at the same time according to a mechanism mentioned above in (4.3.21) can also be seen as making a compromise to meet all the circumstances at the same time that correspond to the simultaneously emerging external stimuli.

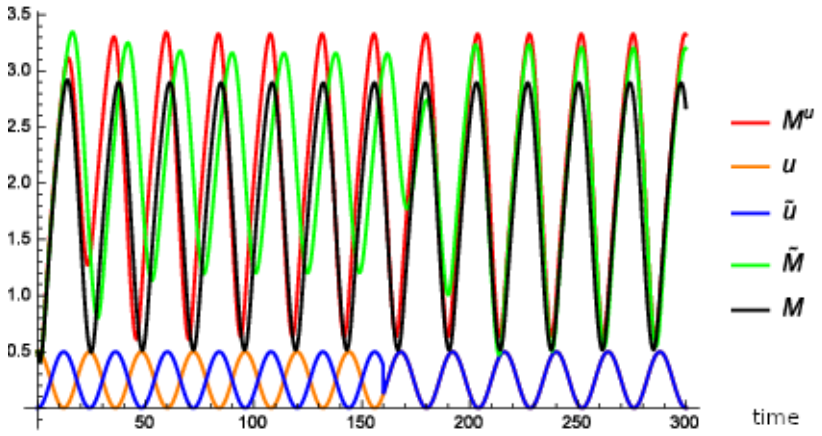

Figure 4.3.24: Time curve of the external stimulus u defined in (4.3.12) and $\tilde{u}$ defined in (4.3.22) with $\tilde{t} = 160$ and $\tilde{\varphi} = \pi$, of M calculated from the model (4.3.1) to (4.3.5), of $\tilde{M}$ calculated by an analogous model like (4.3.1) to (4.3.5) where (4.3.2) is replaced by (4.3.21) with $\tilde{\mu} = 0.3$, $\beta = 2$, $\nu = 0.4$ and of M^u calculated from (4.3.1) to (4.3.5) where (4.3.2) is replaced by (4.3.13) with $\mu = 1$ for (4.3.12) with $\varphi = 0$. The time is plotted in hours on the abscissa and the corresponding concentration with respect to the whole cell volume is plotted on the ordinate.

Notice that the closer $\tilde{\varphi}$ is to φ the smaller the shift of the phases of the two oscillators is and the stronger the stimulus $\tilde{u}$ is the closer the shift of the phases of the two oscillators comes to the phase shift between u and $\tilde{u}$.

Point of singularity

Our framework also provides an explanation for the effects called point of singularity by a principle mechanism. The point of singularity describes the phenomena that one pulse of light can stop the rhythmical behavior of a plant and another pulse of light can restart it again, see [18] for further reading. The following two basic mathematical concepts can be used for explaining this.

The first possibility is to use a macroscopic model that describes a population of microscopic oscillators as a single macroscopic oscillator. To describe the point of singularity the corresponding equations have to contain a point of rest, sometimes called steady state. The discussion in this case is the same as for the system of equations in Chapter 4 for the special choice of equations that are used to model regulatory networks. Further see Section 8.1 in the appendix for a discussion about the characterization of steady states. If the external stimulus brings the system sufficiently close to such a steady state, then the system converges to that point of rest when time evolves. This means that at this special point the values of the agents' concentration are such that their alteration with respect to time is (almost) zero and thus there are no oscillations anymore. If a second pulse of an external stimulus brings the system sufficiently away from that steady state, the oscillations start again. However, in our model based on (4.3.1) to (4.3.5) we have not observed such a behavior.

A second possibility to describe the effect of singularity is to consider several microscopic oscillators whose output then is added up to a macroscopic oscillation. The key is that these microscopic oscillators are coupled inhomogeneously to the external stimulus that means that each coupling constant defers a little bit. This can be for instance because the cells are exposed differently to light because they are covered differently by tissue.

For our experiment we take five oscillators according to (4.3.1) to (4.3.5) where (4.3.2) is replaced by (4.3.13) with $\mu_1 = 0.1$, $\mu_2 = 0.7$, $\mu_3 = 1.1$, $\mu_4 = 1.5$ and $\mu_5 = 2$ for the corresponding oscillator. All oscillators start with the same initial values and thus have the same phase at the beginning. We give four pulses of light. The first one (in hours) at $t_1 = 40$ with the intensity of 2 units, second one at $t_2 = 149$ with the intensity of 5 units, third one at $t_3 = 210$ with intensity of 2 units and the fourth one at $t_4 = 290$ with intensity of 5 units. Since the coupling to the external stimulus is different for each oscillator, the phase shift caused by the light is also different and thus the oscillators are phase shifted to each other. Then the total macroscopic oscillation is weaker as the microscopic

oscillators have different phases and thus the addition of all outputs provides a smaller amplitude of the macroscopic oscillator. The reason for this that some microscopic oscillators are at the lowest point of their oscillation and others are at their highest point. A second pulse brings all the microscopic oscillators to approximately to the same phase again such that the macroscopic oscillation increases or even has the initial amplitude, respectively. This works because the microscopic oscillators are all influenced differently according to their current phase at the time when the second pulse of the external stimulus is given such that all the microscopic oscillators are (almost) in the same phase again. In Figure 4.3.25 we see that the macroscopic oscillation decreases after the first pulse, maybe below a threshold such that it has no effect on the corresponding organism, and increases after the second pulse. Analogously for the third and forth pulse.

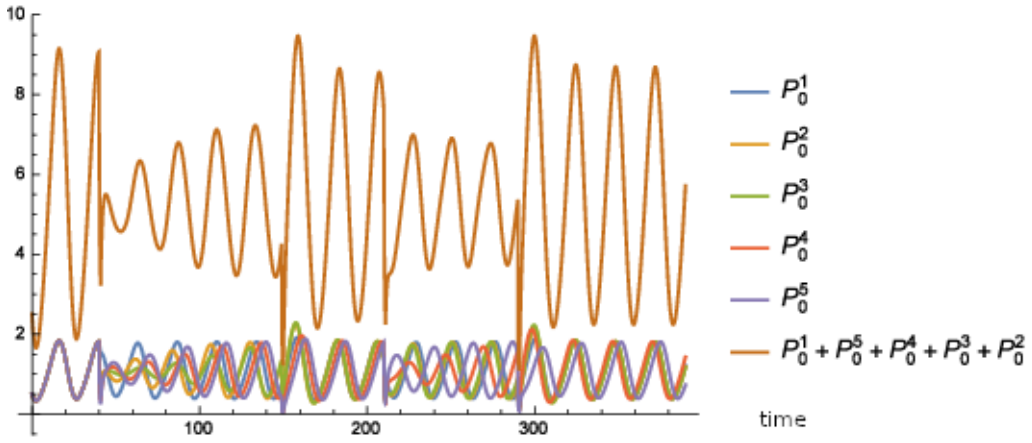

Figure 4.3.25: Five oscillators, each oscillators is described by equations analogous to (4.3.1) to (4.3.5) where (4.3.2) is replaced by (4.3.13) and are coupled differently to light. The PER concentration P_0^i, $i \in \{1, ..., 5\}$ of each microscopic oscillator is on the ordinate as well as the oscillation of the macroscopic oscillator where all the amplitudes of all microscopic oscillators are added up. The time is on the abscissa.

We remark that the pulse 1 and 3 have no effect if the concentration of P_0 is low according to the discussion about the phase response curves above. Furthermore if the intensity of the pulse is too weak, then the shift of the single phases is that weak that the the macroscopic oscillations does not increase noticeably. However if the external stimulus is not too weak, then the increasing of the corresponding duration of application can provide the same effect as an external stimulus with a high intensity shortly applied, see Figure 4.3.26 where pulse 1 and 3 have the intensity of 1 unit and applied for 1 hour and in Figure 4.3.27 applied for 2 hours. The other two pulses are as in the first experiment.

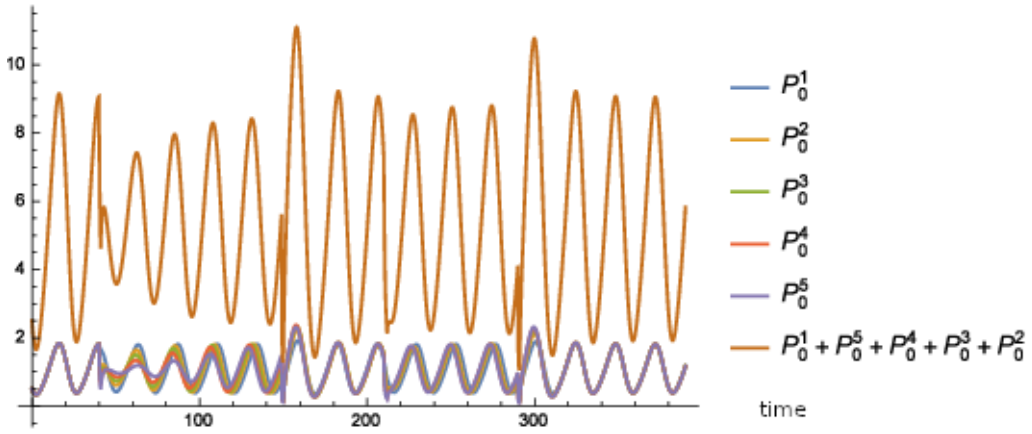

Figure 4.3.26: Five oscillators, each oscillators is described by equations analogous to (4.3.1) to (4.3.5) where (4.3.2) is replaced by (4.3.13) and are coupled differently to light. The PER concentration P_0^i, $i \in \{1, ..., 5\}$ of each microscopic oscillator is on the ordinate as well as the oscillation of the macroscopic oscillator where all the amplitudes of all microscopic oscillators are added up. The time is on the abscissa. The weak external stimulus is applied for one hour.

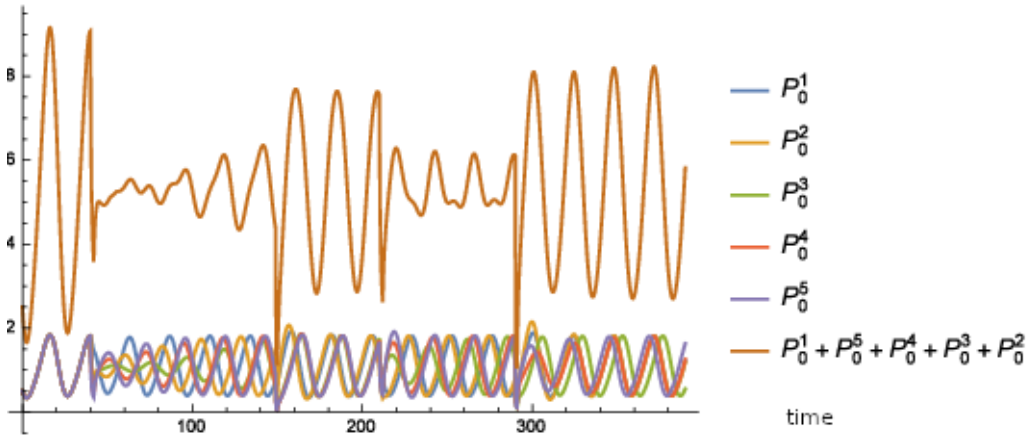

Figure 4.3.27: Five oscillators, each oscillators is described by equations analogous to (4.3.1) to (4.3.5) where (4.3.2) is replaced by (4.3.13) and are coupled differently to light. The PER concentration P_0^i, $i \in \{1, ..., 5\}$ of each microscopic oscillator is on the ordinate as well as the oscillation of the macroscopic oscillator where all the amplitudes of all microscopic oscillators are added up. The time is on the abscissa. The weak external stimulus is applied for two hours.

Chapter 5

Pharmacological intervention as an optimization problem

In the previous sections, we have seen how external stimuli can effectively be included into equations that model biological systems and further how to implement the external stimuli in real biological frameworks. Usually the application of external stimuli to a biological system is connected with a certain purpose. A common task is to find external stimuli that trigger a desired behavior of the biological system. Besides experiments, calculations and simulations are a useful tool to solve this task. For this purpose a biological system is modeled with mathematical equations that are related to the study question. Once the system is modeled and equipped with our framework of external stimuli, we can interpret the task of finding appropriate external stimuli as a mathematical optimal control problem. This represents a systematical way of finding external stimuli that steer the network to the desired state by the virtue of optimization methods that are available to solve mathematical optimal control problems. By this method, the information that is contained in the mathematical equations that have been set up from measurement data can be efficiently exploited. In this section, we show how to set up a mathematical optimal control problem to find external stimuli that steer the network to a desired state and how to solve it numerically to determine the external stimuli sought. This general framework can then be used to figure out optimal drug targets or drug combinations that serve as a treatment where beneficial effects are maximized while side effects are reduced. This method is not restricted to the models proposed in Section 4 but for any well defined system of ordinary differential equations.

5.1 The switch between two different steady states

In this section we present a method how to systematically calculate external stimuli that cause a switch from an initial steady state of the regulatory network to another. That means although the external stimuli are switched off, the expression pattern remains in the new steady state. For the following discussion we assume that the regulatory network is modeled with equations that are analog to the ones discussed in Section 4.1 and Section 4.2. This section is based on [10, Section 3].

5.1.1 The mathematical formulation

In this section we present how to formulate a mathematical optimal control problem from our task to calculate stimuli that steer the regulatory network into a new steady state. For this purpose a given set of nodes is modulated such that a desired network state is achieved. Specifically, we present a way how to calculate external stimuli which are able to switch the regulatory network from one steady state to another.

Let $x_0 := \begin{pmatrix} x_1^0 \\ \vdots \\ x_n^0 \end{pmatrix} \in \mathbb{R}^n$, $n \in \mathbb{N}$ denote the steady state in which our regulatory network starts and

let $x_d \coloneqq \begin{pmatrix} x_1^d \\ \vdots \\ x_n^d \end{pmatrix} \in \mathbb{R}^n$ denote the steady state in which we desire our regulatory network to be. We consider x_d as a constant function over time. To track the desired steady state x_d with the activity level x_k within a time horizon $T > 0$ we use a function that is the smaller the better the activity level fits to the desired steady state. For this purpose we introduce the following sum of integrals

$$\frac{1}{2}\sum_{k=1}^{n}\int_0^T \left(x_k(t) - x_k^d\right)^2 dt. \tag{5.1.1}$$

The smaller the sum of integrals of the term (5.1.1) is, the faster each activity level x_k reaches its desired steady state x_k^d by the action of our external stimuli. Similar, we introduce a term that is the smaller the less external stimuli are used as follows

$$\sum_{j=1}^{m}\int_0^T u_j(t)\, dt. \tag{5.1.2}$$

The smaller the sum of integrals of term (5.1.2) is, the less external stimuli are needed for switching the steady states, both the number of different external stimuli and the time they are applied to the network. By construction, without any external stimuli, the regulatory network rests in the steady state x_0. If we multiply (5.1.2) by $\alpha > 0$ and add it to (5.1.1), we obtain

$$J(x,u) \coloneqq \frac{1}{2}\sum_{k=1}^{n}\int_0^T \left(x_k(t) - x_k^d\right)^2 dt + \alpha\sum_{j=1}^{m}\int_0^T u_j(t)\, dt \tag{5.1.3}$$

where $x \coloneqq \begin{pmatrix} x_1 \\ \vdots \\ x_n \end{pmatrix}$ and $u \coloneqq \begin{pmatrix} u_1 \\ \vdots \\ u_m \end{pmatrix}$. The constant α weights which term of (5.1.3) is more important to be little. If α is big, then it is more important to use few external stimuli than to steer the regulatory network to x_d. Consequently, increasing α can result into the desired behavior of reducing the number of external stimuli while always bringing the network into the desired steady state. However it can happen when α is too big, that the external stimuli are calculated as constant zero functions for all times and the regulatory network remains in its initial steady state because its too costly to have non-zero external stimuli which have the desired perturbation on the network. On the other hand, little α makes it more important that the regulatory network is steered from x_0 to x_d while the number of non-zero external stimuli might be too many for experimental realization.

Minimizing (5.1.3) means to bring the regulatory network from the initial point of rest x_0 as close to the desired state x_d as possible, in the best case to the desired steady state x_d, while using as few external stimuli as possible subject to the constraint $\frac{d}{dt}x_k = f_k(x,u)$, $x_k(0) = x_k^0$ for all $k \in \{1,...,n\}$ and for $t \in (0,T)$ where $f_k(x,u)$ is the right hand-side of one of the models proposed in Section 4, that is (4.2.1), (4.2.2), (4.2.3) and (4.2.4), for example

$$f_k(x,u) \coloneqq \frac{-\mathrm{e}^{\frac{1}{2}h} + \mathrm{e}^{-h\left(\omega_k - \frac{1}{2}\right)}}{\left(1 - \mathrm{e}^{\frac{1}{2}h}\right)\left(1 + \mathrm{e}^{-h\left(\omega_k - \frac{1}{2}\right)}\right)} - \gamma_k x_k + \sum_{j=1}^{m}\sigma_{kj}u_j(1 - x_k) - \sum_{j=1}^{m}\eta_{kj}u_j x_k.$$

We remark that our considerations in this section hold also in the case where $f_k(x,u)$ is the right hand side of any well defined system of ordinary differential equations.

Roughly spoken, the larger T is and the smaller α is, the more it is important, that we obtain external stimuli which steer the regulatory network from the initial steady state to the desired one, according to (5.1.3). Finally, the mathematical formulation of the problem above is as follows.

Minimize (5.1.3) such that

$$\frac{d}{dt}x_k = f_k(x,u),\ x_k(0) = x_k^0 \tag{5.1.4}$$

is fulfilled for all $k \in \{1, ..., n\}$ which reads in mathematical terms as follows

$$\begin{aligned} &\min_{x,u} J(x,u) \\ &\text{such that } \frac{d}{dt}x_k = f_k(x,u), x_k(0) = x_k^0 \text{ for all k} \in \{1, ..., \text{n}\} \end{aligned} \tag{5.1.5}$$

and is called optimal control problem.

5.1.2 A first-discretize-then-optimize approach with a gradient method

The formulation in Subsection 5.1.1 is for continuous functions. In order to find a solution to (5.1.5), one possibility is that we can first discretize the time interval $[0, T]$ and then find a solution to the discretized optimal control problem (5.1.5). The discretization works as follows. We have $t = l\triangle t$ where $\triangle t > 0$ is the time step, $l \in \{0, ..., N\}$ and $T = N\triangle t$. We discretize the ordinary differential equation $\frac{d}{dt}x_k = f_k(x,u)$ with the following explicit Euler scheme for each node k, see [13] for details about discretizing and solving ordinary differential equations numerically. This means that $\frac{d}{dt}x_k = f_k(x,u)$ is approximated by $\frac{x_k^{l+1} - x_k^l}{\triangle t} = f_k\left(x^l, u^l\right)$ for each k where $x^l := \begin{pmatrix} x_1^l \\ \vdots \\ x_n^l \end{pmatrix}$, $u^l := \begin{pmatrix} u_1^l \\ \vdots \\ u_m^l \end{pmatrix}$ and x_k^l denotes the approximation to $x_k(ldt)$ for all $k \in \{1, ..., n\}$ and u_j^l denotes the approximation to or $u_j(ldt)$ for all $j \in \{1, ..., m\}$. Considering $\frac{d}{dt}x_k = f_k(x,u)$ with the initial value x_0 in its discretized form $\frac{x_k^{l+1} - x_k^l}{\triangle t} = f_k\left(x^l, u^l\right)$ we obtain the following system of equations

$$\begin{aligned} x_k^1 &= x_k^0 + \triangle t f_k\left(x^0, u^0\right) \\ x_k^2 &= x_k^1 + \triangle t f_k\left(x^1, u^1\right) \\ &\vdots \\ x_k^N &= x_k^{N-1} + \triangle t f_k\left(x^{N-1}, u^{N-1}\right) \end{aligned} \tag{5.1.6}$$

for every $k \in \{1, ..., n\}$. In the discretized framework, x_k is not a function any more but a vector $x_k := \begin{pmatrix} x_k^1 \\ \vdots \\ x_k^N \end{pmatrix} \in \mathbb{R}^N$ for all $k \in \{1, ..., n\}$ and $x := \begin{pmatrix} x_1 \\ \vdots \\ x_n \end{pmatrix} \in \mathbb{R}^{nN}$. Analogously, the vector $u_j := \begin{pmatrix} u_j^0 \\ \vdots \\ u_j^{N-1} \end{pmatrix} \in \mathbb{R}^N$ and $u := \begin{pmatrix} u_1 \\ \vdots \\ u_m \end{pmatrix} \in \mathbb{R}^{mN}$. If we define

$$F_k(x,u) := -\begin{pmatrix} x_k^1 \\ \vdots \\ x_k^N \end{pmatrix} + \begin{pmatrix} x_k^0 \\ \vdots \\ x_k^{N-1} \end{pmatrix} + \triangle t \begin{pmatrix} f_k\left(x^0, u^0\right) \\ \vdots \\ f_k\left(x^{N-1}, u^{N-1}\right) \end{pmatrix} \in \mathbb{R}^N,$$

then (5.1.6) can be written as $F_k(x,u) = 0$ for all $k \in \{1, ..., n\}$. Discretizing the integrals in (5.1.3) with the Riemann sum [2], we obtain the following discretized optimization problem

$$\begin{aligned} &\min_{x,u} J(x,u) := \frac{1}{2}\sum_{k=1}^{n}\sum_{l=1}^{N}\left(x_k^l - x_k^d\right)^2 \triangle t + \alpha\sum_{j=1}^{m}\sum_{l=0}^{N-1} u_j^l \triangle t \\ &\text{such that } F(x,u) = 0,\ x^0 = x_0 \\ &u \in U_{ad} \end{aligned} \tag{5.1.7}$$

where $F(x,u) := \begin{pmatrix} F_1(x,u) \\ \vdots \\ F_n(x,u) \end{pmatrix} \in \mathbb{R}^{nN}$ and

$$U_{ad} := \left\{u \in \mathbb{R}^{mN} |\ 0 \le u_j^l \le 1 \text{ for all } j \in \{1, ..., m\} \text{ and } l \in \{0, ..., N-1\}\right\}$$

which means that all components of u are constraint according to the definition of the external stimuli u_j in Section 4.2.

One method to determine the external stimuli u which solve (5.1.7), a so called optimal solution to (5.1.7), is the Lagrange approach, see text books about mathematical optimization or Lagrange optimization like [27, 5] for details. For this purpose, we have to formulate the Lagrange function which reads as follows

$$L(x,u,p) \coloneqq \frac{1}{2}\sum_{k=1}^{n}\sum_{l=1}^{N}\left(x_k^l - x_k^d\right)^2 \triangle t + \alpha\sum_{j=1}^{m}\sum_{l=0}^{N-1} u_j^l \triangle t + \sum_{k=1}^{n} p_k^T F_k(x,u)\triangle t \tag{5.1.8}$$

where $p \coloneqq \begin{pmatrix} p_1 \\ \vdots \\ p_n \end{pmatrix} \in \mathbb{R}^{nN}$, $p_k \coloneqq \begin{pmatrix} p_k^1 \\ \vdots \\ p_k^N \end{pmatrix} \in \mathbb{R}^N$, $k \in \{1,...,n\}$ is a vector of so called Lagrange multipliers and $p_k^T F_k$ is the Euclidean scalar product of the vectors p_k and F_k for all $k \in \{1,...,n\}$. The Euclidean scalar product for two vectors $v, w \in \mathbb{R}^n$ is defined by $v^T w \coloneqq \sum_{i=1}^{n} v_i w_i$.

Before we proceed, we introduce some symbols. We use the following scalar product for the following calculations. We have $(v,w) \coloneqq \sum_{k=1}^{n}\sum_{l=1}^{N} v_k^l w_k^l \triangle t$ for any $v, w \in \mathbb{R}^{nN}$. Analogously for vectors $v, w \in \mathbb{R}^{mN}$. The gradient of the Lagrange function L with respect to p is denoted by

$$\nabla_p L = \frac{1}{\triangle t}\begin{pmatrix} \frac{\partial}{\partial p_1^1}L(x,u,p) \\ \frac{\partial}{\partial p_1^2}L(x,u,p) \\ \vdots \\ \frac{\partial}{\partial p_n^N}L(x,u,p) \end{pmatrix} \in \mathbb{R}^{nN},$$

see [2] for details about the connection between gradient and derivative. Analogously, the gradient of the Lagrange function L with respect to x is denoted by

$$\nabla_x L = \frac{1}{\triangle t}\begin{pmatrix} \frac{\partial}{\partial x_1^1}L(x,u,p) \\ \frac{\partial}{\partial x_1^2}L(x,u,p) \\ \vdots \\ \frac{\partial}{\partial x_n^N}L(x,u,p) \end{pmatrix} \in \mathbb{R}^{nN}$$

and the gradient of the Lagrange function L with respect to u is denoted by

$$\nabla_u L = \frac{1}{\triangle t}\begin{pmatrix} \frac{\partial}{\partial u_1^0}L(x,u,p) \\ \frac{\partial}{\partial u_1^1}L(x,u,p) \\ \vdots \\ \frac{\partial}{\partial u_m^{N-1}}L(x,u,p) \end{pmatrix} \in \mathbb{R}^{mN}.$$

Applying these formulas to the Lagrange function (5.1.8), we calculate the gradients for the Lagrange formalism that can be found in [5] for instance. We have

$$\nabla_p L(x,u,p) = F(x,u).$$

Next, we have

$$\nabla_x L(x,u,p) = \begin{pmatrix} \nabla_{x_1} L(x,u,p) \\ \vdots \\ \nabla_{x_n} L(x,u,p) \end{pmatrix}$$

where

$$\nabla_{x_k} L(x,u,p) = \begin{pmatrix} x_k^1 - x_k^d - p_k^1 + p_k^2 + \sum_{i=1}^{n} p_i^2 \frac{\partial}{\partial x_k^1} f_i\left(x^1,u^1\right)\triangle t \\ x_k^2 - x_k^d - p_k^2 + p_k^3 + \sum_{i=1}^{n} p_i^3 \frac{\partial}{\partial x_k^2} f_i\left(x^2,u^2\right)\triangle t \\ \vdots \\ x_k^{N-1} - x_k^d - p_k^{N-1} + p_k^N + \sum_{i=1}^{n} p_i^N \frac{\partial}{\partial x_k^{N-1}} f_i\left(x^{N-1},u^{N-1}\right)\triangle t \\ x_k^N - x_k^d - p_k^N \end{pmatrix} \in \mathbb{R}^N \tag{5.1.9}$$

for all $k \in \{1, ..., n\}$. Notice that $\frac{\partial}{\partial x_k^1} f_i = ... = \frac{\partial}{\partial x_k^{N-1}} f_i$ holds for the derivatives in (5.1.9) if considered as functions from $\mathbb{R}^n \times \mathbb{R}^m$ to $\mathbb{R}$. Finally, we have

$$\nabla_u L(x, u, p) = \begin{pmatrix} \nabla_{u_1} L(x, u, p) \\ \vdots \\ \nabla_{u_m} L(x, u, p) \end{pmatrix}$$

where

$$\nabla_{u_j} L(x, u, p) = \begin{pmatrix} \alpha + \sum_{i=1}^n p_i^1 \frac{\partial}{\partial u_j^0} f_i\left(x^0, u^0\right) \triangle t \\ \vdots \\ \alpha + \sum_{i=1}^n p_i^N \frac{\partial}{\partial u_j^{N-1}} f_i\left(x^{N-1}, u^{N-1}\right) \triangle t \end{pmatrix} \in \mathbb{R}^N \tag{5.1.10}$$

for all $j \in \{1, ..., m\}$. Notice that $\frac{\partial}{\partial u_j^1} f_i = ... = \frac{\partial}{\partial u_j^{N-1}} f_i$ holds for the derivatives in (5.1.10) if considered as functions from $\mathbb{R}^n \times \mathbb{R}^m$ to $\mathbb{R}$.

Following the Lagrange approach as in [5] for instance to determine a solution u of (5.1.7) and thus the desired external stimuli, we have to solve the following system of equations, see also [27, 1.5] for example,

$$\nabla_p L(x, u, p) = 0 \tag{5.1.11}$$

$$\nabla_x L(x, u, p) = 0 \tag{5.1.12}$$

$$\nabla_u L(x, u, p)^T (\tilde{u} - u) \geq 0 \text{ for all } \tilde{u} \in U_{ad}. \tag{5.1.13}$$

There are different strategies available to solve the proposed optimization problem by the virtue of necessary equations like (5.1.11) to (5.1.13). In this subsection, we present the projected gradient method to solve (5.1.11) to (5.1.13) numerically. We explain the procedure in the following.

For a given u and as the initial value x_0 is given, Equation (5.1.11) can be solved as follows. We can calculate x_k^1 for all $k \in \{1, ..., n\}$ from the first row of the corresponding $F_k(x, u)$. Then, we can calculate x_k^2 for all $k \in \{1, ..., n\}$ from the second row of the corresponding $F_k(x, u)$. This procedure can be repeated, going forwards through all the rows of the corresponding $F_k(x, u)$ until x_k^N for all $k \in \{1, ..., n\}$ is calculated from the last row of the corresponding $F_k(x, u)$. Analogously, for a given u and x, (5.1.12) can be calculated, however, starting from the last row of $\nabla_{x_k} L(x, u, p)$ to determine the corresponding p_k^N for each $k \in \{1, ..., n\}$ and then going backwards through all the rows of $\nabla_{x_k} L(x, u, p)$ until the corresponding p_k^1 can be calculated from the first row of $\nabla_{x_k} L(x, u, p)$ for all $k \in \{1, ..., n\}$. The vector $\nabla_u L(x, u, p)$ can be assembled for given u, x and p. Any vector $u \in U_{ad}$ which fulfills (5.1.13) for x and p solving simultaneously (5.1.11) and (5.1.12) is a minimizer of the Lagrange function $L(x, u, p)$. Equation (5.1.13) is a generalization of $\nabla_u L(x, u, p) = 0$ at a minimum. The need for the generalization comes from the fact that the vector u is not calculated in $\mathbb{R}^{mN}$, that means we can choose any value for u, but in U_{ad}, where there are restrictions on the choice of the values of u, see [27, Proposition 1.2].

Remark 3. The gradient $\nabla_u L(x, u, p)$ is associated with the gradient $\nabla \hat{J}(u)$ of the reduced target functional $\hat{J}(u) := J(x(u), u)$, see [27, Proof of Theorem 1.17]. Actually, we have that for variations in u, the function $x(u)$ also varies as x and u are connected via (5.1.6). Furthermore, for a given u, the function $x(u)$ can be calculated by $F(x, u) = 0$ as discussed above. The gradient $\nabla \hat{J}(u)$ can be used for any optimization method based on a steepest descent in order to find an optimal control for (5.1.7), like for a nonlinear conjugated gradient (NCG) method or a Broyden-Fletcher–Goldfarb-Shanno (BFGS) method, see [6] for instance. With these methods one can extend the algorithmic part of this work with respect to the calculation of an optimal solution for (5.1.7).

There are various methods to calculate u such that (5.1.13) and simultaneously (5.1.11) and (5.1.12) are fulfilled, see [5, 6, 27]. We choose a projected gradient method that is formulated in Algorithm 5.1 below since it illustrates the algorithmic method how to minimize the target functional in a very

direct way. For this purpose, we define the projection $Pr : \mathbb{R}^m \to \mathbb{R}^m$ of a vector u as follows

$$Pr(u) = \begin{cases} u_j^l & \text{if } 0 < u_j^l < 1 \\ 1 & \text{if } u_j^l \geq 1 \\ 0 & \text{if } u_j^l \leq 0 \end{cases} \quad \text{for all } j \in \{1, ..., m\} \text{ and } l \in \{0, ..., N-1\}.$$

Algorithmus 5.1 Projected gradient method

1. Choose $\sigma \in (0,1)$, ${}^0s = 1$, $\beta_1 \in (0,1)$, $\beta_2 > 1$, $\epsilon > 0$, $\ell = 0$, ${}^0u \in U_{ad}$
2. Calculate ${}^0x$ from (5.1.11) for ${}^0u$ and ${}^0p$ from (5.1.12) for ${}^0x$ and ${}^0u$
3. While $\left({}^\ell u - Pr\left({}^\ell u - \nabla_u L\left({}^\ell x, {}^\ell u, {}^\ell p\right)\right)\right)^T \left({}^\ell u - Pr\left({}^\ell u - \nabla_u L\left({}^\ell x, {}^\ell u, {}^\ell p\right)\right)\right) > \epsilon$
   For ${}^{\ell+1}s = {}^\ell s \cdot \beta_1^q$, $q \in \mathbb{N}_0$, determine the smallest q such that

$$\begin{aligned} &\hat{J}\left(Pr\left({}^\ell u - {}^{\ell+1}s \nabla_u L\left({}^\ell x, {}^\ell u, {}^\ell p\right)\right)\right) \\ &\leq \hat{J}\left({}^\ell u\right) - \sigma \nabla_u L\left({}^\ell x, {}^\ell u, {}^\ell p\right)^T \left({}^\ell u - Pr\left({}^\ell u - {}^{\ell+1}s \nabla_u L\left({}^\ell x, {}^\ell u, {}^\ell p\right)\right)\right) \end{aligned}$$

   is fulfilled.
   Set ${}^{\ell+1}u = Pr\left({}^\ell u - {}^{\ell+1}s \nabla_u L\left({}^\ell x, {}^\ell u, {}^\ell p\right)\right)$
   Calculate ${}^{\ell+1}x$ from (5.1.11) for ${}^{\ell+1}u$ and ${}^{\ell+1}p$ from (5.1.12) for ${}^{\ell+1}x$ and ${}^{\ell+1}u$
   Set ${}^{\ell+1}s = \beta_2 {}^{\ell+1}s$
   Set $\ell = \ell + 1$
   End

Algorithm 5.1 iteratively determines a solution to the Equations (5.1.11) to (5.1.13). We give an explanation of Algorithms 5.1. By ${}^\ell x \in \mathbb{R}^{nN}$, ${}^\ell u \in \mathbb{R}^{mN}$ and ${}^\ell p \in \mathbb{R}^{nN}$ we denote the vectors that contain the values for the corresponding vectors x, u and p at the corresponding entry after the ℓ-th iteration of Algorithm 5.1. The parameter ϵ is a measure how close the numerical solution of Algorithm 5.1 is to an analytical solution to the Equations (5.1.11) to (5.1.13). The smaller ϵ is, the closer the numerical solution is to an analytical one but the calculation time increases. Typically, the parameter ϵ ranges between 10^{-3} to 10^{-9}. We recommend $\epsilon = 10^{-4}$ to obtain useful results for the original task to determine external stimuli for pharmacological modulation for example. The step size ${}^\ell s$ is determined such that it is associated with reducing $\hat{J}$. The gradient $\nabla_u L(x, u, p) \in \mathbb{R}^{mN}$ points out in the direction of the steepest ascent of $L(x, u, p)$ or $\hat{J}(u)$, respectively and thus $-\nabla_u L(x, u, p)$ points out in the direction of the steepest descent. The projection of ${}^\ell u - {}^{\ell+1}s \nabla_u L\left({}^\ell x, {}^\ell u, {}^\ell p\right)$ on U_{ad} is needed to ensure that each iterate is in U_{ad} and thus the output of Algorithm 5.1 is in U_{ad} which means that the external stimuli only take values between 0 and 1.

This formulation of a projected gradient method noted in Algorithm 5.1 has the advantage that the step size stays in the size of magnitude from the last iteration. According to our experience the step size stays in the same size of magnitude over several iterations. Therefore, in such a case, our formulation has the advantage that the step size does not have to be found in each iteration from the scratch and thus can save calculation time. Additionally, the step size is adaptively found from an initial guess and varied by slightly enlarging it after each iteration in the case that a greater step size might be suitable and thus generate a greater descent of the target functional. From our experience, we recommend $\sigma = 0.01$, $\beta_1 = 0.1$ and $\beta_2 = 1.1$ for a fast convergence of Algorithm 5.1.

5.1.3 A first-optimize-then-discretize approach with the sequential quadratic Hamiltonian scheme

In this section we provide another algorithm that is different from the projected gradient method for the case that for instance the projected gradient method converges slowly for a special setting consisting of a certain network equipped with external stimuli. For this case an alternative method

is implemented and provided with this work which might perform better in such a case. The method provided with this section is based on the Pontryagin maximum principle (PMP) and is a first optimize then discretize approach.

For this reason we first characterize a solution $(\bar{x}, \bar{u})$ to the optimal control problem (5.1.5) with the PMP, see for example [26, 2.4] for further reading on the PMP. Basic for the PMP is the Hamiltonian $H : \mathbb{R} \times \mathbb{R}^n \times \mathbb{R}^m \times \mathbb{R}^n \to \mathbb{R}$, $(t, x, u, p) \mapsto H(t, x, u, p)$ that is defined as follows

$$H(t, x, u, p) := \frac{1}{2} \sum_{k=1}^{n} \left(x_k - x_k^d \right)^2 + \alpha \sum_{j=1}^{m} u_j + \sum_{k=1}^{n} p_k f_k(x, u)$$

for our problem. The PMP says that it holds

$$H(t, \bar{x}(t), \bar{u}(t), \bar{p}(t)) = \min_{w \in [0,1]^m} H(t, \bar{x}(t), w, \bar{p}(t)) \tag{5.1.14}$$

for almost every $t \in [0, T]$ where the functions $(\bar{x}, \bar{u})$ solve (5.1.5) inserted instead of (x, u). Furthermore, the adjoint variable $\bar{p}$ is given componentwise by the following adjoint equation

$$\frac{d\bar{p}_k}{dt} = -\left(\bar{x}_k - x_k^d \right) - \sum_{i=1}^{n} \bar{p}_i \frac{\partial}{\partial x_k} f_i(\bar{x}, \bar{u}) \tag{5.1.15}$$

with $\bar{p}_k(T) = 0$ for all $k \in \{1, ..., n\}$ where $\frac{\partial}{\partial x_k} f_i(\bar{x}, \bar{u}) := \frac{\partial}{\partial x_k} f_i(x, u)|_{(x,u)=(\bar{x},\bar{u})}$ that means the partial derivative of the i-th component of f with respect to the k-th component of $x := \begin{pmatrix} x_1 \\ \vdots \\ x_n \end{pmatrix} \in \mathbb{R}^n$ evaluated at $(\bar{x}, \bar{u})$.

If one has any solution (x^*, u^*) to (5.1.4), $x(0) = x_0$, then minimizing $H(t, x^*(t), w, p^*(t))$ over $w \in [0, 1]^m$ is related to minimizing the target functional (5.1.3) as [26, 2.4.2] indicates where p^* is a solution to (5.1.15) for x^* and u^* instead of $\bar{x}$ and $\bar{u}$, respectively. This connection is made use of in the sequential quadratic Hamiltonian method, see [8] for instance. For this method, the augmented Hamiltonian is crucial which is given by $K_\epsilon : \mathbb{R} \times \mathbb{R}^n \times \mathbb{R}^m \times \mathbb{R}^m \times \mathbb{R}^n \to \mathbb{R}$, $(t, x, u, v, p) \mapsto K_\epsilon(t, x, u, v, p)$ with $K_\epsilon(t, x, u, v, p) := H(t, x, u, p) + \epsilon \sum_{j=1}^{m} (u_j - v_j)^2$. There are a number of different variants to implement Pontryagin's maximum principle. We use the following that can be found for example in [8] where according to our experience this method converges faster to appropriate results than the projected gradient method.

Algorithmus 5.2 Sequential quadratic Hamiltonian method

1. Choose $\epsilon > 0$, $\kappa > 0$, $\sigma > 1$, $\zeta \in (0, 1)$, $\eta \in (0, \infty)$, $u^0 \in U_{ad}$, compute x^0 with (5.1.4) for $u \leftarrow u^0$ and p^0 from (5.1.15) for $\bar{x} \leftarrow x^0$ and $\bar{u} \leftarrow u^0$, set $l \leftarrow 0$

2. Choose u such that

$$K_\epsilon\left(t, x^l(t), u(t), u^l(t), p^l(t)\right) \leq K_\epsilon\left(t, x^l(t), w, u^l(t), p^l(t)\right)$$

for all $w \in [0, 1]^m$ and all gird points $t \in [0, T]$

3. Calculate x from (5.1.4) for u and $\delta := \|u - u^k\|^2 := \sum_{j=1}^{m} \int_0^T \left(u_j(t) - u_j^l(t) \right)^2 dt$

4. If $J(x, u) - J\left(x^l, u^l\right) > -\eta\delta$: Choose $\epsilon \leftarrow \sigma\epsilon$
Else: Choose $\epsilon \leftarrow \zeta\epsilon$, $x^{l+1} \leftarrow x$, $u^{l+1} \leftarrow u$, calculate p^{l+1} from (5.1.15) for $\bar{x} \leftarrow x^{l+1}$ and $\bar{u} \leftarrow u^{l+1}$, $l \leftarrow l + 1$,

5. If $\delta < \kappa$: STOP and return u^l
Else go to 2.

Algorithm 5.2 works as follows. First, one chooses an initial guess for ϵ, recommended $\epsilon = 0.1$, which weights the deviation from the current u^l to the update where l counts the number of updates to the initial guess u^0, a tolerance κ for the convergence criterion, σ for increasing ϵ, ζ for decreasing ϵ, η for the comparison of the value of the target functional for the current control u^k and its update. We recommend $\sigma = 50$, $\zeta = 0.15$ and $\eta = 10^{-12}$ and $\kappa = 10^{-6}$. With the initial guess for the control u^0 we compute x^0 with (5.1.4), $x^0(0) = x_0$, for all $k \in \{1, ..., n\}$ and u^0 instead of u, we write $\bar{u} \leftarrow u^0$, as well as p^0 with (5.1.15) for x^0 instead of $\bar{x}$, we write $\bar{x} \leftarrow x^0$ and $\bar{u} \leftarrow u^0$. Secondly, we determine the minimum of $K_\epsilon\left(t, x^l, w, u^l, p^l\right)$ for every grid point t which is in our case given by $0 = \frac{\partial}{\partial u_j} K_\epsilon\left(t, x^l, u, u^l, p^l\right)$, where $\frac{\partial}{\partial u_j} K_\epsilon\left(t, x^l, u, u^l, p^l\right)$ is the partial derivative of K_ϵ with respect of the j-th component of the control u in the third argument of K_ϵ. As $\frac{\partial f_i\left(x^l, u\right)}{\partial u_j}$, the partial derivative of the i-th component of f with respect to the j-th component of the control u, does actually not depend on u_j in our case, that is the case if the right hand-side $f_k(x, u)$ of (5.1.4) is one of the following (4.2.1), (4.2.2), (4.2.3) and (4.2.4), for instance, we have, considering the upper and lower bound of u, the update

$$u_j(t) = \max\left(0, \min\left(-\frac{\alpha + \sum_{i=1}^n p_i^l(t) \frac{\partial f_i\left(x^l, u\right)}{\partial u_j}}{2\epsilon} + u_j^l(t), 1\right)\right)$$

for each grid point $t \in [0, T]$ for all $j \in \{1, ..., m\}$ where p_i^l is the i-th component of p^l. In the next step, we calculate x from (5.1.4) for u, $x(0) = x_0$ and the norm $\|u - u^k\|^2$ and set $\delta := \|u - u^k\|^2$. In the forth step, we check if the new update on u provides a smaller value of the target functional by at least $-\eta\delta$. If not, we increase ϵ, else we take the update for the state and control, decrease ϵ and calculate p^l from (5.1.15) with $p^l(T) = 0$, with the new x^l, $\bar{x} \leftarrow x^l$ and u^l, $\bar{u} \leftarrow u^l$. If at a certain iteration δ is less than the tolerance κ, we stop and return the last iterate u^l which has provided a descent of the target functional by at least $-\eta\delta$. We remark that we have to discretize $\|u - u^k\|^2$, (5.1.4) and (5.1.15) for an implementation of Algorithm 5.2. We choose the Riemann sum [2] for $\|u - u^k\|^2$ and an explicit Euler scheme [13] for (5.1.4) and (5.1.15).

5.1.4 Direct method to calculate appropriate external stimuli that induce a switch

In this subsection, we present a method to go systematically through all the combinations of external stimuli in order to find a selection of external stimuli that steers the network into the desired steady state. We recall that $m \in \mathbb{N}$ is the number of external stimuli, $n \in \mathbb{N}$ the number of nodes and T the time horizon within the switch is supposed to happen. The method considers all the elements g of the power set $\mathcal{P}$ of the set $\{1, ..., m\}$ up to a cardinality $|g| \leq \text{maxNum}$ where $\text{maxNum} \in \{1, ..., m\}$. Then for each g, we define the following controls

$$u_j(\eta T) := \begin{cases} 1 & \text{for } 0 \leq t \leq \eta T \\ 0 & \text{else,} \end{cases}$$

$0 < \eta < 1$ for all $j \in g$. For $j \in \{1, ..., m\} \setminus g$, we set $u_j(\eta T) = 0$ for all $0 \leq t \leq T$ and define

$$u(\eta T) := \begin{pmatrix} u_1(\eta T) \\ \vdots \\ u_m(\eta T) \end{pmatrix}. \tag{5.1.16}$$

That means we pick systematically combinations of subsets of the index set $\{1, ..., m\}$ and apply the corresponding controls for a certain period of time starting from $t = 0$ until all the controls are switched off after ηT time units. If the perturbation of the selected external stimuli is successful that means that the state $x(T)$ of the network at the final time T equals the desired state x_d in each component up to a tolerance $\text{tol} > 0$, then we figure out if the switch can be achieved with a shorter period of the controls' application than ηT. For this purpose, we take $u\left(\tau^l \eta T\right)$ with the corresponding state calculated by $\frac{d}{dt} x_k = f\left(x, u\left(\tau^l \eta T\right)\right)$ for all $k \in \{1, ..., n\}$, (5.1.5), or $F\left(x, u\left(\hat{\tau^l} \eta T\right)\right) = 0$, (5.1.7),

respectively, with $0 < \tau < 1$, $\hat{l} \in \mathbb{N}_0$ and enlarge $\hat{l}$ until there is a state of one node, x_k, $k \in \{1, ..., n\}$, for which we have $|x_k(T) - (x_d)_k| \geq \text{tol}$. We note the smallest number where the switch does not happen any more $\hat{l}_s \in \mathbb{N}$. Then we take the duration of application $\tau^{\hat{l}_s - 1}\eta T$ such that we define the control $u\left(\tau^{\hat{l}_s - 1}\eta T\right)$ as the output of the combinatorial method. The method is given as follows.

Algorithmus 5.3 Combinatorial method

1. Choose maxNum $\in \{1, ..., m\}$, $0 < \text{tol} < 1$, $0 < \eta < 1$, $0 < \tau < 1$,
2. Choose all the elements $g \in P \subseteq \mathcal{P}$ of the power set $\mathcal{P}$ of $\{1, ..., m\}$ such that the cardinality $|g| \leq \text{maxNum}$
3. For all $g \in P$
   - Set $u = u(\eta T)$ according to (5.1.16)
   - Calculate x with u from $\frac{d}{dt}x_k = f(x, u)$ for all $k \in \{1, ..., n\}$ defined in (5.1.5) or $F(x, u) = 0$ defined in (5.1.7), respectively
   - If $|x_k(T) - (x_d)_k| < \text{tol}$ for all $k \in \{1, ..., n\}$, return $u\left(\tau^{\hat{l}_s - 1}\eta T\right)$ where $\hat{l}_s \in \mathbb{N}$ is the smallest number such that there is one $k \in \{1, ..., n\}$ with $|x_k(T) - (x_d)_k| \geq \text{tol}$ with $\frac{d}{dt}x_k = f\left(x, u\left(\tau^{\hat{l}_s}\eta T\right)\right)$ for all $k \in \{1, ..., n\}$ or $F\left(x, u\left(\tau^{\hat{l}}\eta T\right)\right) = 0$, respectively

Notice that η is chosen sufficiently small such that after the switch off of the external stimuli there is still enough time for the network to relax sufficiently close to the desired steady state if the selected external stimuli are able to steer the network into the desired steady state as the proposed method does not identify the selected external stimuli as successful ones otherwise. On the other hand η must be sufficiently large that the perturbation can last sufficiently long to activate or inactivate corresponding nodes sufficiently long such that networks inertia effects are overcome.

The advantage of Algorithm 5.3 is that it checks directly if the desired switch is achieved with the chosen set of external stimuli. However, the disadvantage is that it needs exponential time with respect to the number of possible external stimuli. In contrast, Algorithm 5.1 or Algorithm 5.2 are linear in time with respect to the number of possible external stimuli and at most quadratic with respect to the total number of nodes and edges as one has to calculate the Jacobi matrix of f, see for example (5.1.9).

We can combine these methods as follows in order to determine a selection of external stimuli supporting the external stimuli determined by Algorithm 5.3 causing the desired switch. Even for a large number of possible external stimuli, the number of combinations is not too big if maxNum is small. If then Algorithm 5.3 returns a set of external stimuli causing the desired switch, we can use this result as an initial guess for the external stimuli for Algorithm 5.1 or Algorithm 5.2 in order to find more external stimuli supporting the desired switch which can be affected by the weight α in (5.1.3). Roughly spoken, the less α is, the more different external stimuli will be found which are different from constant zero function and the bigger α is, the less different controls are returned being different from zero, but the more important these external stimuli are for the switch. In this case the cardinality of the selection of external stimuli that is returned by Algorithm 5.1 or Algorithm 5.2 does not have to change but some external stimuli may be replaced by one that are more effective with respect to steering the network into the desired steady state. By supporting the desired switch we mean that the network is steered faster to the desired state. That can be useful for dynamical reasons when time matters that means a switch in an experiment is supposed to be accelerated or to enlarge the number of external stimuli a bit to choose that ones that can be implemented in an experimental set up in the easiest way.

There is a further reason why to take the result of Algorithm 5.3 for an initial guess of Algorithm 5.1 or Algorithm 5.2. When solving (5.1.5) or (5.1.7), respectively, in order to find a set of external stimuli which causes the switch from the initial state x_0 to the desired state x_d, it may happen, because

of the highly non-linear constraint F or f_k, respectively, that there is a local optimum of the target functional at which there is a node that does not equal its desired state at the final time. This can happen because Algorithm 5.1 and Algorithm 5.2 are so called local optimization methods and therefore they only determine their result with respect to necessary optimality conditions (5.1.13) or (5.1.14), respectively. However, not all optima in this sense contain a switch of steady states. Thus if the initial value x_0 is close to such a local minimum, it may happen that our utilized local optimization method like projected gradient method or sequential quadratic Hamiltonian method, converges to such a mentioned local optimum. Then, the corresponding external stimuli are optimal in the sense of fulfilling the necessary optimality conditions (5.1.13) or (5.1.14) but may not cause the desired switch. Moreover, varying the initial guess for the external stimuli u in Algorithm 5.1 or Algorithm 5.2 can cause convergence to different local optima and thus, considering even just the local minima containing a desired switch, can result in different selections of active external stimuli. In order to ensure converging a local optimum which includes a switch of the network's state, one can take the result of Algorithm 5.3 where the chosen external stimuli already cause the desired switch. Then this initial guess for the external stimuli is maybe sufficiently close to an optimum where the corresponding state equals the desired state at the final time. Notice that the shorter the time is where the external stimuli are active in the result of Algorithm 5.3 the closer the initial guess is to an optimum that contains the desired switch as the duration of application of the external stimuli enlarges the target functional (5.1.3). For this purpose the subroutine in Algorithm 5.3 to approximate a duration of application of the selected external stimuli causing the desired switch that is as short as possible is necessary.

Furthermore, Algorithm 5.3 returns the first combination of external stimuli that it finds. However, there might be a combination that is more effective for the switch that is more likely to be found from Algorithm 5.1 or Algorithm 5.2, especially for big α. For this reason it is worth to additionally start one of these algorithms with the result of Algorithm 5.3 as an initial guess.

Remark 4. We remark that the time horizon T used in Algorithm 5.1, Algorithm 5.2 and Algorithm 5.3 is supposed to be at least that large as in the steady state analysis in which one figures out the steady states of the considered network in order to ensure that there is enough time for the network to relax into the desired state after the external stimuli are switched off. This is reasonable because the oscillations induced by the switch on and switch off of the external stimuli can decay and the network can relax to the desired state x_d sufficiently much such that $x(T)$ is close to x_d within the tolerance tol for all $k \in \{1, ..., n\}$. Also the step size $\triangle t$ is supposed to be at most that size as the one used in the steady state analysis in order to ensure a stable numerical solution of the underlying differential equations assuming that an explicit solver for the steady state analysis is used.

5.2 External stimuli keeping networks in desired expression patterns

In this section, we introduce a mathematical model for the optimal control of regulatory networks where only the activity level of certain nodes is of interest and not necessarily the expression pattern of the whole network. Furthermore the alteration of the activity levels of the nodes caused by the action of the applied external stimuli may decay after the external stimuli are set off. This is in contrast to Section 5.1 where the external stimuli are always supposed to effect the network such that the alterations of the nodes' activity levels stay although the applied external stimuli are switched off due to the switch between two steady states. An application of this framework in the present section is optimal drug targeting or pharmacological modulation which is discussed later. We assume that the different agents of interests of a real (biological) network are modeled by a regulatory network analogously to Section 4.1 and Section 4.2. Each agent is associated with a node $k \in \{1, ..., n\}$ where $n \in \mathbb{N}$ is the number of nodes.

5.2.1 The mathematical formulation as an optimal control problem

Once we have modeled the dynamics of the network, we have desired activity levels for certain nodes of the network that means not necessarily for all nodes of the network. This can be the case if only a few nodes of a network serve or are identified as an output that is relevant for the outcome of an experiment while the other nodes that are left are still important for regulating these nodes of interest. These desired activity levels $x_k^d : \mathbb{R}_0^+ \to [0,1]$ are functions which represent the desired activity level of node k. These functions can be constant or vary their value over time. The set of desired activity levels is defined by $D := \left\{x_k^d |\ k \in N_I\right\}$, $N_I \subseteq \{1,...,n\}$ where N_I only contains the indices of the nodes of interest. Consequently in the case that we are just interested in the activity level of a subset of nodes of the whole network, then the cardinality of D is less than n.

The task for which we develop the framework in this section is to determine external stimuli, and if necessary their time curve, such that each node of interest from the set N_I takes its desired value as well as possible. For this purpose we define $x := \begin{pmatrix} x_1 \\ \vdots \\ x_n \end{pmatrix} \in \mathbb{R}^n$ and $u := \begin{pmatrix} u_1 \\ \vdots \\ u_m \end{pmatrix} \in \mathbb{R}^m$ and the following target functional

$$\tilde{J}(x,u) := \frac{1}{2}\sum_{k=1}^{n} g_k \int_0^T \left(x_k(t) - x_k^d(t)\right)^2 dt, \tag{5.2.1}$$

where $g_k \in \mathbb{R}_0^+$ is the weight of the corresponding tracking term $\int_0^T \left(x_k(t) - x_k^d(t)\right)^2 dt$ with $g_k > 0$ if $k \in N_I$ and $g_k = 0$ else. These weights mean how important it is that the corresponding node achieves its desired value compared to the other nodes of interest. The greater the value g_k of a certain node k is compared to the weights of the other nodes of interest, the more important it becomes that the corresponding node k attains its desired state x_k^d compared with the other nodes of interest where $g_k > 0$.

The value of $\tilde{J}(x,u)$ also serves as a measure how well the desired activity levels are taken by their corresponding nodes of interest subject to the constraint that (x,u) fulfills (5.1.4). That means the smaller $\tilde{J}$ is the better the desired activity levels are taken by the their corresponding node where in the best case $\tilde{J} = 0$ which means that $x_k = x_k^d$ for all $k \in N_I$. In order to include costs of the external stimuli into the target functional, we add the term $\alpha \sum_{j=1}^m \int_0^T u_j(t)\,dt$, $\alpha \geq 0$, to (5.2.1) which extracts the most effective external stimuli by increasing α. This works as follows. As for large values of α it is more likely that the cost of an active external stimuli is greater than its effect on steering the nodes of interest to the desired activity level and thus is set to zero. Then, we have the following extended cost functional

$$J_\alpha(x,u) := \frac{1}{2}\sum_{k=1}^{n} g_k \int_0^T \left(x_k(t) - x_k^d(t)\right)^2 dt + \alpha \sum_{j=1}^{m} \int_0^T u_j(t)\,dt. \tag{5.2.2}$$

Notice that $J_0(x,u) = \tilde{J}(x,u)$. Summarizing, we now have the following optimal control problem

$$\begin{aligned} &\min_{y,u} J_\alpha(x,u) \\ &\text{subject to } \frac{d}{dt}x_k = f_k(x,u) \text{ for all } k \in \{1,...,n\} \end{aligned} \tag{5.2.3}$$

where $f_k(x,u)$ is given by one of the right hand-sides of (4.2.1), (4.2.2), (4.2.3) and (4.2.4) for instance. We remark that these considerations also hold for any well defined system of ordinary differential equations that seems to be appropriate to model a real biological system.

Remark 5. An application of the framework discussed so far can be as follows. An interaction graph can be set up where the governing ordinary differential equations model can be fitted to real data created by the omics technology. All the possibilities of intervention by drugs can be modeled by external stimuli which can affect even more than just one node if one drug has multi target effects. Then by our optimization framework one can figure out the most effective drug combination that brings the

activity level of the nodes of interest as close to the desired activity level as possible. In general it will be not possible the meet the desired state exactly. If for some reason the user wishes to have some certain nodes closer to a desired value than it is in the calculated solution because they are still to far away from their desired value such that it is physiologically still not reasonable, they can increase the corresponding g_k and perform the calculations again. Then these nodes might get closer to the desired state, however maybe at the cost that others might get away a little bit more from their desired state but still close enough such that the new expression pattern caused by the external stimuli makes physiologically sense. If the expression pattern is still not as close to the desired activity level, then one has to include more external stimuli and thus can identify new effective drug targets that have the desired effect. This demonstrates how the optimization framework can be used to extract promising drug combinations or drug targets out of a huge graph, containing all the available information, that steer the experiment close to a physiological desired expression pattern.

Remark 6. Now, we are more specific with respect to the fitting procedure of the model parameters. In order to induce changes in the expression pattern or activity pattern of a real network, the network is perturbed with external stimuli. The resulting time curves of the agents are measured and the model is fitted to them. That means that for the fitting procedure of a network given by for example (4.1.1) we actually need a consistent framework that includes the effect of external stimuli. Such a framework is given by the mechanisms discussed in Section 4.2. Within that framework the whole fitting procedure works as follows. We measure the time curves of all expression levels or activity levels of all nodes and model the time curve of the corresponding external stimulus according to its application in the experiment. For example a scaled concentration of the external stimulus ranging from 0 (no application) to 1 maximum concentration of application. We remark that also the effect of several external stimuli can be measured at once and that there is no need for measuring the effect of each external stimulus individually. Then we do this procedure until at least all external stimuli have been active in at least one experiment. Thus each measurement generates a data set. Next, we have to perform a parameter fitting for all the data sets at once. That means all the model parameters are fitted such that the difference between the theoretical time curves of the activity levels and all the corresponding time curves of the corresponding activity levels of the data sets, measured in a certain norm, is as small as possible.

The procedure is not restricted to (4.2.1), (4.2.2), (4.2.3) or (4.2.4) but can be applied to any model consisting of ordinary differential equations.

Considering Remark 6, we understand the huge beneficial potential of the proposed framework to investigate the issue of determining appropriate external stimuli for a desired network behavior. Instead of measuring different combinations of external stimuli that might have the desired effect, one measures just die effect of each external stimulus on the network, fits the parameters of the model equations from the corresponding data and can extract the information of the most effective intervention that has the desired effect from the model. As the number of combinations of external stimuli depends exponentially on the number of all possible single external stimuli, real experiments can become very time consuming. For this reason it can be very advantageous to use the presented framework to determine promising candidates of network intervention for a desired network behavior since from the information of the effect of each external stimuli the best combination is figured out by our mathematical formalism which may save a lot of time as the required measurements depend only linearly on the number of possible single external stimuli.

5.2.2 Local optimization techniques

In this subsection we give the changes that have to be made to adapt the mathematical framework discussed in Section 5.1 for the situation that not all nodes of the network have to follow a desired activity level.

As in Subsection 5.1.2, we can discretize (5.2.3) before we optimize with a local optimization method like the gradient method that is given by Algorithm 5.1 and obtain for a certain time step size $\triangle t > 0$,

$t = l\triangle t$, $l \in \{0, ..., N\}$ and $T = N\triangle t$ the following optimal control problem

$$\min_{x,u} J(x,u) \coloneqq \frac{1}{2}\sum_{k=1}^{n} g_k \sum_{l=1}^{N} \left(x_k^l - x_k^d(l\triangle t)\right)^2 \triangle t + \alpha \sum_{j=1}^{m}\sum_{l=0}^{N-1} u_j^l \triangle t$$
$$\text{subject to } F(x,u) = 0,\ x^0 = x_0$$

where $F(x,u) \coloneqq \begin{pmatrix} F_1(x,u) \\ \vdots \\ F_n(x,u) \end{pmatrix} \in \mathbb{R}^{nN}$,

$$F_k(x,u) \coloneqq -\begin{pmatrix} x_k^1 \\ \vdots \\ x_k^N \end{pmatrix} + \begin{pmatrix} x_k^0 \\ \vdots \\ x_k^{N-1} \end{pmatrix} + \triangle t \begin{pmatrix} f_k(x^0,u^0) \\ \vdots \\ f_k(x^{N-1},u^{N-1}) \end{pmatrix} \in \mathbb{R}^N$$

for all $k \in \{1, ..., n\}$. Notice that x_k is not a function any more but a vector $x_k \coloneqq \begin{pmatrix} x_k^1 \\ \vdots \\ x_k^N \end{pmatrix} \in \mathbb{R}^N$ for all $k \in \{1, ..., n\}$ and $x \coloneqq \begin{pmatrix} x_1 \\ \vdots \\ x_n \end{pmatrix} \in \mathbb{R}^{nN}$. Analogously, we have the definition for the vector $u_j \coloneqq \begin{pmatrix} u_j^0 \\ \vdots \\ u_j^{N-1} \end{pmatrix} \in \mathbb{R}^N$ and $u \coloneqq \begin{pmatrix} u_1 \\ \vdots \\ u_m \end{pmatrix} \in \mathbb{R}^{mN}$ with $0 \leq u_j^l \leq 1$ for all $j \in \{1, ..., m\}$ and $l \in \{0, ..., N-1\}$. Then, we just have to modify the adjoint equation for $p \coloneqq \begin{pmatrix} p_1 \\ \vdots \\ p_n \end{pmatrix} \in \mathbb{R}^{nN}$, $p_k \coloneqq \begin{pmatrix} p_k^1 \\ \vdots \\ p_k^N \end{pmatrix} \in \mathbb{R}^N$ which is given by

$$0 = \begin{pmatrix} g_k\left(x_k^1 - x_k^d(1dt)\right) - p_k^1 + p_k^2 + \sum_{i=1}^n p_i^2 \frac{\partial}{\partial x_k^1} f_i\left(x^1,u^1\right) dt \\ g_k\left(x_k^2 - x_k^d(2dt)\right) - p_k^2 + p_k^3 + \sum_{i=1}^n p_i^3 \frac{\partial}{\partial x_k^2} f_i\left(x^2,u^2\right) dt \\ \vdots \\ g_k\left(x_k^{N-1} - x_k^d((N-1)dt)\right) - p_k^{N-1} + p_k^N + \sum_{i=1}^n p_i^N \frac{\partial}{\partial x_k^{N-1}} f_i\left(x^{N-1},u^{N-1}\right) dt \\ g_k\left(x_k^N - x_k^d(Ndt)\right) - p_k^N \end{pmatrix} \in \mathbb{R}^N$$

for all $k \in N_I$ and

$$0 = \begin{pmatrix} -p_k^1 + p_k^2 + \sum_{i=1}^n p_i^2 \frac{\partial}{\partial x_k^1} f_i\left(x^1,u^1\right) dt \\ -p_k^2 + p_k^3 + \sum_{i=1}^n p_i^3 \frac{\partial}{\partial x_k^2} f_i\left(x^2,u^2\right) dt \\ \vdots \\ -p_k^{N-1} + p_k^N + \sum_{i=1}^n p_i^N \frac{\partial}{\partial x_k^{N-1}} f_i\left(x^{N-1},u^{N-1}\right) dt \\ -p_k^N \end{pmatrix} \in \mathbb{R}^N$$

for all $k \in \{1, ..., n\} \setminus N_I$.

In order to use the sequential quadratic Hamiltonian method that is given by Algorithm 5.2, we just have to modify some definitions made in Subsection 5.1.3. The Hamiltonian $H : \mathbb{R} \times \mathbb{R}^n \times \mathbb{R}^m \times \mathbb{R}^n$ now is given by

$$H(t,x,u,p) \coloneqq \frac{1}{2}\sum_{k=1}^{n} g_k\left(x_k - x_k^d\right)^2 + \alpha \sum_{j=1}^{m} u_j + \sum_{k=1}^{n} p_k f_k(x,u).$$

The adjoint variables $\bar{p}_k : \mathbb{R}_0^+ \to \mathbb{R}$ are given by the following adjoint equations

$$\frac{d\bar{p}_k}{dt} = -g_k\left(\bar{x}_k - x_k^d\right) - \sum_{i=1}^{n} \bar{p}_i \frac{\partial}{\partial x_k} f_i\left(\bar{x}, \bar{u}\right)$$

if $k \in N_I$ and by the following equations

$$\frac{d\bar{p}_k}{dt} = -\sum_{i=1}^{n} \bar{p}_i \frac{\partial}{\partial x_k} f_i\left(\bar{x}, \bar{u}\right)$$

if $k \in \{1, ..., n\} \setminus N_I$ with $\bar{p}_k(T) = 0$ for all $k \in \{1, ..., \}$ where $\frac{\partial}{\partial x_k} f_i(\bar{x}, \bar{u}) := \frac{\partial}{\partial x_k} f_i(x, u)\,|_{(x,u)=(\bar{x},\bar{u})}$ that means the partial derivative of the i-th component of f with respect to the k-th component of $x := \begin{pmatrix} x_1 \\ \vdots \\ x_n \end{pmatrix} \in \mathbb{R}^n$ evaluated at $(\bar{x}, \bar{u})$ and $(\bar{x}, \bar{u})$ is an optimal solution to (5.2.3).

Remark 7. As in this framework the desired activity level x_d can model a time-dependent expression pattern where the values for each node vary with respect to time, we can think of pharmacological applications where the expression pattern of a network is supposed to be different between day and night time which can be achieved with external stimuli and a fitted regulatory network.

5.2.3 A global optimization technique

Besides local optimization approaches to solve (5.2.3) there is the possibility to systematically try different external stimuli with constant value over the interval $[0, T]$. Moreover we can vary each value of each point of time of each external stimulus and test each combination which of them generates the smallest target functional value. However this method has a great number of different combinations and this number growth exponentially with the number of external stimuli. To keep the number of combinations as small as possible and reasonable in favor of our purpose to find a combination of external stimuli that keep the network close to a desired expression pattern, we implement the following idea in Algorithm 5.4. We choose the maximum number of external stimuli maxNum $\in \{1, ..., m\}$ that are supposed to be active at once and the number numInt $\in \mathbb{N}$ of parts in which the image of the external stimuli $[0, 1]$ is divided into. Then we choose from the power set $\mathcal{P}$ of the set $\{1, ...m\}$ that elements g with cardinality $|g| \leq$ maxNum. This defines the set P. Next, we choose $g \in P$, $val \in \left\{i\frac{1}{\text{numInt}} |\ i = 1, ..., \text{numInt}\right\}$ and set $u_j = val$ if $j \in g$ and $u_j = 0$ else. That means the active external stimuli are constant functions with value val and the inactive external stimuli are constant functions with value 0 in the whole time interval $[0, T]$. Next, we calculate the target functional value $J_\alpha(x, u)$ for the corresponding external stimuli u where (x, u) fulfills (5.1.4). This is done for all $g \in P$ and all $val \in \left\{i\frac{1}{\text{numInt}} |\ i = 1, ..., \text{numInt}\right\}$. We choose the combination of external stimuli that causes the smallest target functional value as the output of Algorithm 5.4.

Algorithmus 5.4 Combinatorial method

---

1. Choose numMax $\in \{1, ..., m\}$, numInt $\in \mathbb{N}$
2. Choose all the elements $g \in P \subseteq \mathcal{P}$ of the power set $\mathcal{P}$ of $\{1, ..., m\}$ such that the cardinality $|g| \leq$ maxNum
3. Calculate $J_\alpha(x, u)$ for all $p \in P$ and all $val \in \left\{i\frac{1}{\text{numInt}} |\ i = 1, ..., \text{numInt}\right\}$ with $u_j = val$ if $j \in g$ and $u_j = 0$ else where (x, u) fulfills (5.1.4)
4. Return (x, u) with the smallest target functional value $J_\alpha(x, u)$ defined in (5.2.2)

Notice that it is worth to parallelize an implementation of Algorithm 5.4 as the calculation for each combination of external stimuli in Step 3 is independent of the others. Furthermore, we remark that the calculation time of Algorithm 5.4 increases exponentially with respect to maxNum.

The output of Algorithm 5.4 can be used as an initial guess of a local optimization method like the projected gradient method, see Algorithm 5.1 or the sequential quadratic Hamiltonian method, see Algorithm 5.2. Based on the initial guess from Algorithm 5.4, a local optimization method finds an optimal solution for (5.2.3) in linear calculation time with respect to the number of external stimuli. As the external stimuli are functions over time, the solution of a local optimization time is not necessary a constant function but its value can vary with time. Determining also time resolved external stimuli with a method as Algorithm 5.4 might be to costly. However the most promising combination determined can be refined by a local optimization algorithm. This refinement of the time curves of the external stimuli corresponding to a minimum of (5.2.3) may contain further information about the relation of each external stimulus to each other. Additionally an optimal solution from a local optimization method can differ with respect to the number of active external stimuli compared with the solution from Algorithm 5.4. The local optimization method's calculation might also be more efficient due to the time scaling depending on the number of external stimuli.

With similar consideration as for Algorithm 5.3 due to the possibly high non-linearity of (5.1.4), a further use of Algorithm 5.4 is to improve the initial guess for the local optimization methods such that they converge to a global optimum of (5.2.3) and not to a local optimum that has possibly a greater target functional value than the global optimum but is optimal in the sense of fulfilling the necessary optimality conditions like (5.1.13) or (5.1.14) though causing that the local optimization methods stop.

5.3 State of research with respect to software solutions

Finally to calculate external stimuli for inducing a switch from one steady states of regulatory network to a different one or for keeping the close to a desired expression pattern, a software solution is useful that creates the system of ordinary differential equations from an interaction graph, fits parameters of the system from experimental data and includes the effects of external stimuli to calculate an effective selection of external stimuli that steers the network in our favor. This section is intended to give an overview of existing software solution and how they are related to the task of determining external stimuli. This section is based on [10, Section 6].

Specifically we point out differences to other software existing to analyze regulatory networks and illustrate how to combine our provided software package with other tools. In particular, there is no calculation of optimal modulation of networks by external stimuli available. However, the selection of an optimal stimulus for a specified number of nodes to be modulated into a new state is central for pharmacological interventions. Moreover, planning of knockdowns, RNAi experiments for instance, or any kind of other inhibition, excitation or modulation of the network would highly profit from such an application and this is offered here.

On the other hand each of them allows an efficient description of the system state including suitable differential equations using either accurate or heuristic solutions. Iterative model refinement can be done including studying the effect of different receptor inputs, activations and inhibitions. However, none of these tools allows to directly calculate the optimal manipulation of the network for changing to a prespecified new system state. Instead there would be numerous trials and iterative steps necessary using any of the software below to achieve this.

We start with the **SQUAD** method (https://sbos.eu/docu/docu/SQUAD/doku.php.htm). One can utilize SQUAD to analyze steady states of a network once one has the topology of the network that means the interaction graph. Additionally, one can perturb the network for example by activating receptors or by changing decay or gain of a node's activity. However, this software does not provide a systematical procedure how to search for perturbations to steer the network to a desired state. Therefore our concept of providing a framework to calculate perturbations by techniques of mathematical optimization supplements the pioneering idea implemented in the SQUAD software.

The next software package is called **JIMENA** (https://www.biozentrum.uni-wuerzburg.de/bioinfo/computing/jimena-c/) which focuses on an efficient numerical steady state analysis. Therefore, this package as well as SQUAD serves as an excellent tool to figure out the steady states of a network between which one would like to switch. Once the steady states are found, our framework proposed in the present work can be utilized for the calculation

of the desired switch.

The **CELL NET ANALYZER** (https://www2.mpi-magdeburg.mpg.de/projects/cna/cna.html) provides, besides metabolic network analysis and steady state analysis, a method to calculate minimal intervention sets that provide a network with desired steady states. However, this means that one gets a list of knockins and knockouts of nodes of the network such that the network attains the desired steady states. This is a very important tool, especially in the case of lacking experimental information or conflicting information about the interaction of the considered agents, to design the topology of the network in order to obtain a notwork that provides the steady states sought. Thus this method is intended to change the topology of the network that means the interaction graph while our approach deals with a fixed topology of the network during all calculations. The CELL NET ANALYZER is hence well suited for metabolic modeling, modeling of signaling networks and the upstream use of SQUAD or JIMENA to design an appropriate network but not for precalculation of the best and most efficient stimulus combination to achieve a desired system state.

The **ODEFY** (https://www.helmholtz-muenchen.de/icb/software/odefy/index.html) is a tool in order to convert boolean networks into networks whose dynamic is described by ordinary differential equations which are the basic models in our framework. Therefore the ODEFY is a key tool to transform network topologies into an ordinary differential equation model which is essential for our framework, especially in the case of networks with many nodes and couplings between them. Thus ODEFY allows the swift formulation of the differential equation system, however, there is no systematic approach to identify the correct combination of external stimuli.

With our framework we provide in addition a straight forward tool to first define and second apply functions $u_j : \mathbb{R}_0^+ \to [0,1]$, $j \in \{1,...,m\}$, $m \in \mathbb{N}$ as pharmacological parameters.

Specifically, the **COPASI** toolbox (http://copasi.org/) focuses on the modeling and on simulating of biochemical reaction networks, especially simulation of time curves and steady states, parameter fitting of an underling model to experimental data, sensitivity analysis and dynamical behavior characterization. Besides steady state analysis, a further step of network analysis is to compare the simulated curves with experimental data. Therefore the COPASI is a very important tool to analyze different models that fit the data best after fitting of the model's parameters. Thus the COPASI can have a big contribution to pharmacological modeling by first fitting parameters and then choose the model that fits the data best which is essential for dose rate calculations, for example. As our framework does not depend on special network equations that are set up from the interaction graph, our presented framework extends the great range of functions in a useful way. Moreover, COPASI is maybe even more powerful then ODEFY and wide ranges of parameters can be tested swiftly. Nevertheless, to find a proper combination of external stimuli to change the system state is a challenge, cumbersome and not systematic.

The software tool **POTTERSWHEEL** (http://www.potterswheel.de/Pages/index.php) can be used for modeling with ordinary differential equations and best parameter fit to experimental data. For this purpose, one can additionally include external driving functions or vary parameters. This can be used to adapt parameters of the system of ordinary differential equations with which one would like to model a particular real network such that the theoretical data fits best to the experimental data. Moreover, POTTERSWHEEL is very efficient in model testing and model refinement. However, for our task, pharmacological network modulation of the change of the network state by the best, most efficient combination of external stimuli, the tool allows to quickly verify that a given combination is right, but to find it is difficult and needs numerous iterations. On the other hand, individual parameters are fast characterized regarding their sensitivity and importance for network behavior. Therefore, as COPASI, the software POTTERSWHEEL is also very helpful to figure out an appropriate model and can be extended by our framework with a further useful feature.

Next, we explain the need for the mentioned extension in detail. The last two software packages are well known examples and perform, among other things, a fit of model parameters of a system of coupled ordinary differential equations. This is similar to our framework. However, the main difference between a parameter fit and our framework is, that the functions u_j, $j \in \{1,...,m\}$ are time dependent while a parameter is constant. Therefore we extend the idea of parameter fit, which is a special application of mathematical optimal control theory, to a more general framework that also includes

time dependent parameter fitting. In our case, the time dependence of the functions u_j is important as they are switched on for a certain time and after the switch off, the network can relax to the desired state such that we can verify, after the application of certain external stimuli, that each node is close to its desired state which would not be possible with a constant parameter as the network could not relax with constitutively activated external stimuli. Furthermore if the desired activity levels are time dependent then there is the need for external stimuli that can also vary in time.

Our framework provides the most important external stimuli that are responsible for a desired network behavior by increasing the weight α in the cost functional (5.1.3). By this procedure, we can reduce the number of pharmacological intervention points to a small but very effective number which is for the purpose of pharmacological treatments. This issue is also not covered by classical parameter fitting that is provided by COPASI and POTTERSWHEEL. However, as we mentioned before, our framework of systematically finding external stimuli that steer the network to a desired expression pattern is not restricted to a special type of ordinary differential equation model. Therefore the provided Matlab files can also be integrated into existing software packages like COPASI or POTTERSWHEEL to extend their already great and helpful tools for model analysis with respect to experimental data.

Chapter 6

Application of the framework to biological examples

In this chapter, we apply the the mathematical formalism from Chapter 5 to biological examples to validate the proposed method and show the principle scope of the proposed framework. For this purpose we first consider a gene regulatory network modeling platelets and a network modeling T-helper cells. For the platelets we determine receptors that are associated with irreversible aggregation in accordance to literature. For the T-helper cells we propose a treatment to switch the T-cell type from Th17 cell type to a regulatory T-cell type and provide illustrating literature. Furthermore we give several calculations to switch between different T-cell types Th1, Th2, Th17 and regulatory T-cell type. In the last two sections we consider a gene regulatory network that models a myocardiocyte and demonstrate how to determine treatment strategies that keep the nodes of interest of this network close to a desired activity level and compare these different treatment strategies quantitatively. Furthermore we show how to find out the most effective intervention points out of several choices. In the following section we introduce into the application of our proposed framework for inducing a switch between two different steady states of a network with basic examples.

6.1 Introducing examples how to determine external stimuli

In this section, which is based on [10, Section 4], we demonstrate how to analyze a regulatory network which includes interactions with external stimuli using our optimization approach presented in Section 5.1 with the model (4.2.1). For our numerical examples, we use the regulatory network from [37, Figure 5], Alternative Th network. The schematic of this network is given in Figure 6.1.1 where IFN-γ is node 1, CSIF is node 2, IL-2 is node 3 and IL-4 is node 4. The network, although it is small, carries a typical feature for for biological systems that is cross connectivity. Examples are the tumor necrosis factor network [41], myocardiocytes [11] or a network describing proliferation vs. apoptosis in cells [52, 21].

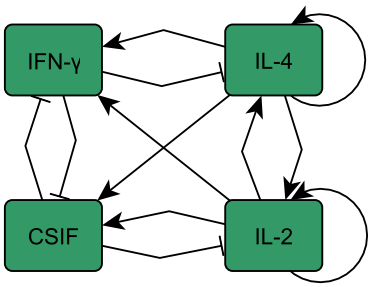

Figure 6.1.1: The schematic of our example network analogous to [37, Figure 5]. Abbreviations are as follows: IFN-γ, interferon γ; IL-x, interleukin x; CSIF, cytokine synthesis inhibitory factor

In our first example, we analyze the transit of one steady state to another for a given set of

external stimuli. We consider the corresponding equations containing external stimuli, see (4.2.1) with u_1 activating node 1, u_2 activating node 4 and u_3 activating node 2, as follows

$$\begin{aligned}
\frac{d}{dt}x_1 &= \frac{-\mathrm{e}^5 + \mathrm{e}^{-10\left(\frac{3}{2}\left(\frac{x_3+x_4}{1+x_3+x_4}\right)\left(1-\frac{11}{10}\frac{10x_2}{1+10x_2}\right)-0.5\right)}}{(1-\mathrm{e}^5)\left(1+\mathrm{e}^{-10\left(\frac{3}{2}\left(\frac{x_3+x_4}{1+x_3+x_4}\right)\left(1-\frac{11}{10}\frac{10x_2}{1+10x_2}\right)-0.5\right)}\right)} - x_1 + u_1\,(1-x_1)\\
\frac{d}{dt}x_2 &= \frac{-\mathrm{e}^5 + \mathrm{e}^{-10\left(\frac{3}{2}\left(\frac{x_3+x_4}{1+x_3+x_4}\right)\left(1-\frac{11}{10}\frac{10x_1}{1+10x_1}\right)-0.5\right)}}{(1-\mathrm{e}^5)\left(1+\mathrm{e}^{-10\left(\frac{3}{2}\left(\frac{x_3+x_4}{1+x_3+x_4}\right)\left(1-\frac{11}{10}\frac{10x_1}{1+10x_1}\right)-0.5\right)}\right)} - x_2 + u_3\,(1-x_2)\\
\frac{d}{dt}x_3 &= \frac{-\mathrm{e}^5 + \mathrm{e}^{-10\left(\frac{3}{2}\left(\frac{x_3+x_4}{1+x_3+x_4}\right)\left(1-\frac{11}{10}\frac{10x_2}{1+10x_2}\right)-0.5\right)}}{(1-\mathrm{e}^5)\left(1+\mathrm{e}^{-10\left(\frac{3}{2}\left(\frac{x_3+x_4}{1+x_3+x_4}\right)\left(1-\frac{11}{10}\frac{10x_2}{1+10x_2}\right)-0.5\right)}\right)} - x_3\\
\frac{d}{dt}x_4 &= \frac{-\mathrm{e}^5 + \mathrm{e}^{-10\left(\frac{3}{2}\left(\frac{x_3+x_4}{1+x_3+x_4}\right)\left(1-\frac{11}{10}\frac{10x_1}{1+10x_1}\right)-0.5\right)}}{(1-\mathrm{e}^5)\left(1+\mathrm{e}^{-10\left(\frac{3}{2}\left(\frac{x_3+x_4}{1+x_3+x_4}\right)\left(1-\frac{11}{10}\frac{10x_1}{1+10x_1}\right)-0.5\right)}\right)} - x_4 + u_2\,(1-x_4)
\end{aligned} \tag{6.1.1}$$

where we choose $h = 10$, $\alpha_k = 1$, $\beta_k = 10$ and $\gamma_k = 1$ for all $k \in \{1,2,3,4\}$. This choice applies for the rest of this section. In our example, we switch the regulatory network (6.1.1) from the steady state $x_0 = \begin{pmatrix} 0 & 0 & 0 & 0 \end{pmatrix}$ to the steady state $\begin{pmatrix} 0.8870 & 5.6662 \cdot 10^{-4} & 0.8870 & 5.6662 \cdot 10^{-4} \end{pmatrix}$. We round the numbers here in this work for the reason of notation. Utilizing Algorithm 5.1 with $\alpha = 0.1$, $T = 20$, $\triangle t = 0.1$, $\epsilon = 10^{-6}$ and ${}^0u = 0$, we obtain the results shown in Figure 6.1.2 and Figure 6.1.3.

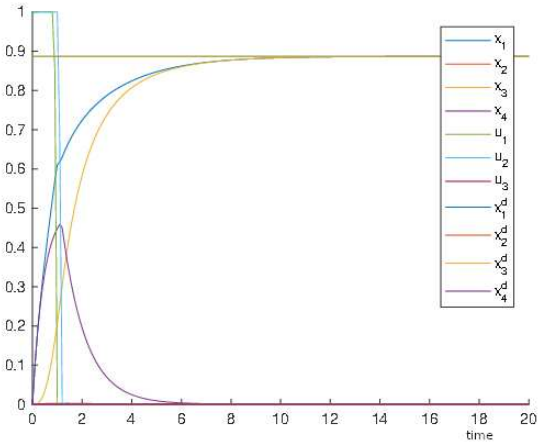

Figure 6.1.2: The time is plotted on the abscissa and the activity level is plotted on the ordinate. Switch from the initial steady state to the desired steady state by the external stimuli u_1, u_2 calculated by Algorithm 5.1.

In Figure 6.1.2, we see that the regulatory network is steered to the desired steady state by the external stimuli u_1 and u_2. For this purpose, only a short application is necessary. Furthermore, we see that the external stimulus u_3 is not needed for this switch. We remark that although we desire the activity level x_4 to be low, it is intermediately activated by u_2 in order to steer the whole regulatory network into the desired steady state. When u_2 is switched off, the activity level x_4 immediately decreases. If the external stimulus 2 is not included into the system of equations (6.1.1), then the desired switch is not performed which demonstrates that the external stimulus 2 is important for the switch. Although it does not activate a node which is desired to have a high activity in the desired state through the cross connectivity the network steers the other nodes into its desired steady state though. This maybe counterintuitive information is revealed by our framework.

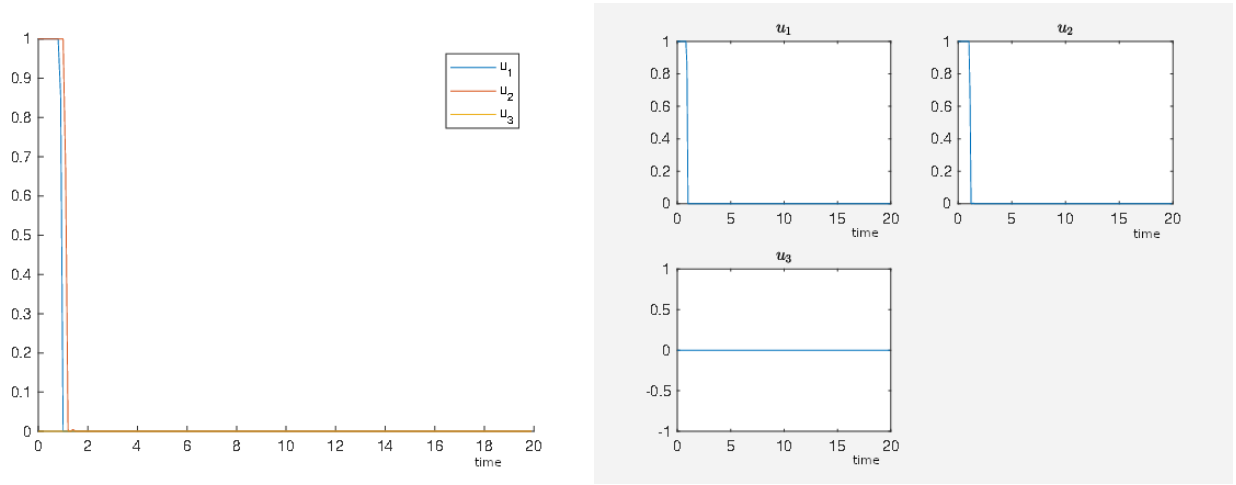

Figure 6.1.3: The time is plotted on the abscissa and the activity level is plotted on the ordinate. The external stimuli u_1, u_2 and u_3 in detail.

Even if we do not know the exact parameters of a system modeled by our equations described in Section 4.2, we can use Figure 6.1.3 as a qualitative information, as the model in Section 4.2 is also intended to be used in the lack of the exact values for the model parameters. The qualitative information is that the external stimuli u_1 and u_2 are essential for the desired switch. Because of the qualitative character in this example, the duration of application proposed by Algorithm 5.1 is hardly able to be recovered in a real experiment in general. However, in Figure 6.1.4, we apply u_1 and u_2 much longer than proposed by Algorithm 5.1 while u_3 is switched off the whole time. Consequently, we see that the model is robust with respect to a duration of application of the external stimuli that is longer than proposed by the calculation of Algorithm 5.1 because we obtain the same switch. This is important for the application in an experiment where it is difficult to apply an external stimuli for an exactly given period. After the external stimuli are switched off, the regulatory network relaxes into the desired steady state. We see that the activity level x_4 of node 4 cannot exceed 0.5 although u_2 is maximum active.

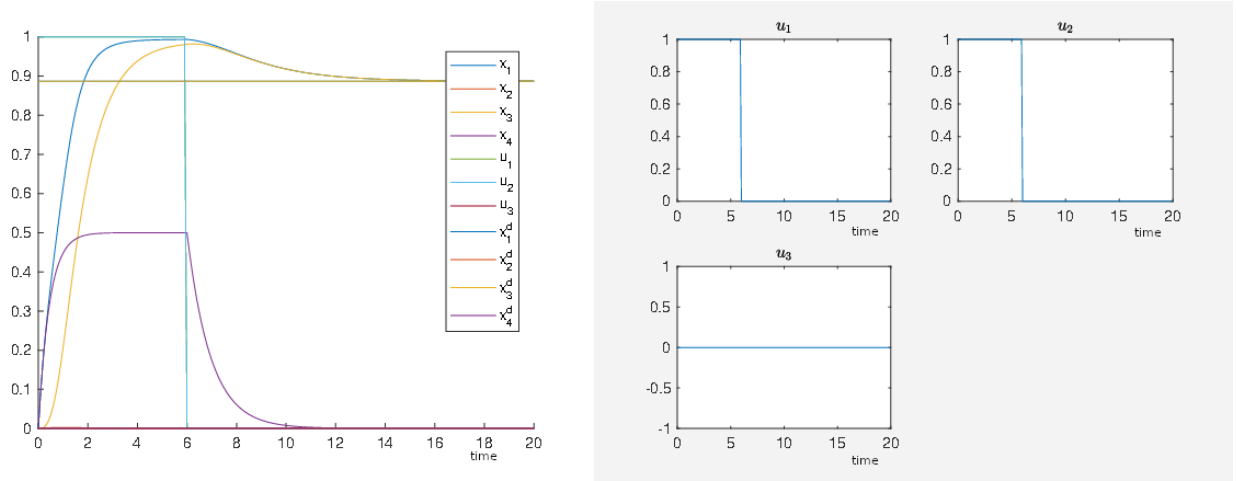

Figure 6.1.4: The time is plotted on the abscissa and the activity level is plotted on the ordinate. Switch from the initial steady state to the desired steady state by the external stimuli u_1 and u_2 applied longer than proposed by Algorithm 5.1.

We remark that there might exist several selections of single external stimuli and their duration of application which steer the regulatory network from one steady state to another. Algorithm 5.1 calculates optimal external stimuli where optimal is meant in the sense of being a (local) solution to (5.1.7). The model presented in Section 4.1 also offers the possibility to find external stimuli for the desired switch by trial and error methods, like Algorithm 5.3. For this purpose, we can set values for

each point of time for the external stimuli and solve (5.1.6) to see if this choice has the desired effect on the regulatory network. Of course, if the choice of external stimuli works, this choice might have a bigger value of the target functional of (5.1.7) than its optimal solution and is not optimal in this sense although it performs the desired switch. However, we focus on finding a selection of external stimuli which performs a desired switch. Solving (5.1.5) or (5.1.7) can be interpreted as an additional tool of systematic inspiration for us to find such a selection.

Algorithm 5.1 or Algorithm 5.2 in combination with the presented optimization approach provides a tool for systematically figuring out what external stimuli are essential to switch the regulatory network between different steady states. This is very useful for network analysis if the modeled system contains a lot of possibilities for activation or inhibition by external stimuli because the number of possible combinations of different external stimuli grows exponentially with the number of external stimuli. Thus a trial and error method to determine a set of essential external stimuli might become cumbersome, see the following example.

We demonstrate the principle procedure with a basic example. The biological relevance of an optimal solution is then that it represents the pharmacological intervention, for instance, that induces the desired switch in the experiment. This switch will surely happen if the model is sufficiently appropriate to describe the corresponding experiment. This example also demonstrates how from the amount of all combinations of all external stimuli that perform a desired switch the most important ones are extracted which is also a crucial issue in pharmacological problems.

Each node is equipped with an activating and an inhibiting external stimulus in order to determine a selection of essential external stimuli. If a system is modeled with a regulatory network, we can generate candidate nodes for which it is worth to develop drugs for activation or inhibition such that we achieve the desired switch in the system. As an illustrative example, we use the following

$$
\begin{aligned}
\frac{d}{dt}x_1 &= \frac{-\mathrm{e}^5 + \mathrm{e}^{-10\left(\frac{3}{2}\left(\frac{x_3+x_4}{1+x_3+x_4}\right)\left(1-\frac{11}{10}\frac{10x_2}{1+10x_2}\right)-0.5\right)}}{(1-\mathrm{e}^5)\left(1+\mathrm{e}^{-10\left(\frac{3}{2}\left(\frac{x_3+x_4}{1+x_3+x_4}\right)\left(1-\frac{11}{10}\frac{10x_2}{1+10x_2}\right)-0.5\right)}\right)} - x_1 + u_1\,(1-x_1) - u_2 x_1 \\
\frac{d}{dt}x_2 &= \frac{-\mathrm{e}^5 + \mathrm{e}^{-10\left(\frac{3}{2}\left(\frac{x_3+x_4}{1+x_3+x_4}\right)\left(1-\frac{11}{10}\frac{10x_1}{1+10x_1}\right)-0.5\right)}}{(1-\mathrm{e}^5)\left(1+\mathrm{e}^{-10\left(\frac{3}{2}\left(\frac{x_3+x_4}{1+x_3+x_4}\right)\left(1-\frac{11}{10}\frac{10x_1}{1+10x_1}\right)-0.5\right)}\right)} - x_2 + u_3\,(1-x_2) - u_4 x_2 \\
\frac{d}{dt}x_3 &= \frac{-\mathrm{e}^5 + \mathrm{e}^{-10\left(\frac{3}{2}\left(\frac{x_3+x_4}{1+x_3+x_4}\right)\left(1-\frac{11}{10}\frac{10x_2}{1+10x_2}\right)-0.5\right)}}{(1-\mathrm{e}^5)\left(1+\mathrm{e}^{-10\left(\frac{3}{2}\left(\frac{x_3+x_4}{1+x_3+x_4}\right)\left(1-\frac{11}{10}\frac{10x_2}{1+10x_2}\right)-0.5\right)}\right)} - x_3 + u_5\,(1-x_3) - u_6 x_3 \\
\frac{d}{dt}x_4 &= \frac{-\mathrm{e}^5 + \mathrm{e}^{-10\left(\frac{3}{2}\left(\frac{x_3+x_4}{1+x_3+x_4}\right)\left(1-\frac{11}{10}\frac{10x_1}{1+10x_1}\right)-0.5\right)}}{(1-\mathrm{e}^5)\left(1+\mathrm{e}^{-10\left(\frac{3}{2}\left(\frac{x_3+x_4}{1+x_3+x_4}\right)\left(1-\frac{11}{10}\frac{10x_1}{1+10x_1}\right)-0.5\right)}\right)} - x_4 + u_7\,(1-x_4) - u_8 x_4
\end{aligned}
\tag{6.1.2}
$$

where each node is equipped with an activating and an inhibiting external stimulus. We desire a switch from the steady state $x_0 = \begin{pmatrix} 0.8870 & 5.6662\cdot 10^{-4} & 0.8870 & 5.6662\cdot 10^{-4} \end{pmatrix}$ to the steady state $\begin{pmatrix} 5.6662\cdot 10^{-4} & 0.8870 & 5.6662\cdot 10^{-4} & 0.8870 \end{pmatrix}$. The results from Algorithm 5.1 with $\alpha = 0.1$, $T = 20$, $\triangle t = 0.1$, $\epsilon = 10^{-6}$ and ${}^0u = 0$ can be seen in Figure 6.1.5. This selection of external stimuli presented in Figure 6.1.5 is able to cause the desired switch of steady states.

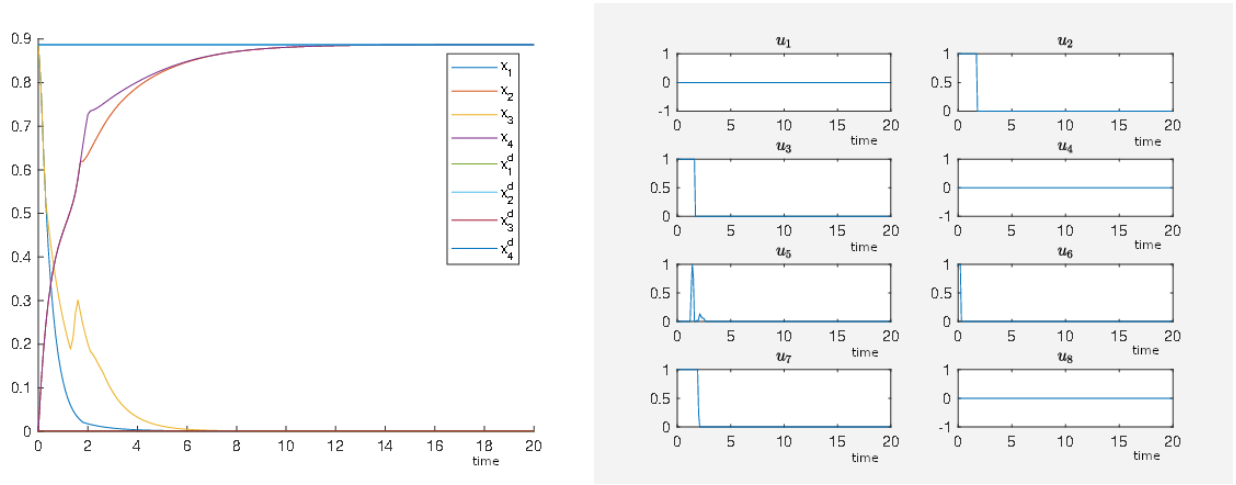

Figure 6.1.5: The time is plotted on the abscissa and the activity level is plotted on the ordinate. An optimal selection of external stimuli performing the desired switch for $\alpha = 0.1$ on the right hand-side and the time course of the nodes' activity level for the corresponding external stimuli on the left hand-side.

For the same setting but with $\alpha = 1.1$ instead of $\alpha = 0.1$, we get a smaller number of non-zero external stimuli, as u_2 and u_6 are constant zero functions now, see Figure 6.1.6. Comparing Figure 6.1.5 and Figure 6.1.6, we see that the desired switch is performed faster in Figure 6.1.5 as more external stimuli are involved. Such investigations are interesting for experiments where a fast switch matters.

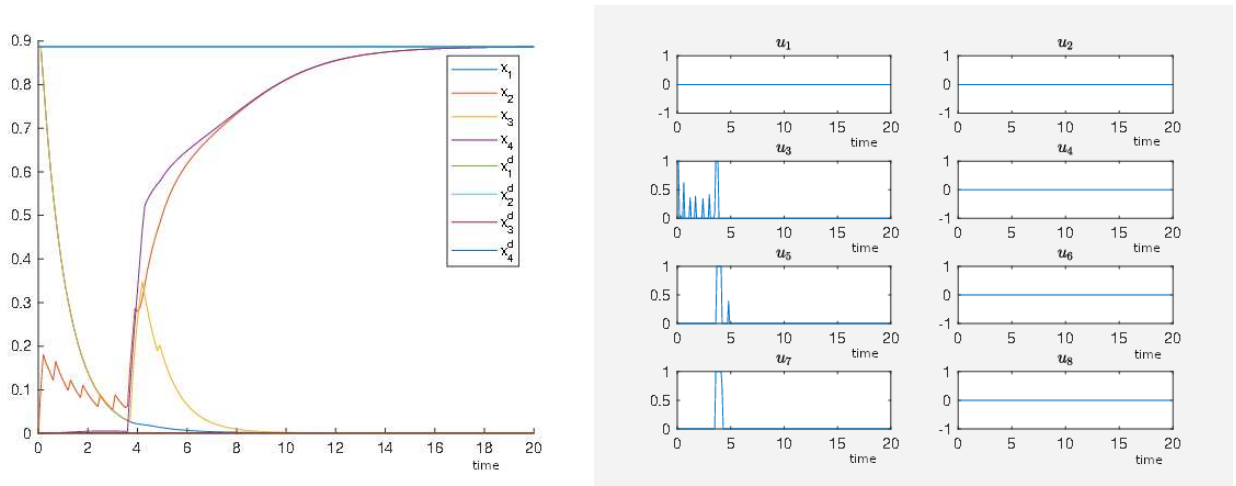

Figure 6.1.6: The time is plotted on the abscissa and the activity level is plotted on the ordinate. An optimal selection of external stimuli performing the desired switch for $\alpha = 1.1$ on the right hand-side and the corresponding time curves of the nodes' activity level on the left hand-side.

From Figure 6.1.6, we see that external stimulus u_3 is applied longer than u_5 and u_7. Applying just u_3 and u_5 or u_3 and u_7 also performs the desired switch, see Figure 6.1.7. In order to obtain the desired switch, we observe a robustness with respect to the duration of application and the time curves of the external stimuli comparing the external stimuli in Figure 6.1.7 with the optimal ones in Figure 6.1.6 since both variants induce the desired switch. Roughly spoken, the exact time curves of the applied external stimuli are not decisive for the desired switch.

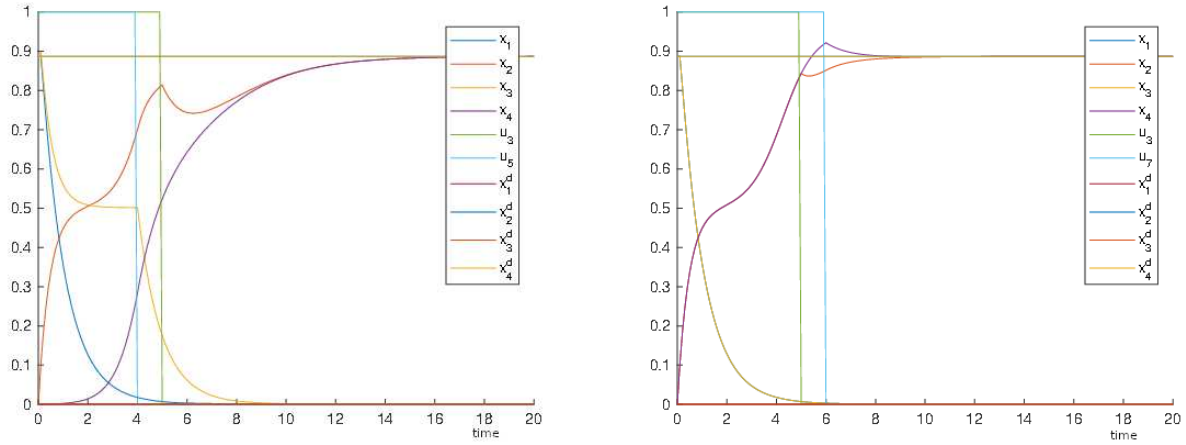

Figure 6.1.7: The time is plotted on the abscissa and the activity level is plotted on the ordinate. Two suitable selections of external stimuli that are able to perform the desired switch.

Applying just u_3 or u_5 and u_7 as in Figure 6.1.8 does not have the desired effect on the network that means the desired switch is not performed. This illustrates the fact that there exist effects in biological networks such that a big duration and an intensive application of a single external stimulus is not able to trigger a desired switch but rather the coordinated occurrence of different external stimuli is crucial for the desired switch. Summarizing this experiment, from all eight external stimuli, we identify five suitable ones and reduce the number of suitable external stimuli from five to three utilizing our optimization framework, especially with Algorithm 5.1 by increasing α. From the three non-zero external stimuli, we extract two tuples consisting each of two external stimuli which perform the desired switch.

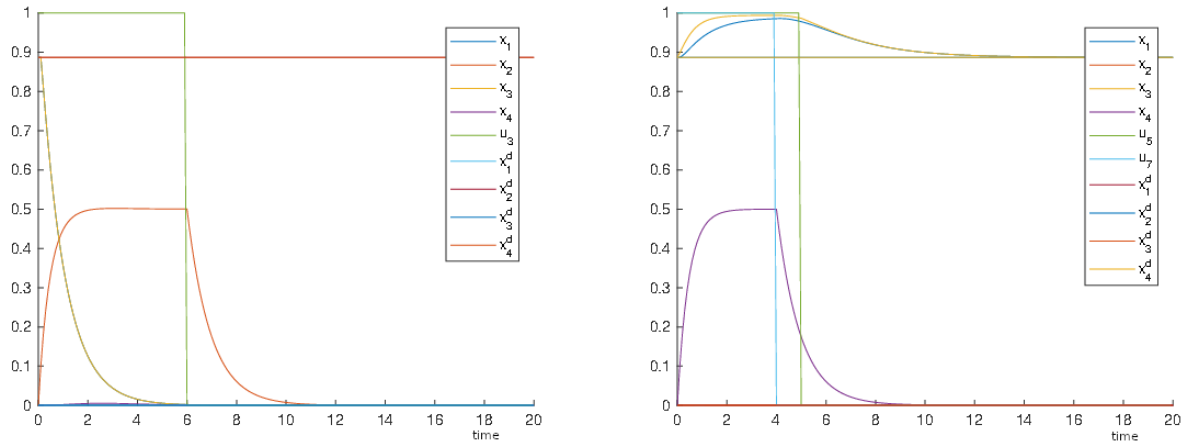

Figure 6.1.8: The time is plotted on the abscissa and the activity level is plotted on the ordinate. These selections of applied external stimuli cannot perform the desired switch.

As well from Figure 6.1.8, we see that the selected external stimuli do not cover sufficient intervention points and do not affect the crucial network nodes and thus are not able to perform the desired switch. That means that the selection of external stimuli has to interfere sufficiently many nodes from which our proposed framework then figures out the external stimuli that perform the desired switch of steady states. Consequently, not any selection of external stimuli can perform any desired switch. This observation can be interpreted as a filter of the network as only selected and rare situations where these coordinated external stimuli occur are able to induce changes of the cell behavior, for example. Since uncoordinated external stimuli do not change the cell's behavior, the need for a coordinated occurrence of external stimuli to trigger the switch ensures that the cell is in the right place and right time to change its behavior assuming that this coordinated occurrence of external stimuli is unlikely

somewhere else where it is not the right place and the right time.

Another example for too few applied external stimuli is (6.1.1) where just u_2 is applied to node 4 in order to switch from $x_0 = \begin{pmatrix} 0 & 0 & 0 & 0 \end{pmatrix}$ to $\begin{pmatrix} 0.8870 & 5.6662 \cdot 10^{-4} & 0.8870 & 5.6662 \cdot 10^{-4} \end{pmatrix}$, see Figure 6.1.9. The switching of the external stimulus u_2 comes from the aim of Algorithm 5.1 of minimizing the target functional of (5.1.5) or (5.1.7), respectively. By this switching of u_2, the activity level x_3 comes closer to the desired state by the activation of x_4 which has less costs than letting u_2 be the constant zero function and the desired switch of steady states cannot be performed yet. If u_2 is switched off, then the activity level x_4 starts to decay immediately.

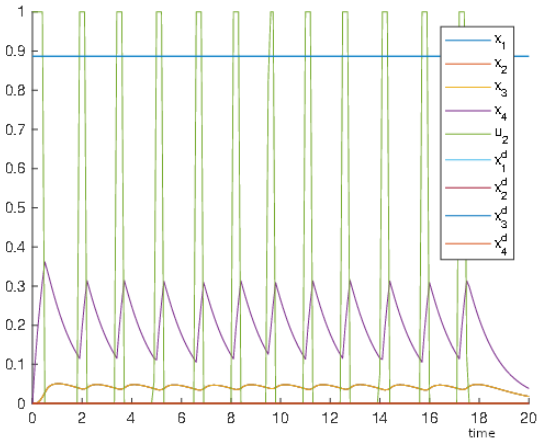

Figure 6.1.9: The time is plotted on the abscissa and the activity level is plotted on the ordinate. The switching of u_2 minimizes the target functional (5.1.5) or (5.1.7), respectively and cannot perform a switch of the steady state yet.

On the other hand if we analyze (6.1.1) where we would like to switch from $x_0 = \begin{pmatrix} 0 & 0 & 0 & 0 \end{pmatrix}$ to the steady state $\begin{pmatrix} 0.8870 & 5.6662 \cdot 10^{-4} & 0.8870 & 5.6662 \cdot 10^{-4} \end{pmatrix}$ and for this purpose once u_1, u_2 and u_3 are applied but u_3 to node 3 instead of node 2, see Figure 6.1.10a and once just u_1 and u_2, see Figure 6.1.10b, then there are more possible intervention points of external stimuli than needed for the desired switch in the first case. As a consequence, the switch of steady states is performed faster.

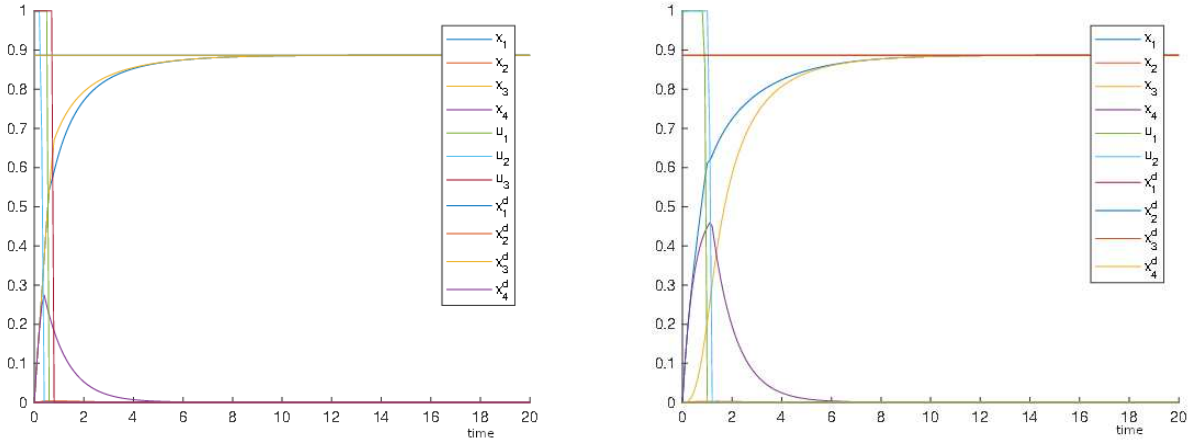

(a) Three external stimuli are applied.

(b) Two external stimuli are applied

Figure 6.1.10: The time is plotted on the abscissa and the activity level is plotted on the ordinate.

Also with the example above we can demonstrate how our framework can figure out the most effective selection of external stimuli that performs the desired switch from all the possible intervention points. This can be very useful if we have a network where the network parameters as well as the

coupling constants of the external stimuli are fitted to data. By the application of Algorithm 5.2 the most effective selection can be figured out that means where the switch can be achieved with the smallest possible use of the potential external stimuli or intervention points, respectively. We remark that the same holds for Algorithm 5.1. For our illustration we let u_1 activate node 1, u_2 activate node 4 where the corresponding coupling constant $\sigma_{42} = 0.23$ instead of 1, see (4.2.1), and let u_3 activate node 3. We first use Algorithm 5.3 for maxNum $= 4$, tol $= 0.1$, $\eta = 0.5$ and $\tau = 0.9$ and obtain that an application of a fully activated u_1 and u_2 for 6.56 time units can perform the desired switch. If we use this output for the initial guess of Algorithm 5.2 for $\alpha = 1$, we obtain that the application of u_1 and u_3 performs the desired switch faster although more shortly applied, see Figure 6.1.11 and thus we can call this selection of external stimuli more efficient compared with the one from Algorithm 5.3. If α is sufficiently small, then Algorithm 5.2 is more likely to detect more external stimuli than needed for the desired switch. These additional external stimuli support the desired switch, see Figure 6.1.12 where $\alpha = 0.5$. This information can be used to fasten up the switch in a real experiment. We obtain the application of external stimulus 1,2 and 3 in our example.

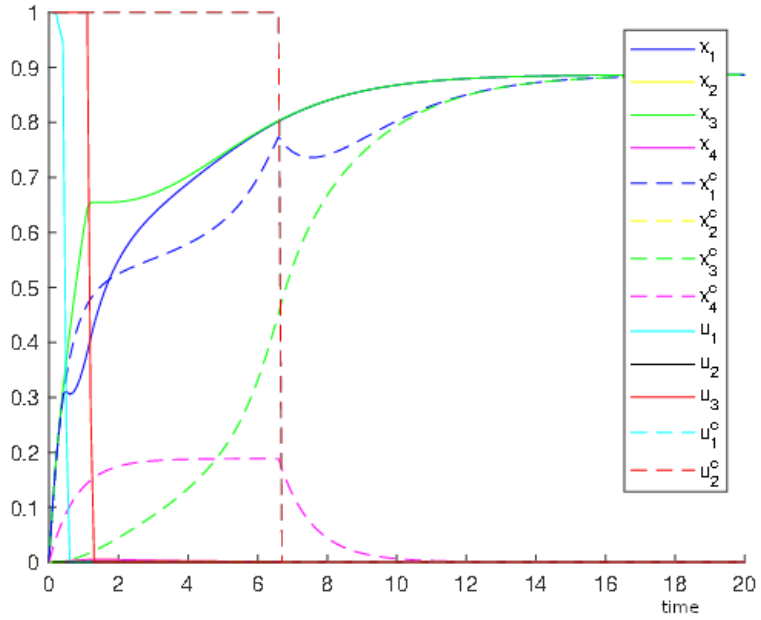

Figure 6.1.11: On the abscissa the time is plotted and on the ordinate the activity level is plotted. The curves with a dashed line belong to the solution from Algorithm 5.3 and the curves with a solid line belong to the solution from Algorithm 5.2 for $\alpha = 1$ where the result from Algorithm 5.3 is used as the initial guess. The curves from the corresponding agents have the same color. We see that the solution from Algorithm 5.2 achieves the desired steady state much faster than the solution from Algorithm 5.3 although the corresponding external stimuli are applied more shortly.

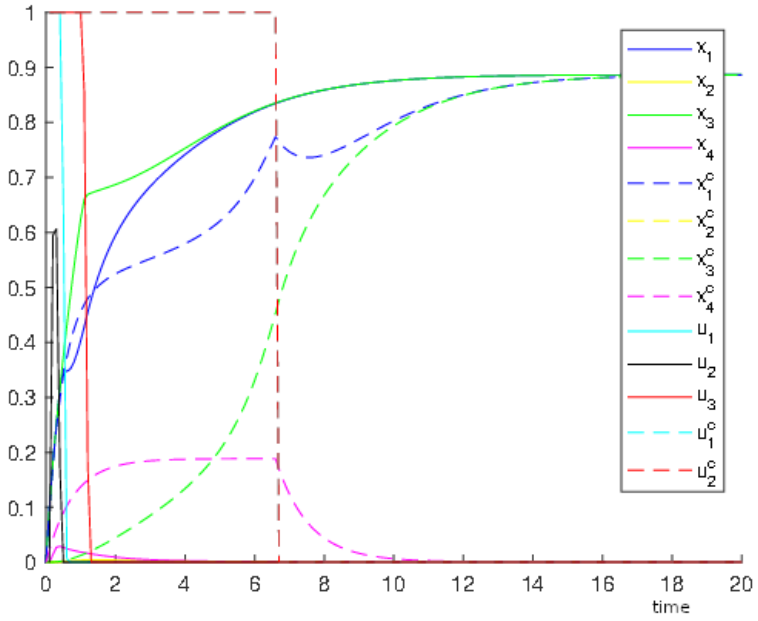

Figure 6.1.12: On the abscissa the time is plotted and on the ordinate the activity level is plotted. The curves with a dashed line belong to the solution from Algorithm 5.3 and the curves with a solid line belong to the solution from Algorithm 5.2 for $\alpha = 0.5$ where the result from Algorithm 5.3 is used as the initial guess. The curves from the corresponding agents have the same color. We see that the external stimuli 1 and 3 from Figure 6.1.11 are supported by the external stimulus 2 which is detected by Algorithm 5.2 as α is sufficiently small such that also small contributions to the switch are worth to be considered.

In our last experiment, we consider external stimuli which affect several nodes at once. This example is the blueprint how our proposed framework can be combined with a data bank driven approach combining the information of an interactom, which is the information what agent in the network affects the others by activation or inhibition, and its affection by drugs. The information of the interactom is used for setting up the system of ordinary equations and all the possible drugs, which can possibly effect more than just one node, are represented within the system of ordinary equations by external stimuli that act on the nodes. Then by the calculations with our optimization framework, we figure out the most effective drug combination as follows for example.

We find a selection of external stimuli which steers our regulatory network from the steady state $x_0 = \begin{pmatrix} 0 & 0 & 0 & 0 \end{pmatrix}$ to the steady state $\begin{pmatrix} 0.8870 & 5.6662 \cdot 10^{-4} & 0.8870 & 5.6662 \cdot 10^{-4} \end{pmatrix}$, called Switch 1, then from the steady state $x_0 = \begin{pmatrix} 0.8870 & 5.6662 \cdot 10^{-4} & 0.8870 & 5.6662 \cdot 10^{-4} \end{pmatrix}$ to the steady state $\begin{pmatrix} 5.6662 \cdot 10^{-4} & 0.8870 & 5.6662 \cdot 10^{-4} & 0.8870 \end{pmatrix}$, called Switch 2 and finally from the steady state $x_0 = \begin{pmatrix} 5.6662 \cdot 10^{-4} & 0.8870 & 5.6662 \cdot 10^{-4} & 0.8870 \end{pmatrix}$ to the steady state $\begin{pmatrix} 0 & 0 & 0 & 0 \end{pmatrix}$ again,

called Switch 3. We consider the following network

$$
\begin{aligned}
\frac{d}{dt}x_1 &= \frac{-\mathrm{e}^5 + \mathrm{e}^{-10\left(\frac{3}{2}\left(\frac{x_3+x_4}{1+x_3+x_4}\right)\left(1-\frac{11}{10}\frac{10x_2}{1+10x_2}\right)-0.5\right)}}{(1-\mathrm{e}^5)\left(1+\mathrm{e}^{-10\left(\frac{3}{2}\left(\frac{x_3+x_4}{1+x_3+x_4}\right)\left(1-\frac{11}{10}\frac{10x_2}{1+10x_2}\right)-0.5\right)}\right)} - x_1 + u_1(1-x_1)\\
\frac{d}{dt}x_2 &= \frac{-\mathrm{e}^5 + \mathrm{e}^{-10\left(\frac{3}{2}\left(\frac{x_3+x_4}{1+x_3+x_4}\right)\left(1-\frac{11}{10}\frac{10x_1}{1+10x_1}\right)-0.5\right)}}{(1-\mathrm{e}^5)\left(1+\mathrm{e}^{-10\left(\frac{3}{2}\left(\frac{x_3+x_4}{1+x_3+x_4}\right)\left(1-\frac{11}{10}\frac{10x_1}{1+10x_1}\right)-0.5\right)}\right)} - x_2 + u_3(1-x_2)\\
\frac{d}{dt}x_3 &= \frac{-\mathrm{e}^5 + \mathrm{e}^{-10\left(\frac{3}{2}\left(\frac{x_3+x_4}{1+x_3+x_4}\right)\left(1-\frac{11}{10}\frac{10x_2}{1+10x_2}\right)-0.5\right)}}{(1-\mathrm{e}^5)\left(1+\mathrm{e}^{-10\left(\frac{3}{2}\left(\frac{x_3+x_4}{1+x_3+x_4}\right)\left(1-\frac{11}{10}\frac{10x_2}{1+10x_2}\right)-0.5\right)}\right)} - x_3 + u_2(1-x_3) + u_1(1-x_3) - u_3x_3\\
\frac{d}{dt}x_4 &= \frac{-\mathrm{e}^5 + \mathrm{e}^{-10\left(\frac{3}{2}\left(\frac{x_3+x_4}{1+x_3+x_4}\right)\left(1-\frac{11}{10}\frac{10x_1}{1+10x_1}\right)-0.5\right)}}{(1-\mathrm{e}^5)\left(1+\mathrm{e}^{-10\left(\frac{3}{2}\left(\frac{x_3+x_4}{1+x_3+x_4}\right)\left(1-\frac{11}{10}\frac{10x_1}{1+10x_1}\right)-0.5\right)}\right)} - x_4 + u_2(1-x_4) - u_1x_4
\end{aligned}
\tag{6.1.3}
$$

where u_1 activates node 1 and node 3 and inhibits node 4, u_2 activates node 3, u_3 activates node 2 and inhibits node 3. The results from Algorithm 5.1 with $\alpha = 0.1$, $T = 20$, $\triangle t = 0.1$, $\epsilon = 10^{-6}$ and ${}^0u = 0$ for Switch 1 can be seen in Figure 6.1.13, for Switch 2 in Figure 6.1.14 where the oscillations of u_2 and u_3 are not necessary for the switch, see Figure 6.1.15 and finally, for Switch 3, see Figure 6.1.16.

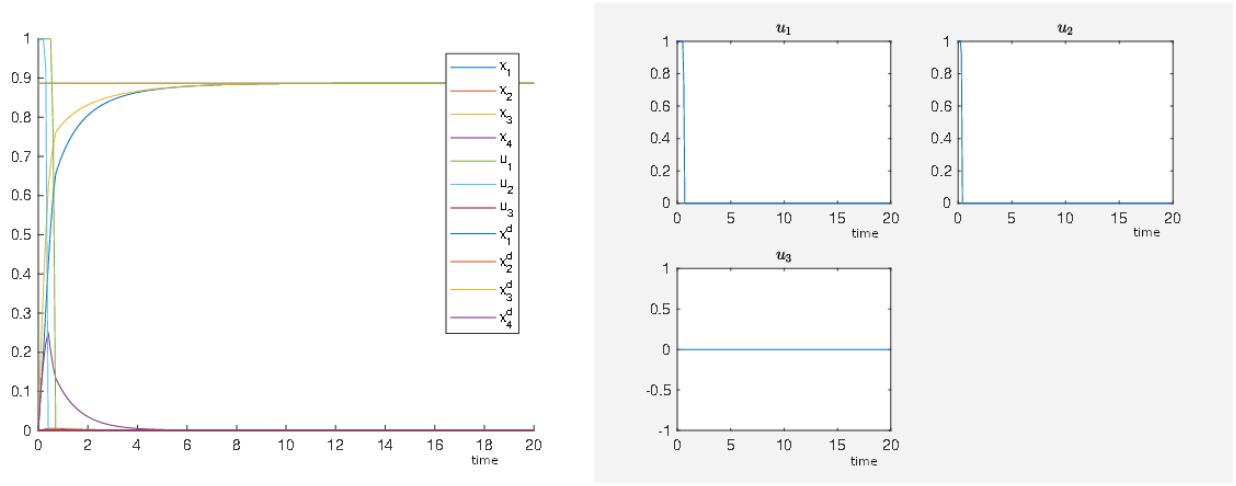

Figure 6.1.13: Switch 1. The time is plotted on the abscissa and the activity level is plotted on the ordinate.

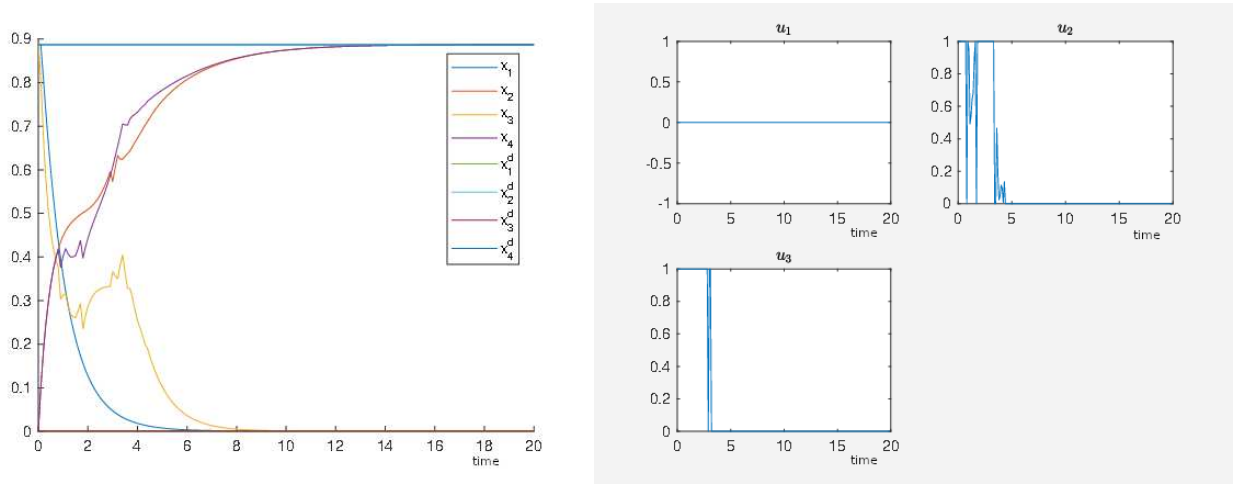

Figure 6.1.14: Switch 2. The time is plotted on the abscissa and the activity level is plotted on the ordinate.

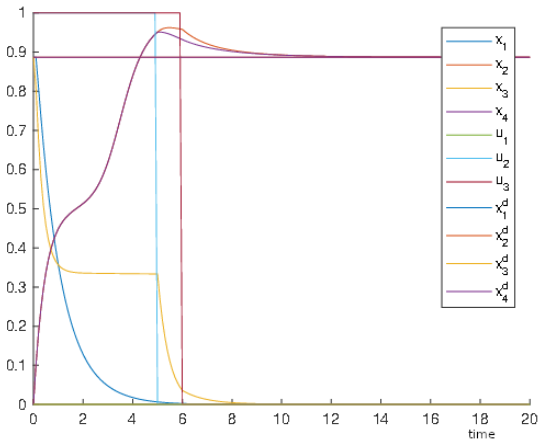

Figure 6.1.15: The time is plotted on the abscissa and the activity level is plotted on the ordinate. Applying u_2 and u_3 in this way performs the desired Switch 2 as well.

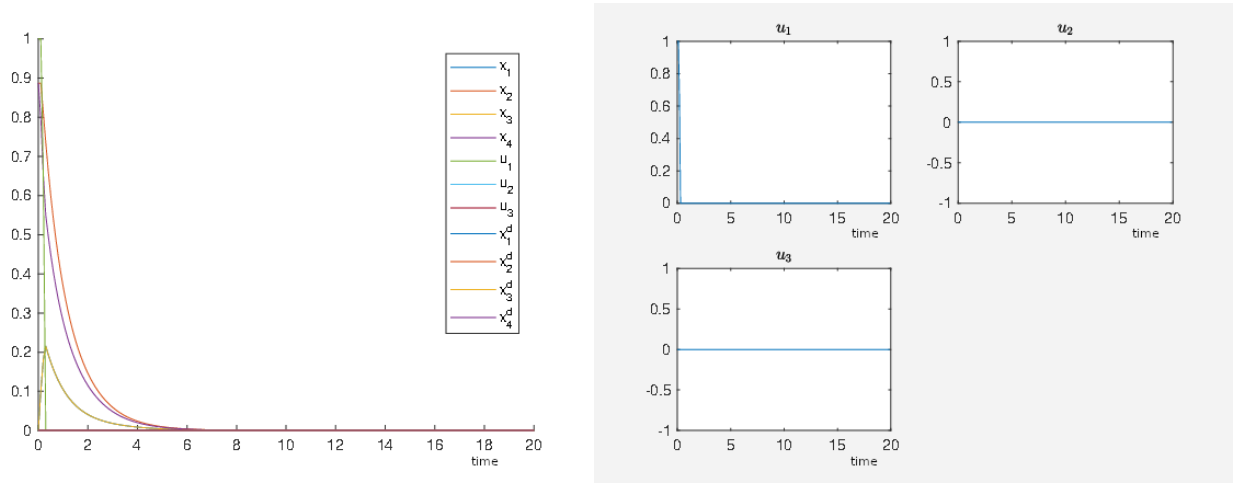

Figure 6.1.16: Switch 3. The time is plotted on the abscissa and the activity level is plotted on the ordinate.

6.2 Induced switches in a platelet network and in a T-cell network

While in Section 6.1 we demonstrate the principal function of the proposed optimal control problem that is utilized for the search for effective network intervention, we relate the framework to well established biological models in order to show the biological relevance of the method.

6.2.1 Application to a platelet network to trigger irreversible aggregation

This section is based on [10, Section 7] and presents a pharmacological illustration for which we use a model that describes the aggregation of platelets. Furthermore we provide also experimental data validating our work. For this purpose, we use the so called SQUAD model that can be found in the supplementary information of [39]. The model is fitted to experimental data with the software Potterswheel that is mentioned in Section 5.3. A schematic of the network can be seen in Figure 6.2.1. For our Matlab implementation, we have the following numbers of the nodes. We have P2Y12 is node 1, P2Y1 is node 2, Ca is node 3, Rap1 is node 4, Akt is node 5, Int is node 6, Src is node 7, PI3K is node 8, PTP is node 9, Throm is node 10 and ThromR is node 11. According to [39] a high integrin (Int) activity is associated with irreversible platelet aggregation. We have identified two steady states. The first one is $\begin{pmatrix} 0 & 0 & 0 & 0 & 0 & 0.91 & 0 & 0 & 0 & 0.1 & 0 \end{pmatrix}$ which has a high integrin activity and thus it is associated with irreversible platelet aggregation. The second one is $\begin{pmatrix} 0 & 0 & 0 & 0 & 0 & 0 & 0 & 0 & 0 & 0.1 & 0 \end{pmatrix}$ which has a low integrin activity and thus it is associated with the reversible platelet aggregation. In [39], we find that adenosine diphosphate (ADP) activates the irreversible aggregation by stimulating the G-protein-coupled receptors (P2Y1 and P2Y12). For all our calculations we use a time horizon $T = 100$ time units and a discretization of the time $\triangle t = 0.01$ to obtain a stable numerical solution of the system of ordinary differential equations with the correct asymptotic behavior.

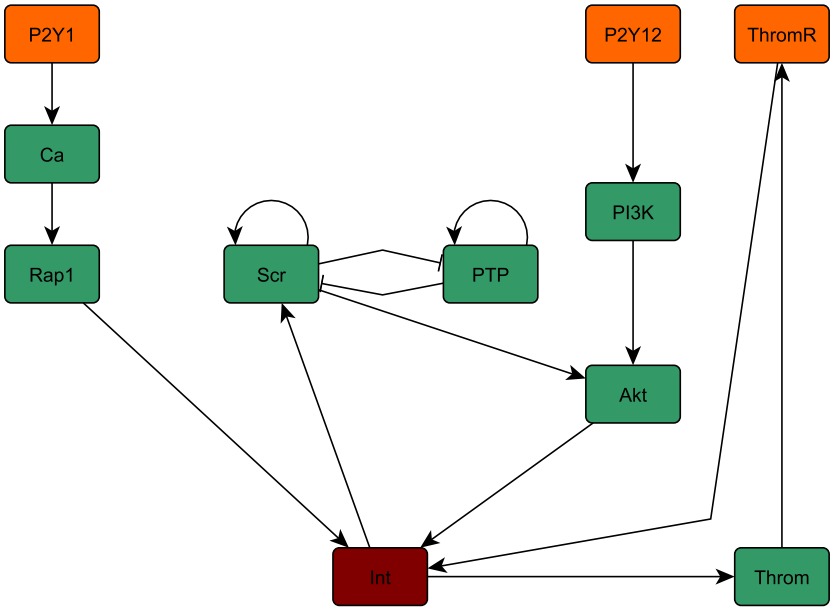

Figure 6.2.1: Schematic of the platelet network analogous to [39, Figure 1]. The nodes are associated with agents as follows. G-protein-coupled receptors, P2Y1 and P2Y12; Calcium, Ca; the small GTPase Rap1, Rap1; sarcoma, Src; protein tyrosine phosphatases, PTP; phosphoinositide-3 kinase, PI3K; protein kinase B, Akt; thromboxane A2, Throm; thromboxane A2 receptor, ThromR.

In the following experiment, we would like to induce a switch from the steady state that is associated with the reversible aggregation of the platelets to the steady state which is associated with the irreversible aggregation of the platelets to demonstrate that the framework is able to find a biological meaningful solution. We have the same system of equation as in [39, SQUAD model] where the corresponding values for the parameters are shown in Table 6.1 with the parameters denoted in our notation and $h = 9.32960030789937$.

parameter	value	parameter	value
γ_2	0.473605541589502	α_7^7	3.50022125981342
γ_1	1.311224584243	β_9^7	29479.7033034441
α_2^3	0.262564903033411	β_7^9	2.1894335236633
γ_3	1.16006274259696	α_9^9	0.00192534456141202
α_3^4	$2.98605802899337 \cdot 10^{-5}$	γ_9	5.90147225148781
γ_4	0.115178489403329	α_6^7	0.000212925981051457
α_8^5	0.0928794298272352	γ_7	0.474687549992427
α_7^5	18.0666459776589	α_1^8	3.54074679376809
γ_5	6.55297153762532	γ_8	190.994110206951
α_5^6	38078.3609932499	α_6^{10}	3744.26406968954
α_4^6	0.476931510419281	γ_{10}	9.37989945700861
α_{11}^6	17.5203571996	α_{10}^{11}	0.0407260335395034
γ_6	1.00168195221449	γ_{11}	5.73705603581402

Table 6.1: Values for the parameters of the corresponding system of ordinary differential equations according to (4.1.1).

However the activation of P2Y1 and P2Y12 is modeled as follows. We have

$$\frac{d}{dt}x_1 = -1.3x_1 + 0.6u_1$$
$$\frac{d}{dt}x_2 = -0.47x_2 + 0.6u_2$$

where u_1 and u_2 are activating external stimuli, like ADP for example, for P2Y12 and P2Y1, respectively. As by the fitting of the data, the nodes' activity levels are not restricted to the interval $[0, 1]$ and thus we do not have to multiply the activating external stimuli by an additional term considering the maximum activity level of the node forcing the activating external stimuli terms to zero if the node's activity level reaches its maximum, see (4.2.4). Furthermore, we equip PTP with an activating external stimulus, ThromR with an inhibiting external stimulus and Akt with an inhibiting external stimulus. We use the output from Algorithm 5.3 for maxNum $= 2$, tol $= 0.1$, $\eta = 0.5$ and $\tau = 0.9$ as an input for Algorithm 5.2 for $\alpha = 0.1$ that converges here faster than the projected gradient method (Algorithm 5.1). From Algorithm 5.3, we obtain that applying stimulus u_1 for 22 time units induces already a switch. From Algorithm 5.1, we also obtain that additionally external stimulus u_2 steers the system towards irreversible platelet aggregation which is in accordance with the results that can be found in [39]. The results from Algorithm 5.2 can be seen in Figure 6.2.2.

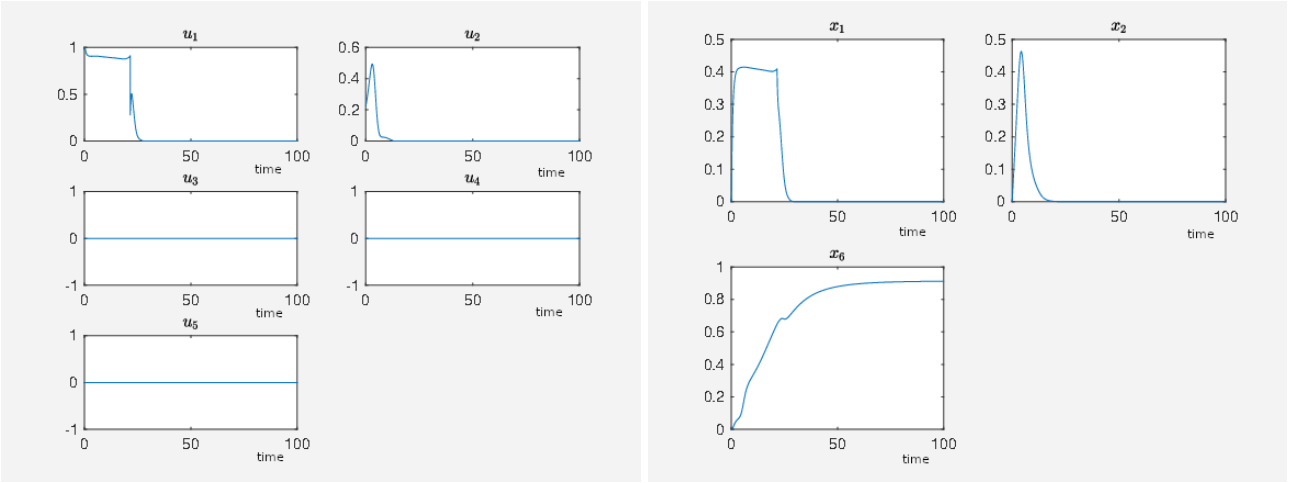

Figure 6.2.2: On the left hand-side, we see the active external stimuli u_1 (activating P2Y12) and u_2 (activating P2Y1) where the others are not active. The others are u_3 activating PTP, u_4 inhibiting ThromR and u_5 inhibiting Akt if they are active. On the right hand-side we have the activity levels of P2Y12 (x_1), of P2Y1 (x_2) and of integrin (x_6) where we see the decay of the receptors' activity (P2Y12, P2Y1) while the activity level of integrin converges to 90%. The time is plotted on the abscissa and the activity level is plotted on the ordinate.

6.2.2 Application to a T-helper cell network to switch between types of T-cells

In this subsection, which is based on [10, Section 8], we consider T-cell maturation and predict intervention points to change T-helper cell types. Specifically, one switch is discussed detailed and confirmed with literature while for the others the results of the calculations are presented in a table. For this purpose we analyze a network with 36 nodes modeling the differentiation of different types of T-helper cells as well as CD4+ Foxp3+ regulatory T-cells (Treg) where the activity levels x_k, $k \in \{1, ..., 36\}$ are restricted to the interval $[0, 1]$. For our calculations we use the numbering of the nodes as in Table 6.2 and the schematic of the model is given in Figure 6.2.3. This model is investigated in [36] with respect to its steady states and it is shown there that this network has five steady states, see [36, Table 2]. These steady states and the corresponding number of the nodes in our calculations are shown in Table 6.2. There is one steady state for each special type of CD4+ T-helper cell, namely Th0, Th1, Th2, Th17 and, in addition, Treg.

Number of node	Name of node	Th0	Th1	Th2	Th17	Treg
1	Foxp3	0	0	0	0	0.9998
2	GATA3	0	0	1	0	0
3	IFN-β	0	0	0	0	0
4	IFN-βR	0	0	0	0	0
5	IFN-γ	0	0.9981	0	0	0
6	IFN-γR	0	1	0	0	0
7	IL-10	0	0	1	0	0
8	IL-10R	0	0	1	0	0
9	IL-12	0	0	0	0	0
10	IL-12R	0	0	0	0	0
11	IL-17	0	0	0	1	0
12	IL-18	0	0	0	0	0
13	IL-18R	0	0	0	0	0
14	IL-2	0	0	0	0	0
15	IL-23	0	0	0	0	0
16	IL-23R	0	0	0	0	0
17	IL-2R	0	0	0	0	0
18	IL-4	0	0	1	0	0
19	IL-4R	0	0	1	0	0
20	IL-6	0	0	0	1	0
21	IL-6R	0	0	0	1	0
22	IRAK	0	0	0	0	0
23	JAK1	0	0	0	0	0
24	JAK3	0	0	0	1	0
25	NFAT	0	0	0	0	0
26	RORγt	0	0	0	1	0
27	SOCS1	0	1	0	0	0
28	STAT1	0	0	0	0	0
29	STAT3	0	0	1	0	0
30	STAT4	0	0	0	0	0
31	STAT5	0	0	0	0	0
32	STAT6	0	0	1	0	0
33	TCR	0	0	0	0	0
34	TGF-β	0	0	0	0	0
35	TGF-βR	0	0	0	0	0
36	Tbet	0	1	0	0	0

Table 6.2: Numbering of the nodes from the T-helper cell network and its steady states.

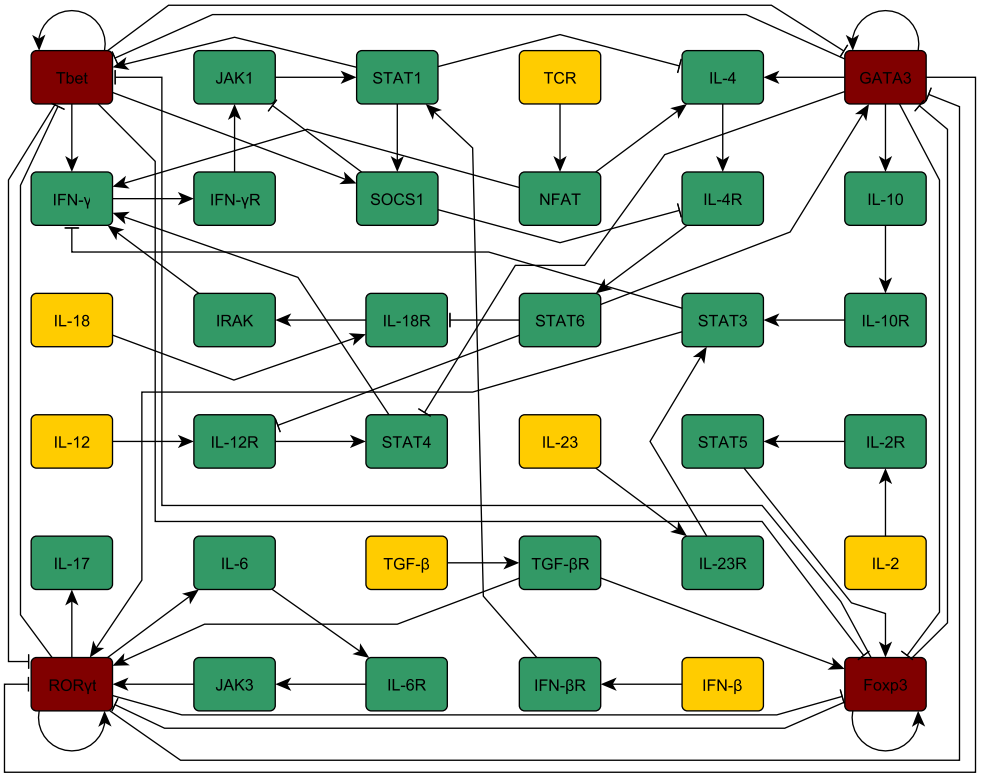

Figure 6.2.3: Schematic of the CD4+ T-helper and Treg network analogous to [36, Figure 2]. The nodes are associated with the following agents. The lineage-specifying transcription factors (dark red nodes) Tbet for Th1, GATA3 for Th2, Foxp3 for Treg and RORγt for Th17; xR, receptor for agent x; IL-x, interleukin x; IFN-x, interferon x; JAKx, Janus kinase x; STATx, signal transducer and activator of transcription x; TCR, T-cell receptor; SOCS1, suppressor of cytokine signaling 1; NFAT, nuclear factor of activated T-cells; IRAK, interleukin receptor-associated kinase; TGF-β, transforming growth factor.

We use (4.2.1) where all the parameters are set to 1 except $h = 50$, see [36, Table 1]. First, we concentrate on the switch from a Th17 cell to a Treg cell. For this purpose we introduce the following external stimuli. External stimulus u_1 activates IFN-β, external stimulus u_2 activates IL-12, external stimulus u_3 activates IL-18, external stimulus u_4 activates IL-2, external stimulus u_5 activates IL-23, external stimulus u_6 activates TCR, external stimulus u_7 activates TGF-β, external stimulus u_8 inhibits RORγt, u_9 inhibits IL-6 and u_{10} inhibits IL-6R which is the receptor for IL-6. With this selection of external stimuli, we intend to induce a switch from Th17 with the corresponding steady state of the network $[0,0,0,0,0,0,0,0,0,0,1,0,0,0,0,0,0,0,0,1,1,0,0,1,0,1,0,0,0,0,0,0,0,0,0,0]$ which serves as initial state for the network to Treg with the corresponding steady state $[0.9998,0,0,0,0,0,0,0,0,0,0,0,0,0,0,0,0,0,0,0,0,0,0,0,0,0,0,0,0,0,0,0,0,0,0,0]$, see Table 6.2 for all the steady states.

In Figure 6.2.4a, we see the result from Algorithm 5.3 for maxNum = 4, tol = 0.1, $\eta = 0.5$ and $\tau = 0.9$. We have that according to our model, inactivation of RORγt and activation of IL-2 and TGF-β for about 4.4 time units perform the desired switch. We take the result from Algorithm 5.3 as an initial guess ${}^0u$ for Algorithm 5.1 with the parameters $\alpha = 0.5$, $T = 20$ and $\triangle t = 0.1$ where the remaining parameters are set as in Subsection 5.1.2. In Figure 6.2.4b we see the results. We have that the inhibition of IL-6, u_9 and IL-6R, u_{10} supports the switch, that means that by the supporting external stimuli the network switches faster to the Treg cell. We stress that by virtue of the self activation of RORγt, according to our model, a direct knock down of RORγt is necessary to induce the switch.

A switch from Th17 to Treg is described for example in the tumor setting [17] where soluble factors contained in ovarian cancer ascites are capable of mediating the transdifferentiation from Th17 to

Treg. While the Foxp3-inducing effect of the cancer ascites is mimicked by the addition of recombinant TGF-β this is not the case concerning suppression of IL-17A expression. Consequently, the cancer ascites must contain additional factors which suppress RORγt expression. This is according to what we show in the present work a prerequisite to complete the switch from Th17 to Treg.

Also with the example we can see the advantage of the presented framework with respect to finding essential molecular agents in the ascites that are important for the switch from Th17 to Treg. We get a hint by the calculation what other molecular agent is necessary for the switch. Then the molecular agents contained in the ascites can be analyzed with respect to the question if they have the required feature and thus decrease the number of experiments that have to be done in order to find the responsible molecular agents. Another way to use the framework favorably for shorten series of experiments is the following. We only have to analyze systematically the effect of the single molecular agents contained in the ascites on the regulatory network. Once this information is available we can figure out a promising selection out of all the molecular agents that is responsible for the switch instead of performing real experiments for all combinations of possible molecular agents. This number of experiments scales exponentially while the number of measuring each effect of each single molecular agent scales only linearly. The method becomes more important the more different agents necessarily have to interact for an observed outcome of an experiment and the more possible agents exist that might contribute to the outcome of an experiment.

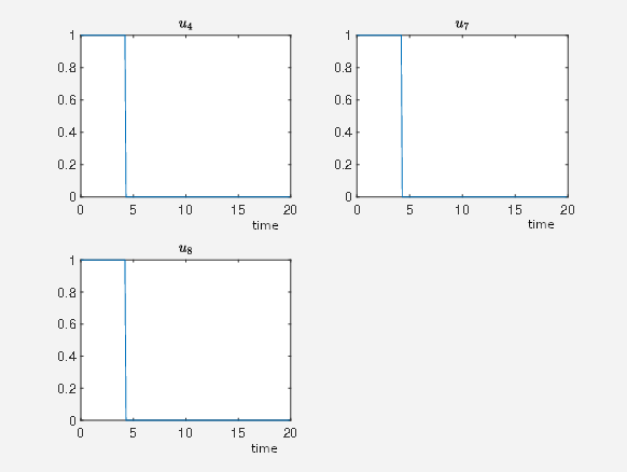

(a) External stimuli calculated by Algorithm 5.3 where u_4 activates IL-2, u_7 activates TGF-β and u_8 inhibts RORγt.

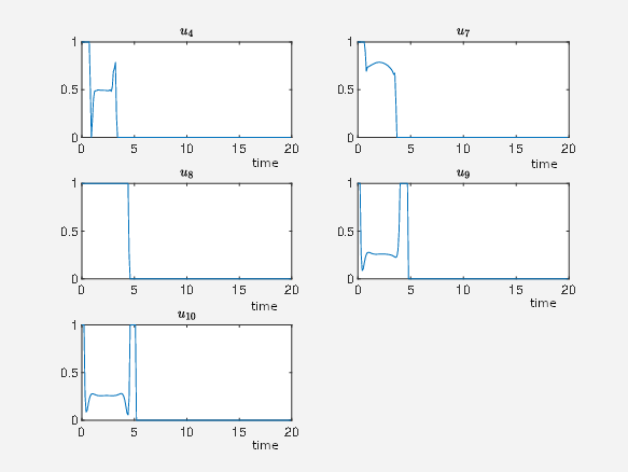

(b) Result calculated by Algorithm 5.1 where u_4 activates IL-2, u_7 activates TGF-β, u_8 inhibits RORγt, u_9 inhibits IL-6 and u_{10} inhibits IL-6R.

Figure 6.2.4: External stimuli that cause a switch from Th17 to Treg where in the left figure there is a small set of external stimuli that performs the desired switch calculated by Algorithm 5.3 and in the right figure we calculate further external stimuli that support the desired switch with Algorithm 5.1. The time is on the abscissa and the activity level is on the ordinate.

In our experiments which we perform with the present network, we notice that once the network has taken a steady state corresponding to a T-cell type Th1, Th2, Th17, Treg, the corresponding attractor is quite robust under perturbations of our external stimuli and is stable with respect to switches between different cell types. However, according to our model presented here in the external stimuli framework for desired switches, roughly spoken, mostly, one has to knock down the lineage-specifying transcription factor of the cell type in which one starts and activate the related cytokines and lymphokines of the desired cell type in order to induce the desired switch of cell types into any desired one, that means Th1, Th2, Th17 or Treg, see Table 6.4.

We remark that perturbations by our external stimuli framework proposed in (4.2.1) or (4.2.2) differ from just perturbing the initial values of the network. In the proposed framework of external stimuli, the duration of application can be varied that cannot be done in the case of perturbing initial values of the network's nodes. Activating or inhibiting external stimuli can act sufficiently long such that inertial network effects can be overcome, for example activated nodes can decay and inactivated

nodes can be activated sufficiently long by others until they reach a certain threshold such that the network relaxes into its desired state. For example, if one takes the steady state associated with the Th17 cell type as an initial state of the network where additionally the initial value for RORγt is set to zero and the initial value for IL-2 and TGF-β is set to one according to the external stimuli proposed in Figure 6.2.4a, then the network relaxes back to the steady state corresponding to the Th17 cell type. This behavior results as just the perturbation of the initial state does not reach a necessary threshold of the activity levels which would cause the relaxation of the network to the desired state, which is the steady state associated with Treg. Thus these perturbations are not sufficient to perform the desired switch. This shows that the inertial network effects can overcome perturbations of the initial states or initial values, respectively, but not if the perturbations of the corresponding nodes last sufficiently long and go beyond a perturbation of an initial state. Then a desired switch can happen. Furthermore, in contrast to our external stimuli framework, it is difficult to implement perturbations of the initial state of a real biological network in an experimental setting because this means, based on the example of the Th17 cell mentioned above, that one has to set up a cell with an expression level where the expression of RORγt is low while at the same time the expression level of IL-17 and IL-6 is high. This might not be possible as the transcription of IL-17 and IL-6 directly depends on the presence of RORγt, see Figure 6.2.3.

For the experimental realization of our predictions, cytokines and cytokine receptors can be readily inhibited, for example by monoclonal antibodies or the receptors stimulated by recombinant cytokines. For the T-cell lineage-specifying transcription factors like RORγt therapeutic targeting is more difficult in principle. However, in the case of RORγt with digoxin or with compounds like GSK805 specific inhibitors are available also for clinical use [60, 59].

In addition a knock out of lineage-specifying transcription factors is also possible, but the knock out changes the topology of a network and thus is not covered by our model so far. Nevertheless knocking out the T-cell lineage-specifying transcription factor and activating cytokines for cell polarization into the desired T-cell type might also work to induce the desired switch. This intuition comes from the fact that each lineage-specifying transcription factor is connected to each other, see Figure 6.2.3, which might provide a robustness with respect to a knock out of a lineage-specifying transcription factor since an active lineage-specifying transcription factor is connected to all the others and thus inhibits the remaining ones.

Next, we equip the network with the following external stimuli and calculate sufficient external stimuli to switch from one T-cell type to another. The dark red nodes are equipped with an inhibiting stimulus that means Tbet with u_1, GATA3 with u_2, Foxp3 with u_3 and RORγt with u_4. All the yellow nodes are equipped with an activating stimulus. That means TCR with u_5, IL-18 with u_6, IL-12 with u_7, IL-23 with u_8, TGF-β with u_9, IL-2 with u_{10} and IFN-β with u_{11}. It is summarized in Table 6.3 on which node the external stimulus acts where a minus sign indicates that the external stimulus inhibits the corresponding node.

Tbet	GATA3	Foxp3	RORγt	TCR	IL-18	IL-12	IL-23	TGF-β	IL-2	IFN-β
-u_1	-u_2	-u_3	-u_4	u_5	u_6	u_7	u_8	u_9	u_{10}	u_{11}

Table 6.3: The external stimuli that act on the corresponding node where a minus sign indicates inhibition.

We take the output of Algorithm 5.3 as an initial guess for Algorithm 5.1 where the parameters are set as above for the first experiment in this subsection. The results are shown in Table 6.4 where the calculations are performed with two different α in (5.1.3). In the case where no external stimulus is found we would have to insert more external stimuli into the network and in this way new network interventions or targets can be found that cause the desired switch. We remark if no external stimulus is found by our algorithms does not necessarily mean that there is no switch possible with the given external stimuli. Next, we see that we do not find any external stimulus to dedifferentiate Th2 or Th17 back into Th0. However it is possible to transform a Th2 cell into a Th1, Th17 or Treg cell and a Th17 cell into a Treg cell. This might indicate that it is not necessary to completely first dedifferentiate a cell and then differentiate it again into a new cell but to switch the molecular effects in a cell at a certain

point such that the cell develops its expression pattern into the desired cell type without completely shutting the specific expression pattern down.

Switch	$\alpha = 0.1$	$\alpha = 2$	Algorithm 5.3
Th0 to Th1	u_6	u_6	u_6
Th0 to Th2	u_5	u_5	u_5
Th0 to Th17	u_8	u_8	u_8
Th0 to Treg	u_9, $(+u_4;\ \alpha = 0.001)$	u_9	u_9
Th1 to Th0	u_1	u_1	u_1
Th1 to Th2	u_1, u_5	u_1, u_5	u_1, u_5
Th1 to Th17	u_1, u_8	u_1, u_8	u_1, u_8
Th1 to Treg	u_1, u_9	u_1, u_9	u_1, u_9
Th2 to Th0	no stimulus	no stimulus	no stimulus
Th2 to Th1	u_2, u_{11}, $(+u_4;\ \alpha = 0.0001)$	u_2, u_{11}	u_2, u_{11}
Th2 to Th17	u_2, u_9, u_{11}	u_2, u_9, u_{11}	u_2, u_9, u_{11}
Th2 to Treg	u_2, u_4, u_9, u_{10}	u_2, u_4, u_9, u_{10}, $(-u_4;\ \alpha = 3)$	u_2, u_9, u_{10}
Th17 to Th0	no stimulus	no stimulus	no stimulus
Th17 to Th1	u_4, no switch	no stimulus	no stimulus
Th17 to Th2	u_4, no switch	no stimulus	no stimulus
Th17 to Treg	u_4, u_9, u_{10}	u_4, u_9, u_{10}	u_4, u_9, u_{10}
Treg to Th0	u_3	u_3	u_3
Treg to Th1	u_3, u_6	u_3, u_6	u_3, u_6
Treg to Th2	u_3, u_5	u_3, u_5	u_3, u_5
Treg to Th17	u_3, u_8	u_3, u_8	u_3, u_8

Table 6.4: External stimuli causing the desired switch between two types of T-cells. The information in brackets means that for the given α further external stimuli are found, indicated by the plus sign and a minus sign indicates that if α is sufficiently big, Algorithm 5.1 reduces the corresponding selection of external stimuli by the external stimulus given in brackets. For further explanation see the text above.

6.3 Finding external stimuli causing a desired expression pattern

In this section, we demonstrate how in principle the framework discussed in Section 5.2 can be used to calculate external stimuli that keep the network in a desired expression pattern where not necessarily all nodes have to have a given expression level. For this purpose, we consider a gene regulatory network for a myocardiocyte given in [11] that is fitted to experimental data. The activity levels of the nodes are restricted to $[0, 1]$. We equip the network with different selections of external stimuli several times and compare the different results of the method that determines the optimal combination of certain external stimuli. These external stimuli can be associated for instance with pharmacological targets or any intervention that is intended with the corresponding experiment. Moreover, we show how (5.2.1) can be used to order different selections of external stimuli with respect to their capability of steering the network to its desired expression pattern. Based on this, we illustrate why the presented framework is an objective method to compare different treatment strategies. The network's graph, which we use, is shown in Figure 6.3.1.

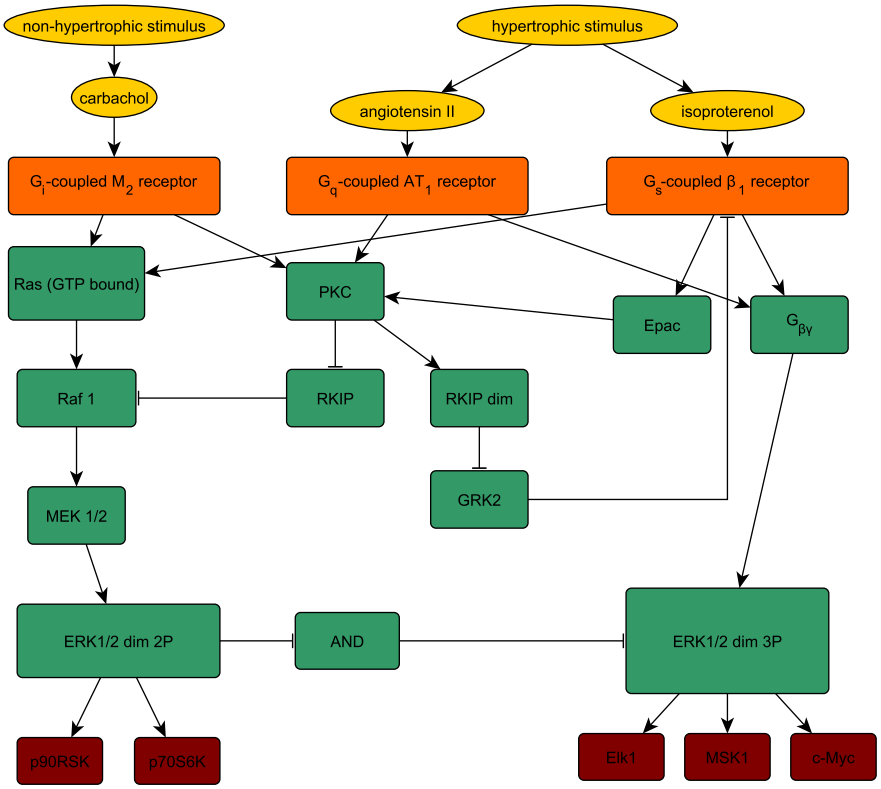

Figure 6.3.1: The graph of a network associated with a myocardiocyte analogous to [11, Fig. 1]

We use (4.2.2) if not otherwise stated where $h = 10$ and ω_k, $k \in \{1, ..., 26\}$ are taken from [11] and are given as in Table 6.5. The mechanism that implements the external stimuli is defined for each experiment separately except $\eta_{kj} = 0$ for all $k \in \{1, ..., m\}$ and all j. The nodes AND and SYSTEM STATE have no biological equivalent. The node SYSTEM STATE is not in the network but is used to permanently activate RKIP and GRK2 to model their constitutive expression in our model of a myocardiocyte. Furthermore, the node SYSTEM STATE activates the node AND such that we have that ERK1/2 dim 3P can only be activated if ERK1/2 dim and $G_{\beta\gamma}$ are active at the same time. The equations for node 1, node 10 and node 26 are given as follows $\frac{dx_1}{dt} = -x_1$, $\frac{dx_{10}}{dt} = -x_{10}$ that can be supplemented by activating external stimuli according to (4.2.2) and $\frac{dx_{26}}{dt} = 1 - x_{26}$ that ensures that the activity level of SYSTEM STATE is constantly one in order to activate node 14, node 16 and node 17.

k	name of the node	ω_k
1	non-hypertrophic stimulus	
2	carbachol	$\frac{11x_1}{1+10x_1}$
3	G_i-coupled M_2 receptor	$\frac{11x_2}{1+10x_2}$
4	RAS (GTP bound)	$\frac{\frac{13}{12}(10x_3+x_{12}+x_{19})}{1+10x_3+x_{12}+x_{19}}$
5	Raf1	$\frac{11x_4}{1+10x_4}\left(1-\frac{1.01x_{14}}{1+0.01x_{14}}\right)$
6	MEK1/2	$\frac{2x_5}{1+x_5}$
7	ERK1/2 dim 2P	$\frac{1.001x_6}{1+0.001x_6}$
8	p90RSK	$\frac{1.01x_7}{1+0.01x_7}$
9	p70S6K	$\frac{1.01x_7}{1+0.01x_7}$
10	hypertrophic stimulus	
11	angiotensin II	$\frac{2x_{10}}{1+x_{10}}$
12	G_q-coupled AT_1 receptor	$\frac{6x_{11}}{1+5x_{11}}$
13	PKC	$\frac{\frac{31}{30}(10x_3+10x_{12}+10x_{20})}{1+10x_3+10x_{12}+10x_{20}}$
14	RKIP	$\frac{2x_{26}}{1+x_{26}}\left(1-\frac{11x_{13}}{1+10x_{13}}\right)$
15	RKIP dim	$\frac{11x_{13}}{1+10x_{13}}$
16	GRK2	$\frac{2x_{26}}{1+x_{26}}\left(1-\frac{31x_{15}}{1+30x_{15}}\right)$
17	AND	$\frac{2x_{26}}{1+x_{26}}\left(1-\frac{101x_7}{1+100x_7}\right)$
18	isoproterenol	$\frac{11x_{10}}{1+10x_{10}}$
19	G_s-coupled β_1 receptor	$\frac{11x_{18}}{1+10x_{18}}\left(1-\frac{1.1x_{16}}{1+0.1x_{16}}\right)$
20	Epac	$\frac{11x_{19}}{1+10x_{19}}$
21	$G_{\beta\gamma}$	$\frac{\frac{21}{20}(10x_{12}+10x_{19})}{1+10x_{12}+10x_{19}}$
22	ERK1/2 dim 3P	$\frac{101x_{21}}{1+100x_{21}}\left(1-\frac{2x_{17}}{1+x_{17}}\right)$
23	Elk1	$\frac{9x_{22}}{1+8x_{22}}$
24	MSK1	$\frac{8x_{22}}{1+7x_{22}}$
25	c-Myc	$\frac{7x_{22}}{1+6x_{22}}$
26	SYSTEM STATE	

Table 6.5: Parameters for the network shown in Figure 6.3.1 according to the model (4.2.2).

We have for the parameters $\sigma_{kj} = \zeta_{kj} = 0$ if the external stimulus u_j has no effect on the node k, $\sigma_{kj} = 1$ if the external stimulus has an activating effect on the node k and $\zeta_{kj} = 1$ if external stimulus has an inhibiting effect on node k. It is stated if we use different values for the parameters than these ones in the present section.

In our case, we associate a high activity of the nodes p90RSK (node 8) and p70S6K (node 9) with beneficial effects and a high activity of the nodes Elk1 (node 23), MSK1 (node 24) and c-Myc (node 25) with maleficent effects. Therefore, we desire a high activity for p90RSK and p70S6K and a low activity for Elk1, MSK1 and c-Myc. We define these five nodes as our nodes of interest and choose for the desired expression pattern the first two agents constant one and the last three agents constant zero. The weights g_k for the first two agents in the target functional (5.2.2) are equal $\frac{3}{2}$ and for the other three equal 1 to compensate the fact, that we have two beneficial nodes and three maleficent ones and thus give the beneficial effect altogether the same weight as the maleficent effect. However it is not necessary that beneficial and maleficent effects have that same weight. It is just an exemplary choice of the g_k, see Remark 5 for what g_k can be utilized.

For our experiments, we always have x_0 the constant zero vector except the last entry is set to 1 which is the initial value of the node SYSTEM STATE. Furthermore, for the experiments, we use Algorithm 5.4 for numMax = 10 or at most the number of external stimuli if there are less than 10 external stimuli and numInt = 3 to obtain the initial guess for the sequential Hamiltonian (SQH)

method, see Algorithm 5.2, with its recommended parameter values except $\kappa = 10^{-14}$ and $\alpha = 0$ if not otherwise stated. The final time is chosen by $T = 20$.

For our first experiment, we have an activating external stimulus on the node carbachol, angiotensin II and isoproterenol. When the SQH method converges, we have $J_0 = 4.802759$ and in Figure 6.3.2, we can see the time curves of the external stimuli which are not the zero function and the time curves of the states of interest. We see that we mainly obtain an activation of carbachol which one can expect according to the schematic depicted in Figure 6.3.1. We see that an activation of carbachol leads to the activation of the beneficial nodes. The short pulse of angiotensin II supports this effect and the maleficent nodes decay after a short and weak activation.

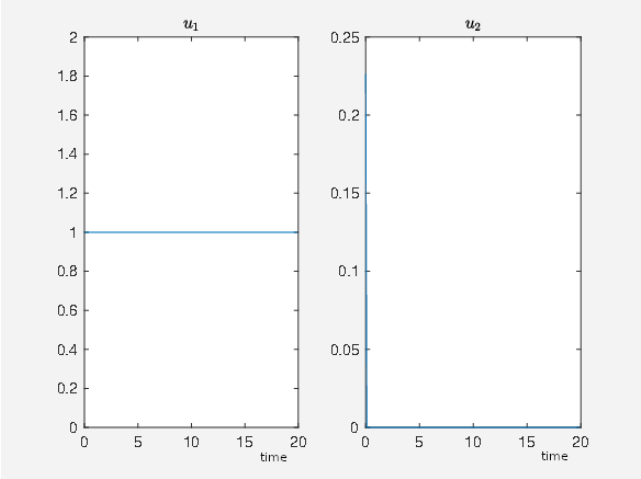

(a) Time curve of the external stimuli where u_1 activates carbachol and u_2 activates angiotensin II.

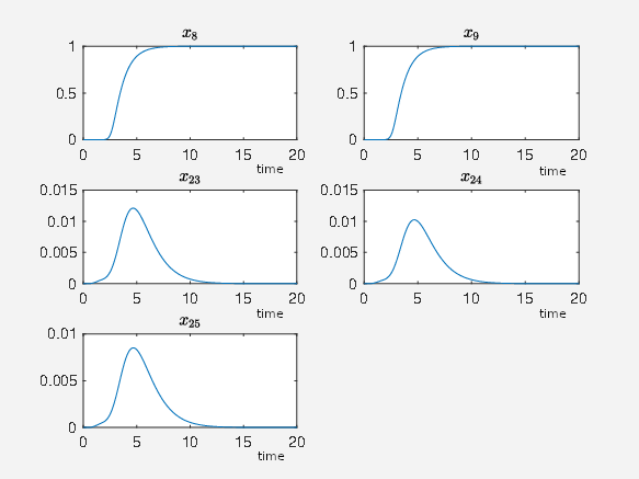

(b) Time curve of the nodes of interests where x_8 is the activity level of p90RSK, x_9 is the activity level of p70S6K, x_{23} is the activity level of Elk1, x_{24} is the activity level of MSK1 and x_{25} is the activity level of c-Myc.

Figure 6.3.2: The time is plotted on the the abscissa and the activity level is plotted on the ordinate.

In Figure 6.3.3, we see the result where we just have an activating external stimulus on carbachol. The target functional value $J_0 = 4.805384$ when the SQH method converges. If we compare the target functional value with the first experiment, we see that it is just a bit bigger and thus both selections of external stimuli can be seen as equivalent with respect to causing an activity level close to the desired one.

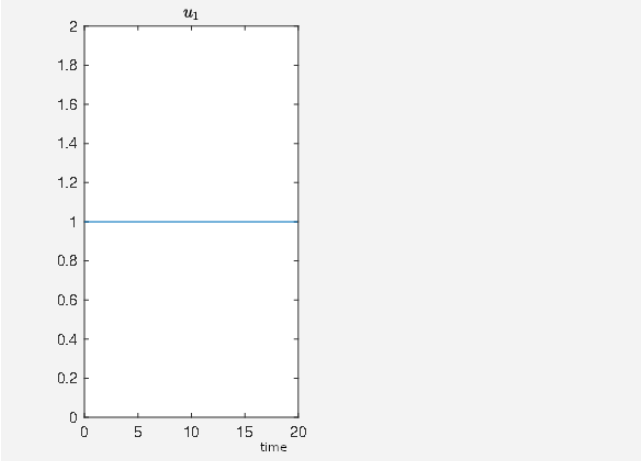

(a) Time curve of the external stimulus where u_1 activates carbachol.

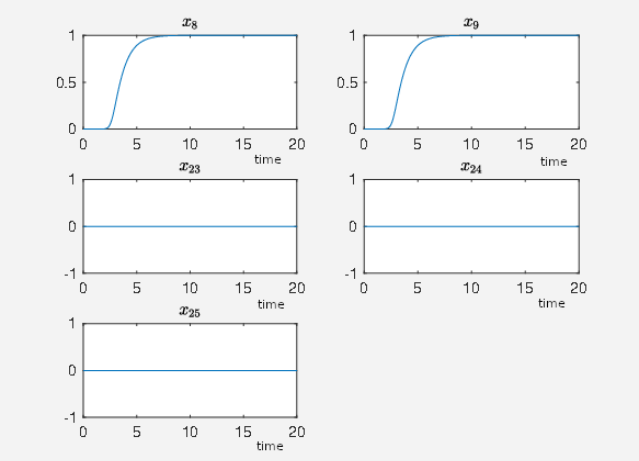

(b) Time curve of the nodes of interests where x_8 is the activity level of p90RSK, x_9 is the activity level of p70S6K, x_{23} is the activity level of Elk1, x_{24} is the activity level of MSK1 and x_{25} is the activity level of c-Myc.

Figure 6.3.3: The time is plotted on the the abscissa and the activity level is plotted on the ordinate.

In our third experiment, we have an activating external control just on angiotensin II and isoproterenol. When the SQH method converges, we have $J_0 = 28.70478$. In Figure 6.3.4, we have the time curves of the external stimuli which are not zero and of the nodes of interest. Compared with the two other experiments, the target functional is much higher which means that an activating external stimulus on carbachol is essential for an activity level of the network's nodes of interest close to our desired activity level compared among carbachol, angiotensin II and isoproterenol.

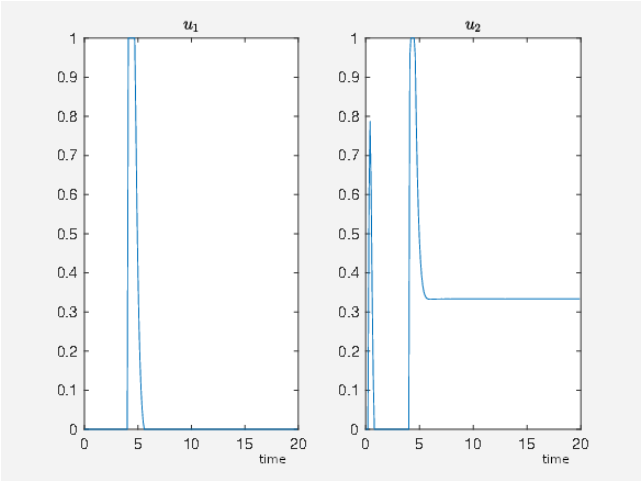

(a) Time curve of the external stimuli where u_1 activates angiotensin II and u_2 activates isoproterenol.

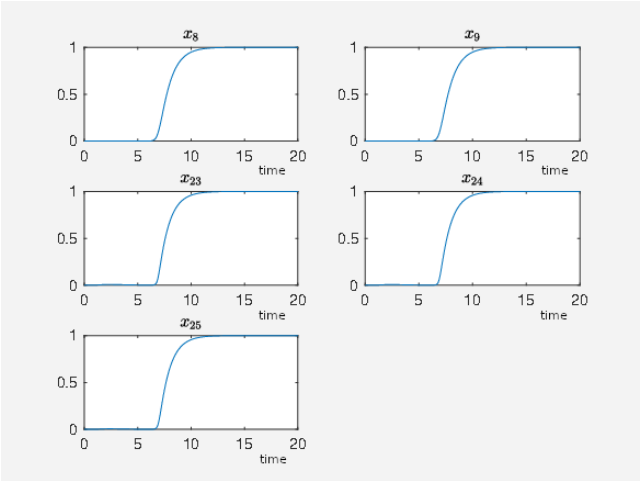

(b) Time curve of the nodes of interests where x_8 is the activity level of p90RSK, x_9 is the activity level of p70S6K, x_{23} is the activity level of Elk1, x_{24} is the activity level of MSK1 and x_{25} is the activity level of c-Myc.

Figure 6.3.4: The time is plotted on the the abscissa and the activity level is plotted on the ordinate.

In our fourth experiment of the present section, we have activating external stimuli on angiotensin II and isoproterenol and one inhibiting external stimuli on ERK1/2 dim 3P. When the SQH method converges, we have $J_0 = 5.513235$ and the corresponding time curves shown in Figure 6.3.5. As the target functional value is close to the one with the experiments where carbachol is activated, we can say that the selection of external stimuli activating angiotensin II and isoproterenol while inhibiting ERK1/2 dim 3P is equivalent to the one where we just activate carbachol compared on the basis of the corresponding target functional values J_0.

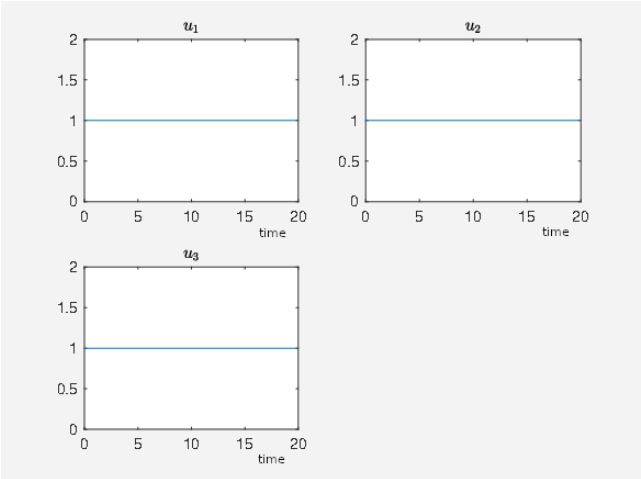

(a) Time curve of the external stimuli where u_1 activates angiotensin II, u_2 activates isoproterenol and u_3 inhibits ERK1/2 dim 3P.

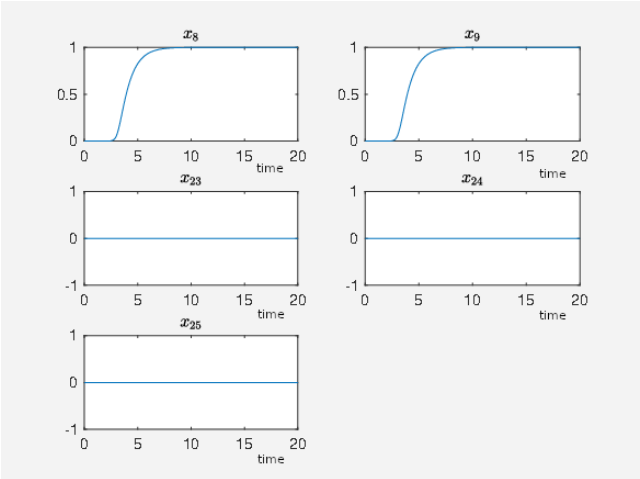

(b) Time curve of the nodes of interests where x_8 is the activity level of p90RSK, x_9 is the activity level of p70S6K, x_{23} is the activity level of Elk1, x_{24} is the activity level of MSK1 and x_{25} is the activity level of c-Myc.

Figure 6.3.5: The time is plotted on the the abscissa and the activity level is plotted on the ordinate.

In Figure 6.3.6 left one, we have the activity level of ERK1/2 dim 3P which is of course an extreme case as we have a very strong inhibition. However, it demonstrates that for a strong inhibition of the ERK1/2 dim 3P, this treatment strategy is almost as good as using an activating external stimulus only on carbachol, see the first two experiments in the present section.

It is possible to fit an external stimulus's ability for inhibition by the parameter ζ_{kj} in (4.2.4) such that the corresponding node has the measured activity level when the inhibitor is active. For this purpose, the parameter $\zeta_{22,3}$ can be decreased and thus the activity level of ERK1/2 dim 3P increases for $\zeta_{22,3}$ tending to zero, see Figure 6.3.6 right one.

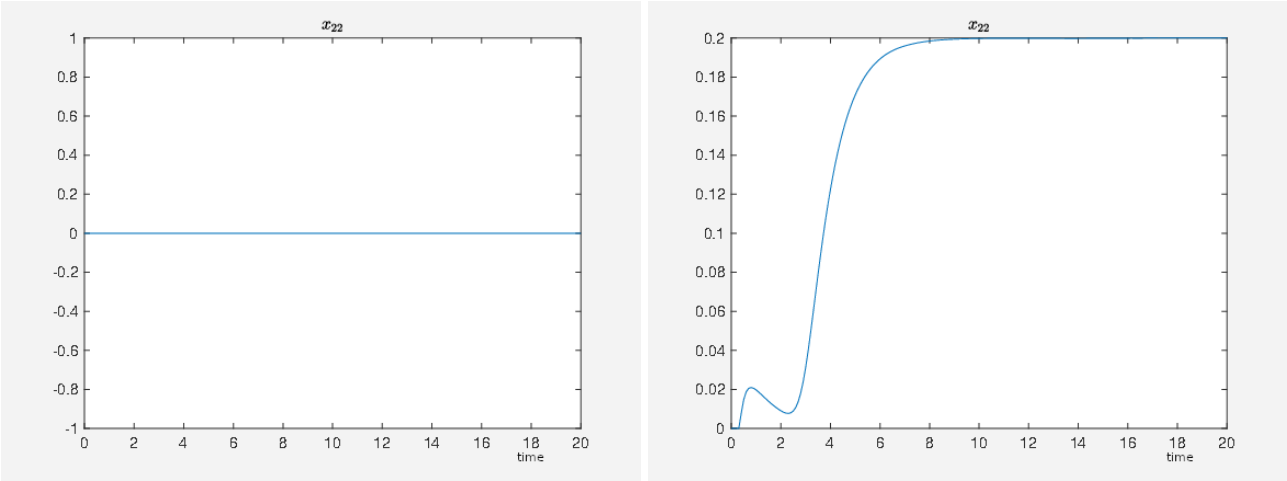

Figure 6.3.6: The time is plotted on the the abscissa and the activity level of the ERK1/2 dim 3P in the forth experiment is plotted on the ordinate. Left figure with $\zeta_{22,3} = 1$ and right one with $\zeta_{22,3} = 0.8$ in (4.2.2).

These four experiments of this section demonstrate how our optimization framework can be used to compare different control strategies with respect to their ability for steering the activity level to the desired activity level of the network's nodes. Once the parameter like T and weights g_k are fixed, then the smaller the target functional value of a certain control strategy is, the more beneficial effects and the less maleficent effects the selection of external stimuli causes. By this procedure, we can determine the most efficient external stimuli that drive the notwork to a desired state and then sort different selections of external stimuli or asses them with respect to their corresponding target functional value given by (5.2.1). The optimization framework serves as an objective method to determine the time curves of the external stimuli such that we have the lowest target functional value possible for the given selection of external stimuli. That means, by our calculations, we figure out the best achievable target functional value that is possible with a certain selection of external stimuli. That means any application of the corresponding treatment is objectively determined by the optimization algorithm and is not liable to the user. We stress that the user just influence on which node an external stimuli acts. Each time curve is then automatically given by the optimization framework, namely by solving (5.2.3). This is where the objectivity comes in. See for example Figure 6.3.4.

However it is clear, that in a real experiment it may be difficult to meet the exact theoretically time curve with the corresponding external stimulus. Also in this case, our framework provides the possibility to compare in silico the corresponding treatments by comparing the target functional values given by (5.2.1) where the time curves of the corresponding external stimuli are set according to their application in the real experiment. The optimization framework gives the theoretically best value of the target functional in order to compare treatment strategies in principal if one applies the external stimuli according to the corresponding time curves given by the optimization. This means that the target functional value from the optimization method is a lower bound for all the target functional values that can be created with a therapy due to different time dependent applications where the intensity of application varies.

6.4 Comparing different treatment strategies quantitatively

In this section, we consider the case where a constitutively activated node alters the activity pattern of a network. A constitutively activation of receptors can be caused by mutations in the receptor itself or its corresponding signal protein. Another example is cell-cell-interaction where a constitutively activated receptor can be caused by secretory cells that constitutively secret the corresponding signal molecule. The presented framework in combination with constitutively activated receptors can also be used in modeling oncogenesis where constitutively activated pathways play a role [14, 20, 29]. Another example is the inhibition of p53 or Retinoblastoma (Rb) protein after a virus infection. This is caused by constitutively translated proteins that bind to p53 or Rb to enhance cell proliferation which is needed for the virus reproduction [44, 33, 63]. This can be modeled analogous to the constitutively activated receptors where the other way round the activity level of the corresponding node is constitutively inhibited by the external stimuli associated with this effect of the virus infection. That illustrates that an external stimulus can also be a virus or the effect of its infection, respectively which the presented framework is able to cover in the described way.

In our example we use the network from Section 6.3 where the G_s-coupled β_1 receptor (node 19) is constitutively activated such that it has continuously about 30% of its maximum activity level. To model this, we equip its corresponding activating node isoproterenol (node 18) with the term $+0.058 - x_{18}$ such that the corresponding equation is given by $\frac{dx_{18}}{dt} = 0.058 - x_{18}$. Furthermore in our experiment node 10 (hypertrophic stimulus) is not activated and thus stays at zero if an initial value of zero is chosen. This ensures that isoproterenol stays at a constant level of 5.8% of its maximum activation which has the consequence that the G_s-coupled β_1 receptor has about 30% of its maximum activity level, see Figure 6.4.1.

As in Section 6.3, we associate a high activity of the nodes p90RSK (node 8) and p70S6K (node 9) with beneficial effects and a high activity of the nodes Elk1 (node 23), MSK1 (node 24) and c-Myc (node 25) with maleficent effects, that is why we desire a low activity for them. We define these five nodes as our nodes of interest and choose the desired state for the first two ones constant one and for the last three constant zero. The weights g_k for the the first two are again equal $\frac{3}{2}$ and for the other three equal 1. We always have x_0 equal the constant zero vector except the activity level for AND, GRK2 and SYSTEM STATE equal 1 and we use Algorithm 5.4 for numMax = 10 and numInt = 3 to obtain the initial guess for the sequential quadratic Hamiltonian (SQH) method (Algorithm 5.2) with its recommended parameter values except $\kappa = 10^{-14}$ and $\alpha = 0$ if not otherwise stated. The final time is chosen by $T = 60$.

If the network is unperturbed, that means no further intervention to the network depicted in Figure 6.3.1 is done, then the constitutively activated G_s-coupled β_1 receptor causes the following activity pattern in the network, where we show the activity level of some nodes in Figure 6.4.1 with $J_0 = 160.1896$ given in (5.2.2). We see that the activity level of the nodes associated with maleficent effects (node 23, 24, 25) are highly active while the nodes associated with beneficial effects (node 8, 9) are at a very low activity level. Furthermore, we see that a constitutively activated receptor is able to hold the network in a certain state that means a constant expression pattern. Thus the expression pattern of the network is also constitutively altered compared to the steady state in which the network would be if the receptor was totally inactive.

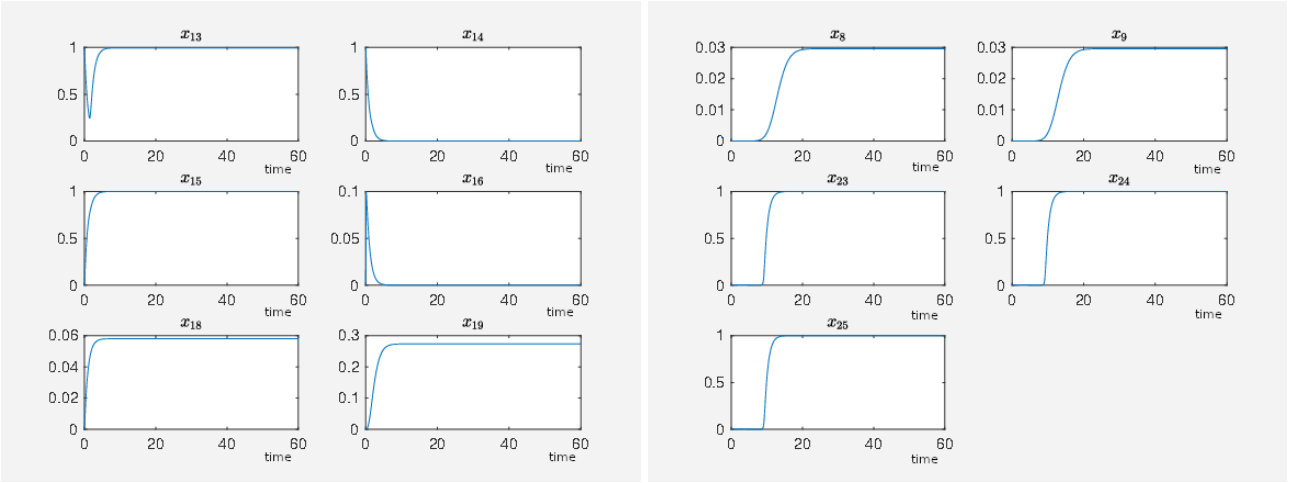

Figure 6.4.1: On the abscissa, we have the time and on the ordinate the activity level for PKC (node 13), RKIP (node 14), RKIP dim (node 15), GRK2 (node 16), isoproterenol (node 18), G_s-coupled β_1 receptor (node 19), p90RSK (node 8), p70S6K (node 9), Elk1 (node 23), MSK1 (node 24), c-Myc (node 25).

Now, we show how to apply our framework to discuss different treatment strategies that improve the expression pattern in our favor. A strategy to reduce the target functional value which means that it increases the beneficial effects is to inhibit the G_s-coupled β_1 receptor which we call the β-block strategy in this work. When the SQH method converges, we have $J_0 = 90.09628$. The results are shown in Figure 6.4.2 and some activity levels of nodes in Figure 6.4.3. The time curve of the corresponding external stimulus is maybe a delicate issue in a real experiment. With a constant external stimulus with value 0.2, we have the value of the cost functional $J_0 = 90.10581$. Therefore, it is not needed to have such a highly structured time curve as shown in Figure 6.4.2 because we get the same order of magnitude of the target functional with the corresponding constant external stimulus. Notice that it is sufficient to reduce the activity level of the G_s-coupled β_1 receptor from about 30% to about 24% such that the activity level of Elk1, MSK1 and c-Myc drops from about 100% to 1%. That means that we have identified a threshold in the activity of the G_s-coupled β_1 receptor for the activity of these three nodes Elk1, MSK1 and c-Myc.

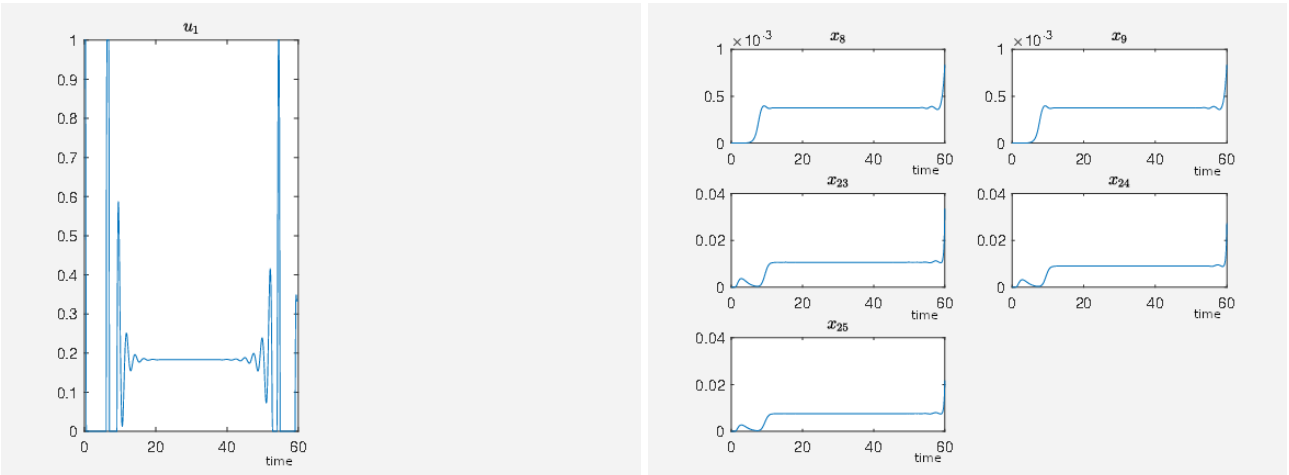

(a) The external stimulus u_1 inhibits the G_s-coupled β_1 receptor.

(b) Time curve of the nodes of interests where x_8 is the activity level of p90RSK, x_9 is the activity level of p70S6K, x_{23} is the activity level of Elk1, x_{24} is the activity level of MSK1 and x_{25} is the activity level of c-Myc.

Figure 6.4.2: The time is plotted on the the abscissa and the activity level is plotted on the ordinate.

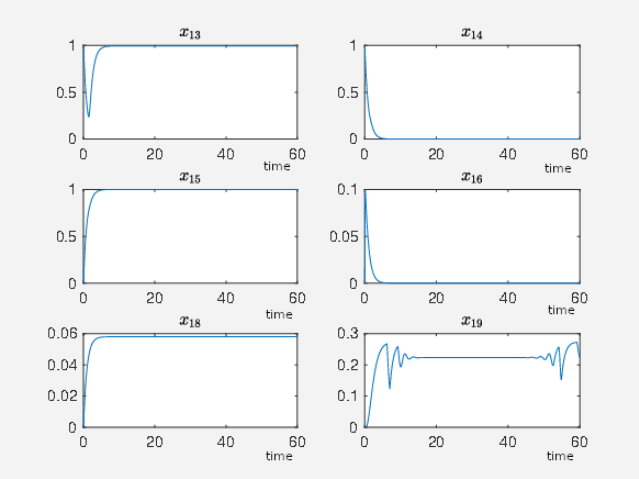

Figure 6.4.3: On the abscissa, we have the time and on the ordinate the activity level for PKC (node 13), RKIP (node 14), RKIP dim (node 15), GRK2 (node 16), isoproterenol (node 18) and G_s-coupled β_1 receptor (node 19) where the G_s-coupled β_1 receptor is inhibited.

If it is not possible to inactivate the G_s-coupled β_1 receptor, then one can inhibit the PKC instead. The results are shown in Figure 6.4.4 with $J_0 = 90.09628$.

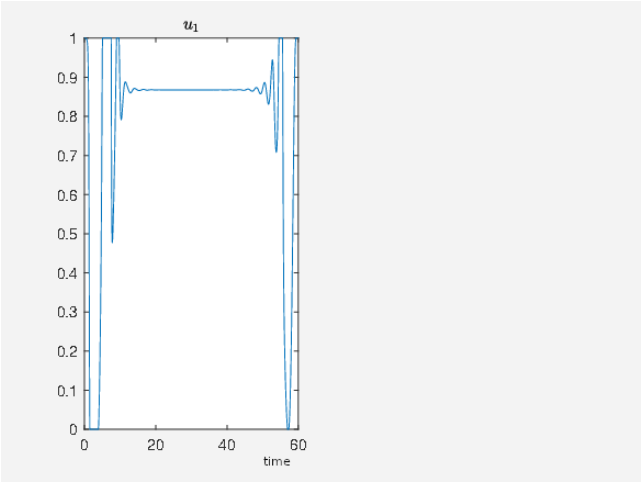

(a) The external stimulus u_1 inhibits PKC.

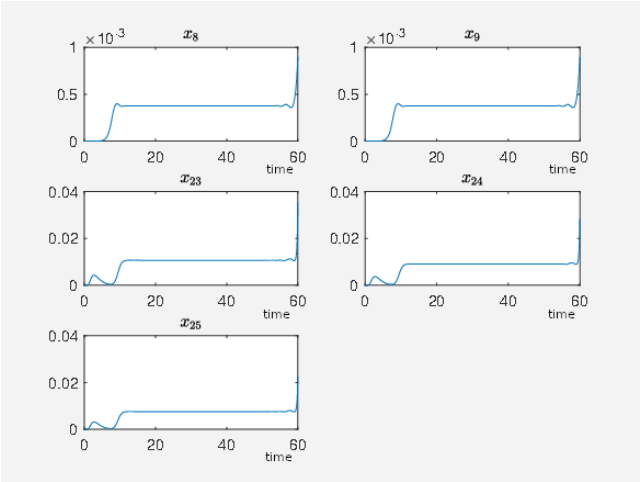

(b) Time curve of the nodes of interests where x_8 is the activity level of p90RSK, x_9 is the activity level of p70S6K, x_{23} is the activity level of Elk1, x_{24} is the activity level of MSK1 and x_{25} is the activity level of c-Myc.

Figure 6.4.4: The time is plotted on the the abscissa and the activity level is plotted on the ordinate.

Alternatively, we can remove RKIP from the system. Notice that then there is no RKIP dim, which is the dimerization of RKIP, in the system and thus, we have to inhibit the node corresponding to RKIP dim simultaneously such that the activity level of RKIP dim decays. That means that the corresponding external stimulus effects two nodes at once and appears in both corresponding equations describing the evolution of the node RKIP and RKIP dim, respectively. The results can be seen in Figure 6.4.5 with $J_0 = 90.09642$. This means that this treatment strategy is equivalent to the one presented in Figure 6.4.4. This comes from the fact that both treatment strategies inactivate Elk1, MSK1 and c-Myc.

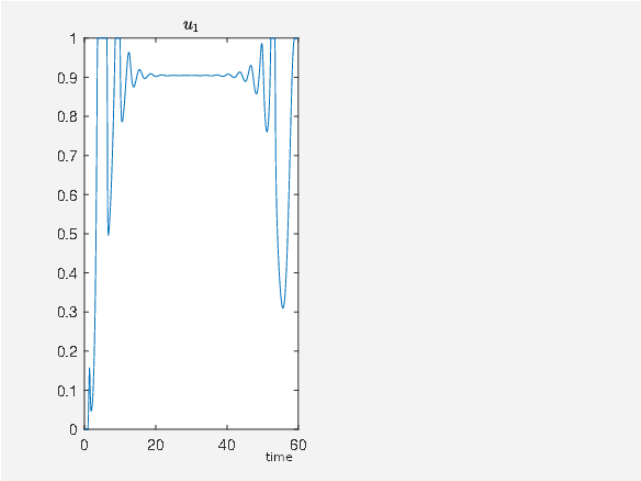

(a) The external stimulus u_1 inhibits RKIP and RKIP dim at once.

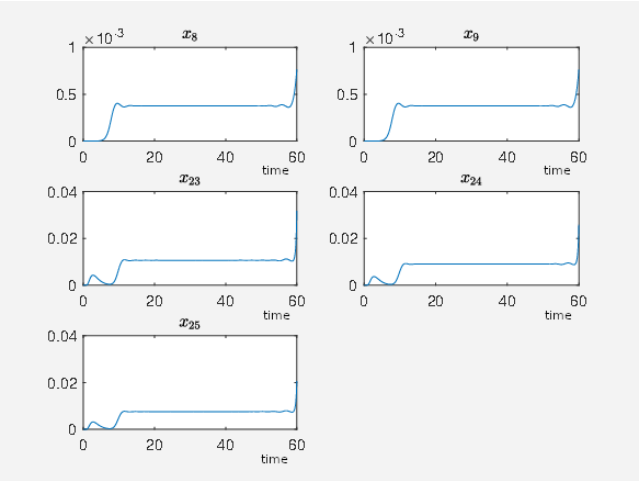

(b) Time curve of the nodes of interests where x_8 is the activity level of p90RSK, x_9 is the activity level of p70S6K, x_{23} is the activity level of Elk1, x_{24} is the activity level of MSK1 and x_{25} is the activity level of c-Myc.

Figure 6.4.5: The time is plotted on the the abscissa and the activity level is plotted on the ordinate.

In Figure 6.4.6, we can compare the time curves for PKC, RKIP and RKIP dim for inhibiting PKC (left picture) and inhibiting RKIP/RKIP dim. We see that it is sufficient to lower the activity level of RKIP dim just from 1 to about 0.8, compare with Figure 6.4.1 for instance, in order to decrease the activity levels of of Elk1, MSK1 and c-Myc to a low level. This makes sense according to the schematic shown in Figure 6.3.1 because GRK2 is not inhibited and inhibits in turn the G_s-coupled β_1 receptor. By the fitting of the network we have in this example that already a small decreasing of the activity level of RKIP dim causes the desired decreasing of the activity level of Elk1, MSK1 and c-Myc.

These treatments results at least in a low activity of Elk1, MSK1 and c-Myc. However, the time curves for the nodes p90RSK and p70S6K stay at a very low level. This means that the used strategy is not able to activate these nodes. However it reduces the activity level of the nodes Elk1, MSK1 and c-Myc. To have a further improvement, we equip the network with further external stimuli in the next experiment.

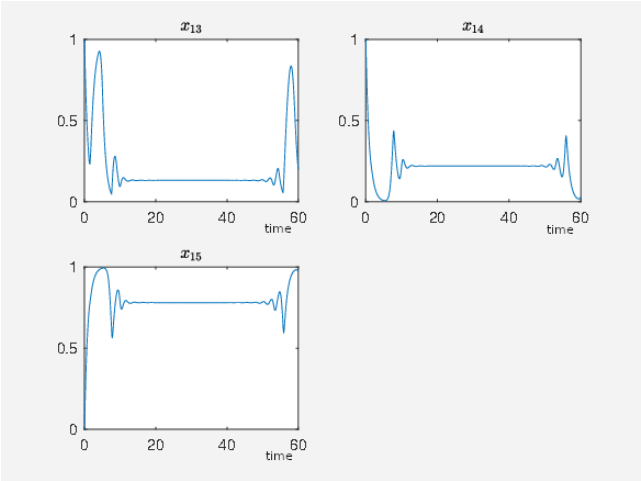

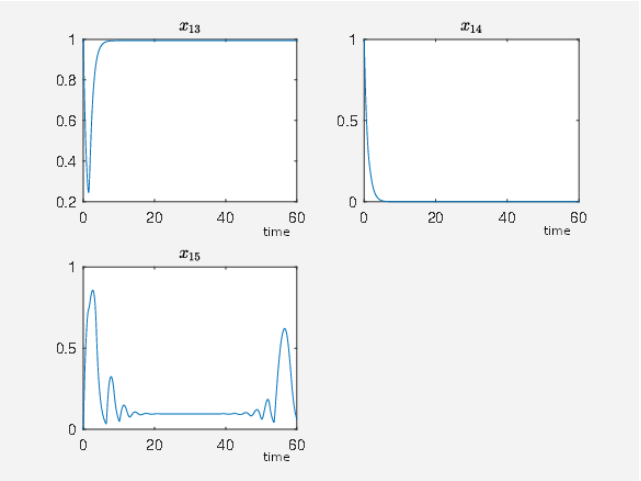

Figure 6.4.6: On the abscissa, we have the time and on the ordinate we have the activity level of PKC (node 13), RKIP (node 14) and RKIP dim (node15). On the left hand-side PKC is inhibited and on the right hand-side RKIP and RKIP dim is inhibited which can be realized by for example removing RKIP and RKIP dim from the system in a real experiment.

We equip the nodes PKC (u_1), RKIP (u_2), RKIP dim (u_2), ERK1/2 dim 3P (u_3), G_s-coupled β_1 receptor (u_4) and Ras (GTP bound) (u_5) with inhibiting external stimuli and the nodes angiotensin II

(u_6) and isoproterenol (u_7) with activating external stimuli. We set $\zeta_{22,3} = 0.95$ which means that the external stimuli u_3 cannot totally inactivate ERK1/2 dim 3P. In Figure 6.4.7, we can see the results. Notice that we now have high activity levels for the nodes p90RSK and p70S6K and still a low activity level for the nodes Elk1, MSK1 and c-Myc which results in a lower target functional value than in the last experiment. We have a target functional value $J_0 = 6.594448$.

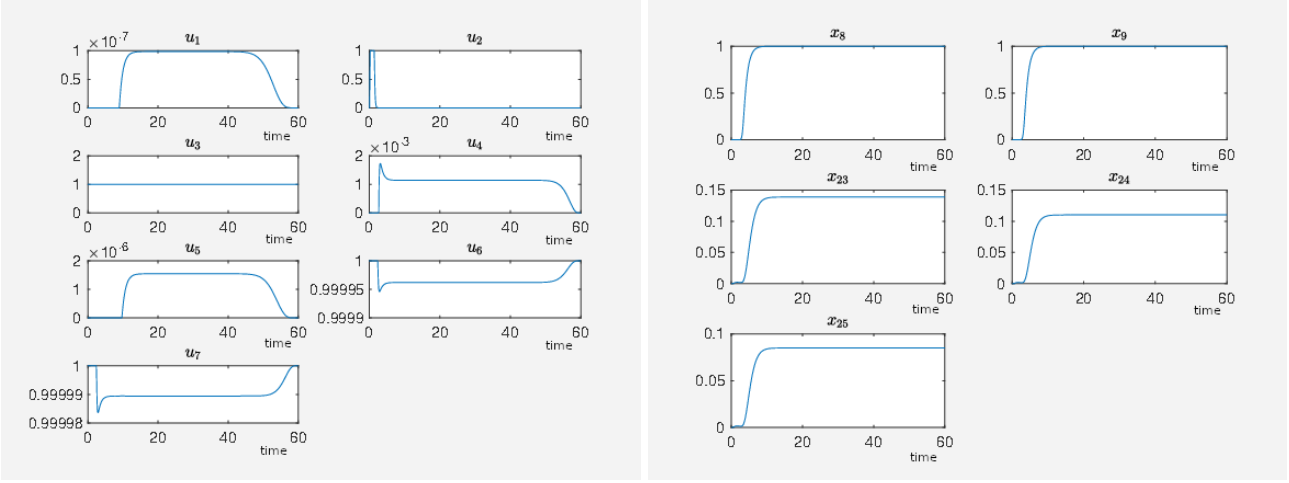

(a) Time curves of external stimuli where u_1 inhibits PKC, u_2 inhibits RKIP and RKIP dim, u_3 inhibits ERK1/2 dim 3P, u_4 G_s-coupled β_1 receptor, u_5 inhibits Ras (GTP bound), u_6 activates angiotensin II and u_7 activates isoproterenol.

(b) Time curves of the nodes of interests where x_8 is the activity level of p90RSK, x_9 is the activity level of p70S6K, x_{23} is the activity level of Elk1, x_{24} is the activity level of MSK1 and x_{25} is the activity level of c-Myc.

Figure 6.4.7: The time is plotted on the the abscissa and the activity level is plotted on the ordinate.

In Figure 6.4.7, there are many active external stimuli. By increasing $\alpha > 0$, we reduce the number of active external stimuli and thus we extract the most effective external stimuli which have much effect on reducing the target functional value. For $\alpha = 0.8$, we only have u_3, u_6 and u_7 as active external stimuli. The results can be seen in Figure 6.4.8.

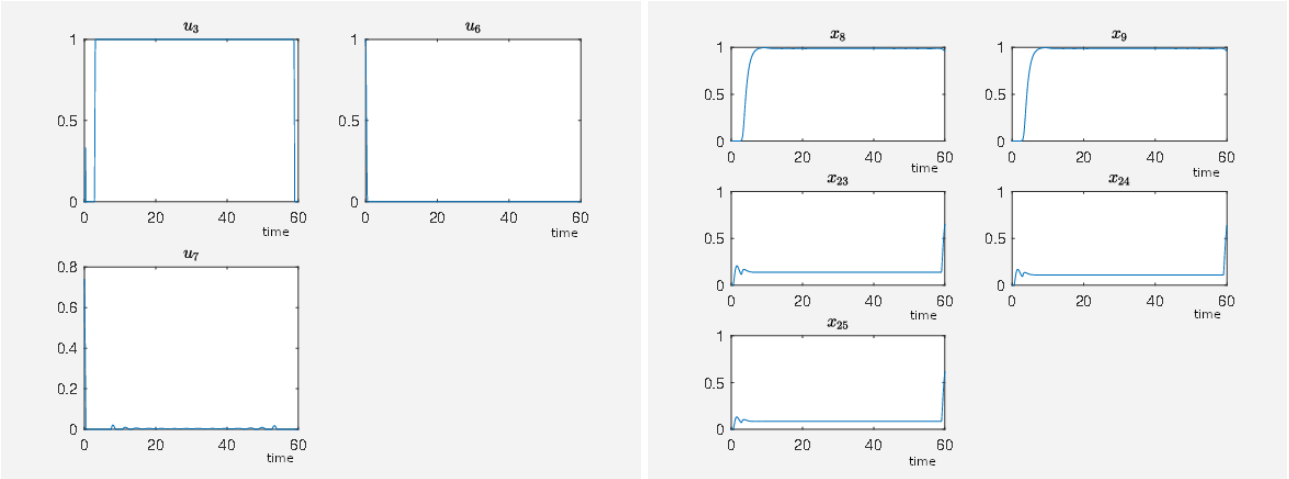

(a) Time curve of external stimuli where u_3 inhibits ERK1/2 dim 3P, u_6 activates angiotensin II and u_7 activates isoproterenol.

(b) Time curve of the nodes of interests where x_8 is the activity level of p90RSK, x_9 is the activity level of p70S6K, x_{23} is the activity level of Elk1, x_{24} is the activity level of MSK1 and x_{25} is the activity level of c-Myc.

Figure 6.4.8: The time is plotted on the the abscissa and the activity level is plotted on the ordinate.

If we perform the same experiment just with the active external stimuli from Figure 6.4.8 for $\alpha = 0$ where we only use Algorithm 5.4, then we obtain $J_0 = 7.118559$ for the full activity of u_3 and u_7 where the activity level of the G_s-coupled β_1 receptor is about 98% of its maximum activity level and

$J_0 = 7.107087$ for full activity of u_3 and u_6 where the activity level of the G_q-coupled AT_1 receptor is about 98% of its maximum activity level which is almost the same target functional value as in the case with many external stimuli more shown in Figure 6.4.7. This demonstrates that this combination of external stimuli u_3 and u_7 or u_3 and u_6 are the essential ones to obtain a beneficial effect on the network, which means to have a low target functional value. While the other external stimuli also have beneficial effects, their contribution is minor compared to the effects of u_3 and u_7 or u_3 and u_6. We can say that compared with the value of the target functional of the unperturbed system ($J_0 = 160.1896$) the treatment strategies u_3 and u_7 or u_3 and u_6 are equivalent with the one shown in Figure 6.4.7 where the big advantage is that only two stimuli have to be applied instead of seven.

We remark without the external stimulus u_3, we are just able to obtain a target functional value of $J_0 \approx 89$, which stresses the importance of the inhibition of ERK1/2 dim 3P for achieving of a beneficial state for the network.

Next, we investigate to what activity level we have to knock down ERK1/2 dim 3P in order to be still as good as just inhibiting the G_s-coupled β_1 receptor, PKC or RKIP/RKIP dim, that means to obtain a target functional value $J_0 \approx 90$ where only the maleficent nodes have a low activity level, however also the beneficial nodes. We choose the treatment strategy where u_3 inhibits ERK1/2 dim 3P (node 22) and u_6 activates angiotensin II (node 11). For this purpose, we use Algorithm 5.4 for different values of $\zeta_{22,3}$ which models the strength how much the activity level of ERK1/2 dim 3P can be inhibited by the external stimulus u_3. The results are presented in Table 6.6, where for each experiment the external stimuli are fully active. We see that if the activity level of ERK1/2 dim 3P is at least at 10% of its maximum activity then, we still have a small target functional value $J_0 \approx 20$ compared with $J_0 \approx 90$ which is achieved by just applying our $\beta-$block strategy mentioned above. Furthermore, as the activity level of p90RSK and p70S6K are at 1 for all $\zeta_{22,3}$ in Table 6.6, we have that at about 5% of the maximum activity level of ERK1/2 dim 3P the maleficent effects abruptly rise (activity levels of Elk1, MSK1 and c-Myc), see also Figure 6.4.9, which can be associated with an abrupt worsening of the treatment which does not mean that the treatment is already worse. For example it can be that also higher values of J_0 are tolerable in vivo for the desired beneficial effects while the maleficent effects are still not noticeable.

In addition if one has a further restriction like that the activity level of Elk1, MSK1 and c-Myc is supposed to be below 15%, then one can see from Table 6.6 that the activity level of ERK1/2 dim 3P is supposed to stay below 5% of its maximum activity level. Additionally we still have a high activity level of p90RSK and p70S6K in contrast to the treatment strategy where one inhibits just the G_s-coupled β_1 receptor or PKC or RKIP/RKIP dim. Furthermore, we see from Table 6.6 that the more we are able to inhibit ERK1/2 dim 3P the better it is for the treatment, that means the lower the activity levels of Elk1, MSK1 and c-Myc are.

In Figure 6.4.10, we can see the corresponding time curve for the activity level of ERK1/2 dim 3P at 10% of its maximum level. In this case the activity level of p90RSK and p70S6K is 1 and of Elk1, MSK1 and c-Myc is between 0.3 and 0.5. We conclude that if the activity levels of p90RSK and p70S6K are low in spite of a constitutively activated G_s-coupled β_1 receptor, one can recommend to activate the G_s-coupled β_1 receptor even more by angiotensin II until the activity levels of p90RSK and p70S6K are high if one can manage it at the same time to have the activity level of ERK1/2 dim 3P at at most 10% of its maximum activity level by some treatment. In other words, when inhibiting ERK1/2 dim 3P, we can have that a hypertrophic stimulus becomes a non-hypertrophic stimulus.

$\zeta_{22,3}$	J_0	Activity level in %			
		ERK1/2 dim 3P	Elk1	MSK1	c-Myc
1	6.08	0	0	0	0
0.99	6.08	1	1	1	1
0.95	7.12	5	14	11	8
0.92	12.89	8	35	29	22
0.9	20.81	10	50	43	35
0.8	63.57	20	88	85	80
0.7	78.90	30	96	95	93
0.6	83.98	40	98	97	97

Table 6.6: Results for different $\zeta_{22,3}$ from Algorithm 5.4.

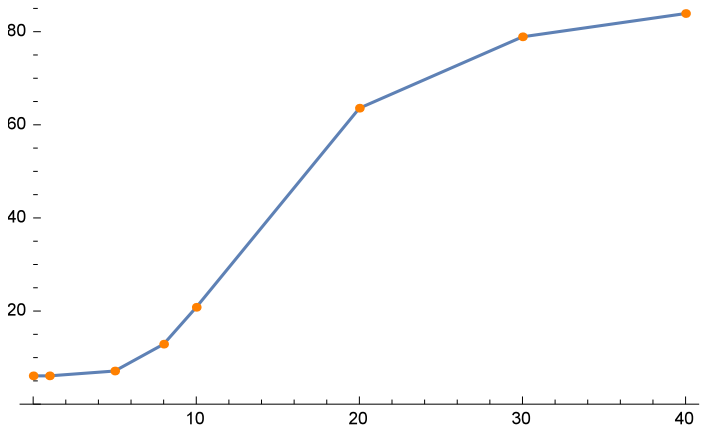

Figure 6.4.9: The activity level of ERK1/2 dim 3P is plotted on the abscissa and the value of J_0 is plotted on the ordinate. We see an abrupt rising of the value of J_0 which can be interpreted as an abrupt deterioration of the corresponding treatment. Data points are taken from Table 6.6.

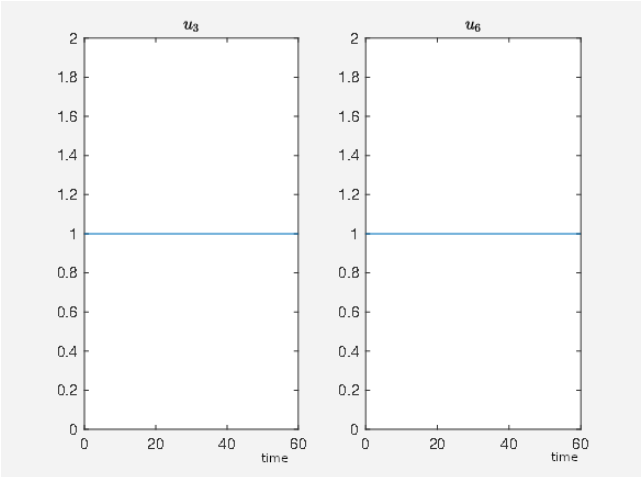

(a) Time curve of external stimuli where u_3 inhibits ERK1/2 dim 3P and u_6 activates angiotensin II.

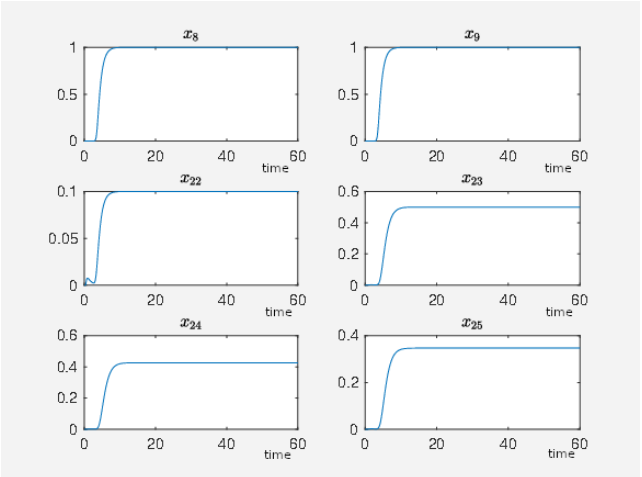

(b) Time curve of the nodes of interests where x_8 is the activity level of p90RSK, x_9 is the activity level of p70S6K, x_{22} is the activity level of ERK1/2 dim 3P, x_{23} is the activity level of Elk1, x_{24} is the activity level of MSK1 and x_{25} is the activity level of c-Myc.

Figure 6.4.10: The time is plotted on the the abscissa and the activity level is plotted on the ordinate.

Remark 8. The framework used in this section and introduced in Section 5.2 can also be used to induce a switch between two different steady states of a network. We repeat the experiment from Subsection

6.2.1 with the corresponding model to demonstrate that the presented framework also figures out the receptors that are associated with irreversible platelet aggregation. We recall that as known from [39] the irreversible platelet aggregation is associated with a high activity of integrin. We start with the steady state associated with the reversible platelet aggregation where the activity of integrin is low and choose as the node of interest the node that is associated with integrin. We desire this node to have an activity level that equals 1. We use the result from Algorithm 5.4 for $\alpha = 0.01$, numMax $= 2$ and numInt $= 3$ as the initial guess for the external stimuli for Algorithm 5.2 with the recommended parameters except $\kappa = 10^{-14}$. The constant non zero external stimuli from Algorithm 5.4 are set to zero at the end of the interval $[0, T]$ from Algorithm 5.2 and thus the network relaxes into the desired steady state. We obtain the results in accordance to Figure 6.2.2 left one which means that the system is in the desired steady state and the same external stimuli are active and the same are inactive.

We also repeat the experiment from Subsection 6.2.2 with the corresponding model to induce a switch from the steady state that is associated with a Th-17 cell to the steady state that is associated with a regulatory Treg cell. The lineage-specifying transcription factor for Treg is Foxp3. For this purpose, we choose only Foxp3 as our only node of interest and desire it to have the value 1. We use the result from Algorithm 5.4 for $\alpha = 0.1$, numMax $= 5$ and numInt $= 3$ for the initial guess for the external stimuli for Algorithm 5.2 with the recommended parameters except $\kappa = 10^{-14}$ and obtain results in accordance to Figure 6.2.4. This means that the network is in the same desired state at the end of the interval $[0, T]$ where the non zero external stimuli from Algorithm 5.4 are set to zero at the end of the interval $[0, T]$ by Algorithm 5.2 such that the same external stimuli are active and the same are inactive.

Part III

Discussion and appendix

Chapter 7

Discussion of the results

This section is devoted to a concluding discussion of the results that were presented in this thesis and their relation to biology. The basic idea of this work was to apply the well developed theory of mathematical optimal control problems to biomedical problems and to demonstrate its advantages for the systematical search for new intervention points in molecular networks. The principal aim of the work was to set up a framework based on mathematical control theory that allows a further exploiting of already existing data for the issue of efficient manipulation of molecular networks to induce desired effects to support biomedical and biological research. Thus a bioinformatic tool was generated that contributed to efficient network analysis.

The work completely focused on tailoring the abstract formulation of optimal control theory to concrete biological and biomedical applications. For this purpose the work firstly collected all the theoretical mathematical concepts and methods that were necessary, secondly linked them to their biological meaning and thirdly also provided a software implementation based on Mathworks Matlab in order to perform concrete calculations whose results were reinterpreted for the initial biological problem. The corresponding examples also validated the framework. These Matlab implementations provided with this work can be integrated in already existing software, like Potterswheel (http://www.potterswheel.de/Pages/index.php) or Copasi (http://copasi.org/). In Jimena2 (https://www.biozentrum.uni-wuerzburg.de/bioinfo/computing/jimena2/) the Matlab implementations have already been integrated for additional network analysis. This software package generates the necessary equations automatically from an interaction graph like Figure 6.2.1 or Figure 6.2.3 and from a table in which it is denoted where and in which matter certain external stimuli act. The result is an executable Matlab file where also pre-assembled functions are provided to plot the results to enhance the practical using.

Because of focusing on a framework that applies existing mathematical theory to biological and biomedical problems in a practicable way, the presented work contained no mathematical proofs as it would have been usual if it had been a mathematical thesis. Instead the mathematical equations, concepts and results of calculations were linked to biology by developing a framework in which the mathematics was interpreted as a tool for rational analysis of biological and biomedical problems.

Specifically, it was proceeded as follows. Mathematical models of molecular networks consisting of ordinary differential equations were extended with terms that included the effect of external stimuli, which could be the action of an experimenter, on the molecular network. Ordinary differential equations are common to model biological molecular networks, see for example [11, 37, 36, 22, 39]. This extension was validated on the example of a model of circadian clocks. For this purpose the following results of experimental work were generated with a single model. In the following the experiments are named and linked to evidence in literature. The synchronization of the circadian clock to external Zeitgebers can be found in [25] and in the presented work in Figure 4.3.3, Figure 4.3.4, Figure 4.3.5 and Figure 4.3.10. The restart of the endogenous clock can be found in [61] and in this work in Figure 4.3.9. The entrainment to different external periods can be found in [4] and in this thesis in Figure 4.3.12. In addition the effect of relative coordination can be found in [43] and in the present thesis in Figure 4.3.13 and in Figure 4.3.14. The behavior upon a permanent light stimulus with constant intensity can be found in [3, 30] and in this work in Figure 4.3.17. Phase response curves based on experimental

data can be found in [46, 42, 45] and the theoretical curves can be found in Figure 4.3.20 in the present work. The synchronization of peripheral clocks to central clocks where also further external stimuli like food intake for liver cells are considered can be found in [24, 16] and in the present thesis in Figure 4.3.21, Figure 4.3.22, Figure 4.3.23 and Figure 4.3.24.

Next based on the models that include the effect of external stimuli, a general framework was developed to consider the issue of determining systematically intervention points and corresponding external stimuli, like chemical agents or physical external stimuli that were detected by receptors. For this purpose a target functional was defined where the squares of the difference between the setpoint and the actual value of each relevant molecular agent were added up. Then the task was to determine the stimuli such that they minimized this functional by steering the corresponding values of molecular agents as close as possible to the desired values. This concept is also used for biological problems where model parameters are fit to experimental data such that the theoretical curves fit best to the experimental curves of the corresponding quantities. However the existing software solutions like Potterswheel and Copasi are not yet optimized for the systematical investigation of molecular networks with respect to the analysis of intervention points. The main reason is that these parameters are constants that cannot change in time which is necessary for certain cases of network analysis for example if external stimuli after a pulse have to be switched off. Furthermore in the presented framework there was the possibility given to reduce the possible intervention point to a small number where only the efficient external stimuli remain. This was done by increasing the weight α in the cost functional (5.1.3) which was also not covered by the mentioned already existing software packages. For a further discussion, see Section 5.3. In order to deal with the mathematical task to solve the mentioned optimal control problem, several mathematical tools and their implementations in Matlab were provided with this work. In the numerical experiments sometimes the local optimization algorithms took long for convergence. Therefore for future work it can be put effort into figuring out termination criteria that stop these algorithms at an iteration where the solution is already sufficiently good for biological interpretation since mostly there is no need for a mathematical optimal solution in the sense discussed in Chapter 5, especially (5.1.11) to (5.1.13) or (5.1.14).

The presented optimal control framework was then validated with different biological examples.

For this purpose a gene regulatory network of a platelet was considered with respect to the issue of triggering irreversible platelet aggregation. The corresponding network had been fitted to experimental data [39]. Several external stimuli were added to the network. The result of the optimization framework was that clearly only the two receptors were found that were associated with irreversible platelet aggregation if activated by adenosine diphosphate, see [39].

In a second example a gene regulatory network concerning the maturation of T-cells from a naive T-cell into four types, namely Th1, Th2, Th17 and a regulatory T-cell, was investigated. Specifically the transdifferentiation from Th17 to a regulatory T-cell was considered as it is reported in a tumor setting [17] where soluble factors contained in an ovarian cancer ascites were capable of mediating the transdifferentiation from Th17 to a regulatory T-cell. From experiments it was known that transforming growth factor β (TGF-β) induced the expression of the lineage-specifying transcription factor of the regulatory T-cell. However exposing the Th17 cells to TGF-β did not perform the transdifferentiation in vitro. The results of our calculations was that on the one hand TGF-β was necessary, which was in accordance to the experimental experience, but had to be supplemented by an agent or agents that also knocked down the expression of the lineage-specifying transcription factor of the Th17 cell. Additionally IL-2 is a necessary molecular agent for the transdifferentiation. For that matter it makes no difference whether the expression of IL-2 is activated in the cell or exogenic IL-2 is given to the cell and ends up in the cell nucleus. This example reveals another advantage that our framework has for the biological experiments. By the theoretical investigation promising options are generated for the observed effects and pave the way what to look for in a biological experiment. This can save a lot of time when figuring out the responsible biologically active substances. Considering our example with the T-cells an ascites may contain a lot of biologically active agents where, as it can be seen that, not necessarily only one agent is responsible for an observed outcome. Thus also all combinations of substances from the ascites would have to be considered. Once having a promising option of chemical agents for an explanation of the observed outcome, for example from theoretical considerations as in

the present case, it is only necessary to check the molecular agents contained in an ascites for their potential with respect to activate or inhibit a certain gene according to the theoretical investigation and finally check only that single option whether it causes the observed outcome. In the best case only one experiment has to be done since there is no need for the procedure of finding promising options by experiments as the already existing information is better exploited by mathematical methods.

In a third example, a gene regulatory network of a myocardiocyte was considered where it was demonstrated how the presented framework, in particular the target functional, could be used to compare different treatment strategies quantitatively. The model had been fitted to experimental data and was taken from [11]. Once a certain selection of external stimuli is included into a model, the optimization method serves as an objective method to compute the smallest target functional possible. This means that the time curves of the external stimuli, which model the treatment, are determined by objective and rational methods and are not subject to the user's subjectivity. This way allows a reasonable comparison of treatment strategies in silico. Furthermore the framework also makes it possible to filter out the most effective external stimuli from a selection of external stimuli that are in favor of a desired effect. This reduction of options to only few effective molecular agents is an important consideration of pharmacological modulation. This is further discussed in the next paragraph.

In the case of the myocardiocyte, a constitutive activated receptor was modeled that triggered a permanent hypertrophic stimulus which was associated with undesirable effects. In the thesis it was demonstrated how to use the proposed framework to find an effective treatment that turned the effects of the pathologically activated receptor into a non-hypertrophic beneficial effect. It turned out that for this purpose a homo-dimerization of two proteins had to be inhibited. The level of inhibition was figured out up to which the treatment was as good as activating a receptor that was directly associated with a non-hypertrophic stimulus. Additionally a threshold of a maximum activity of homo-dimerization was predicted up to which no hypertrophic effects occurred which made the framework further checkable.

In this last two paragraphs an outlook is given how the presented framework can be extended to a data driven approach based on databases where experimental time curves of molecular agents and the time curves of the corresponding external stimuli are stored. In connection with the omics technology time resolved measurements of many agents of a molecular network are possible. Additionally the effect of almost any number of available external stimuli like molecular agents can be step-by-step systematically measured and the data can be stored in databases. Now several models can be set up like standardized qualitative models as in [37], extended by an appropriate mechanism that includes the effects of external stimuli as discussed in Chapter 4 and tested which model fits the data best. For this test procedure software is already available like the software package Potterswheel where the procedure of choosing the best data fitting model is demonstrated in [39] for example. The best fitting model that includes all the possible interventions can then be further processed by the proposed optimization framework where the mathematical methods calculate the most efficient external stimuli combination for the desired effects that are to be induced on the molecular network. The most effective combination of external stimuli represents the drug combination for the pharmacological modulation. All these steps can be performed automatically with a software package if there is access to such a database mentioned above. On the other hand, if the results are not satisfactory as for example the target functional value is still too big which indicates that the desired expression pattern is not very well taken by the molecular network with the given options of external stimuli or single expression levels of molecular agents are too far away from a physiologically reasonable value, then further external stimuli can be added to the existing ones and the calculations can be performed again until there is a satisfactory result. If a new added external stimulus is active in the results of the calculations, then this external stimulus represents a new pharmacological intervention point. This motivates the development of its experimental realization since it is very likely that the effort results in the desired effect in the corresponding experiment. In this case the experimental search for new intervention points can be highly focused on relevant molecular targets coming from a rational theoretical investigation. Consequently the development of drugs that later turn out to be inefficient can be avoided.

In general the advantage of the proposed framework is that first only measurements have to be performed to obtain the effect of the external stimuli on the network and that second also very complex models, containing many cross connections going beyond human comprehension, can be built up

module-wise and processed. The number of measurements scales at most with the number of external stimuli that are to be considered. There is no need for performing measurements for each combination of external stimuli to determine the combination that has the desired effect. This information is already contained in the model where the proposed framework serves as a powerful tool, even for large molecular networks with many agents and interactions between them, to make the desired information of the best combination of external stimuli obvious for its user.

Chapter 8

Appendix

In the appendix, we provide background information about steady states of systems of ordinary equations. In addition, we illustrate characterizing steady states in regulatory networks with examples. Then we consider important issues for the numerical treatment of ordinary differential equations.

8.1 The characterization of steady states of regulatory networks

As discussed in Section 4.1 a regulatory network in its basic form, that means without external stimuli, in general is modeled usually by a system of ordinary differential equations of the form

$$\begin{cases} \frac{d}{dt}x = f(x) \\ x(0) = x_0. \end{cases} \tag{8.1.1}$$

The right hand-side $f(x)$ models a network of nodes interacting with each other where $x(t) : \mathbb{R} \to \mathbb{R}^n$, $n \in \mathbb{N}$, is a vector whose components are the activity levels of the corresponding nodes and $x_0 \in \mathbb{R}^n$ is the initial value of the activity levels. In our simulations where the activity level is modeled by the state x, we observe that for certain networks the activity levels converge to an equilibrium, that means that the activity levels do not change their values any more after a certain time. We say that the system has gone to a steady state. This is characterized by

$$0 = \frac{d}{dt}x = f(x).$$

That means that the steady states are the roots of the right hand-side f. Another interpretation is that the time derivative $\frac{d}{dt}x$ is zero for all times. That means that the function x has to be constant for all times. We label a steady state by $\bar{x} \in \mathbb{R}^n$. If the network is in a steady state $\bar{x}$, then we have that the right hand side $f(\bar{x}) = 0$. Thus, by (8.1.1), we have that the state x is constant, namely $x(t) \equiv \bar{x}$ for all the times left as the derivative with respect to time equals zero once the values of the nodes have reached $\bar{x}$. Especially that means that there cannot occur oscillations between points of rest without external stimuli.

We distinguish three different types of steady states. There are unstable ones. That means that a little deflection from the steady state can cause that the system never reaches that steady state again. There are stable ones. That means that a little deflection from the steady state lets the system remain in a certain neighborhood around the steady state for all times. In this case, we observe that the values of the corresponding quantities of x oscillate around their value of the steady state. The third type is called asymptotically stable. That means that after a little deflection, the system converges to the steady state again.

In order to investigate the type of a steady state, we need to know the behavior of the system within an at least small environment around the steady state. Having the Taylor series of f around $\bar{x}$, there is a small environment $E(\bar{x})$ around $\bar{x}$ such that the Taylor series up to the first term is a good approximation for f, that means

$$f(\tilde{x}) \approx f(\bar{x}) + Df(\bar{x})(\tilde{x} - \bar{x}) \tag{8.1.2}$$

where $Df(\bar{x})$ is the Jacobian of f evaluated at $\bar{x}$ and $\tilde{x} \in E(\bar{x})$, see for example [2, VII] for details about the Taylor series. As $\bar{x}$ is a steady state and thus $f(\bar{x}) = 0$, we have that in a small environment around $\bar{x}$, the system (8.1.1) behaves like a system of liner differential equations which is given by

$$\frac{d}{dt}\tilde{x} = f(\tilde{x}) \approx Df(\bar{x})(\tilde{x} - \bar{x})$$

due to (8.1.2) with the system matrix $Df(\bar{x})$. After a coordinate transformation where we set $x \coloneqq \tilde{x} - \bar{x}$, we have approximately

$$\frac{d}{dt}(x + \bar{x}) = Df(\bar{x})\, x$$

which is equivalent to

$$\frac{d}{dt}x = Df(\bar{x})\, x$$

as $\bar{x}$ is a constant. The general solution to a homogeneous system can always be calculated and the asymptotic behavior is characterized by the real part of the eigenvalues of the matrix $Df(\bar{x})$, roughly spoken. See textbooks about ordinary differential equations like [50, 53] for more details about solving systems of homogeneous differential equations and their asymptotic behavior. The most important case for our purpose is that the eigenvalues of the matrix $Df(\bar{x})$ are of the structure $a + ib$ where the real part $a < 0$ and the imaginary part $b \in \mathbb{R}$. Illustratively stated, the real part is a measure for the damping of the oscillations around the steady state $\bar{x}$, which means how fast the system reaches its point of rest again once deflected where $a = 0$ means that there is no damping and the absolute value of the imaginary part $|b|$ is a measure for how fast the values x oscillate where $b = 0$ means that there is no oscillation. The sign of b affects the direction of the oscillation's rotation. More detailed, the steady states are characterized by the eigenvalues $\lambda_k,\ k = \{1, ..., n\}$ of the Jacobian $Df(\bar{x})$ evaluated at the corresponding steady state $\bar{x}$. We have an unstable one, if the real part of one eigenvalue is greater than zero, i.e. $\mathrm{Re}(\lambda_k) > 0$ for one $k = \{1, ..., n\}$. We have an asymptotically stable one if all the real parts of the eigenvalues are less than zero, i.e. $\mathrm{Re}(\lambda_k) < 0$ for all $k = \{1, ..., n\}$. A stable steady state is for purely imaginary eigenvalues, i.e. $\mathrm{Re}(\lambda_k) = 0$ and $\mathrm{Im}(\lambda_k) \neq 0$ for all $k = \{1, ..., n\}$ and if all the eigenvalues are pairwise different.

We illustrate the discussion above with two examples. We consider a two dimensional system of ordinary differential equations, namely a Lotka-Volterra system, given by

$$\frac{d}{dt}x_1 = \gamma x_1 - \beta x_1 x_2$$
$$\frac{d}{dt}x_2 = \alpha x_1 x_2 - \delta x_2$$

where $\gamma, \beta, \alpha, \delta > 0$. We define

$$f_1(x_1, x_2) \coloneqq \gamma x_1 - \beta x_1 x_2$$
$$f_2(x_1, x_2) \coloneqq \alpha x_1 x_2 - \delta x_2$$

and further

$$f(x_1, x_2) \coloneqq \begin{pmatrix} f_1(x_1, x_2) \\ f_2(x_1, x_2) \end{pmatrix}.$$

In order to find the steady states, that means these points where the values of the quantities x_1, x_2 do not chance any more for any time, we search for the roots of f, that means

$$f_1(x_1, x_2) = 0$$
$$f_2(x_1, x_2) = 0$$

and equivalently,

$$\gamma x_1 - \beta x_1 x_2 = 0$$
$$\alpha x_1 x_2 - \delta x_2 = 0$$

where we have two steady states. The first one is for $\bar{x}_1 = 0$ and $\bar{x}_2 = 0$. The second and interesting one is for $\bar{x}_1 = \frac{\delta}{\alpha}$ and $\bar{x}_2 = \frac{\gamma}{\beta}$.

For the mathematical characterization, we need the Jacobian of the the system. The Jacobian is given by the first derivative as follows

$$Df(x_1, x_2) = \begin{pmatrix} \frac{\partial}{\partial x_1} f_1(x_1, x_2) & \frac{\partial}{\partial x_2} f_1(x_1, x_2) \\ \frac{\partial}{\partial x_1} f_2(x_1, x_2) & \frac{\partial}{\partial x_2} f_2(x_1, x_2) \end{pmatrix}$$

where $\frac{\partial}{\partial x_1}$ is the partial derivative with respect to x_1 and $\frac{\partial}{\partial x_2}$ is the partial derivative with respect to x_2. For the Lotka-Volterra system, we obtain

$$Df(x_1, x_2) = \begin{pmatrix} \gamma - \beta x_2 & -\beta x_1 \\ \alpha x_2 & \alpha x_1 - \delta \end{pmatrix}.$$

Evaluating $Df(x_1, x_2)$ at the point of rest $(x_1, x_2) = \left(\frac{\delta}{\alpha}, \frac{\gamma}{\beta}\right)$ for our Lotka-Volterra system, we obtain

$$Df\left(\frac{\delta}{\alpha}, \frac{\gamma}{\beta}\right) = \begin{pmatrix} 0 & -\frac{\beta\delta}{\alpha} \\ \frac{\alpha\gamma}{\beta} & 0 \end{pmatrix}.$$

The eigenvalues of $Df\left(\frac{\delta}{\alpha}, \frac{\gamma}{\beta}\right)$ are $\lambda_1 = -\sqrt{-\gamma\delta} = -\mathrm{i}\sqrt{\gamma\delta}$ and $\lambda_2 = \sqrt{-\gamma\delta} = \mathrm{i}\sqrt{\gamma\delta}$ and therefore purely imaginary and pairwise different. That means that x_1 and x_2 oscillate around the point of rest $\left(\frac{\delta}{\alpha}, \frac{\gamma}{\beta}\right)$ once deflected at most up to certain distance from the point of rest $\left(\frac{\delta}{\alpha}, \frac{\gamma}{\beta}\right)$.

The next example is according to our model (4.1.1). We have

$$\begin{aligned}
\frac{d}{dt}x_1 &= \frac{-\exp\left(\frac{1}{2}h\right) + \exp\left(-h\left(1 - \frac{1+\beta}{\beta}\frac{\beta x_2}{1+\beta x_2} - \frac{1}{2}\right)\right)}{\left(1 - \exp\left(\frac{1}{2}h\right)\right)\left(1 + \exp\left(-h\left(1 - \frac{1+\beta}{\beta}\frac{\beta x_2}{1+\beta x_2} - \frac{1}{2}\right)\right)\right)} - x_1 \\
\frac{d}{dt}x_2 &= \frac{-\exp\left(\frac{1}{2}h\right) + \exp\left(-h\left(\frac{1+\alpha_{12}+\alpha_3}{\alpha_{12}+\alpha_3}\frac{\alpha_{12}x_1+\alpha_3 x_3}{1+\alpha_{12}x_1+\alpha_3 x_3} - \frac{1}{2}\right)\right)}{\left(1 - \exp\left(\frac{1}{2}h\right)\right)\left(1 + \exp\left(-h\left(\frac{1+\alpha_{12}+\alpha_3}{\alpha_{12}+\alpha_3}\frac{\alpha_{12}x_1+\alpha_3 x_3}{1+\alpha_{12}x_1+\alpha_3 x_3} - \frac{1}{2}\right)\right)\right)} - x_2 \\
\frac{d}{dt}x_3 &= \frac{-\exp\left(\frac{1}{2}h\right) + \exp\left(-h\left(\frac{1+\alpha_4}{\alpha_4}\frac{\alpha_4 x_4}{1+\alpha_4 x_4} - \frac{1}{2}\right)\right)}{\left(1 - \exp\left(\frac{1}{2}h\right)\right)\left(1 + \exp\left(-h\left(\frac{1+\alpha_4}{\alpha_4}\frac{\alpha_4 x_4}{1+\alpha_4 x_4} - \frac{1}{2}\right)\right)\right)} - x_3 \\
\frac{d}{dt}x_4 &= \frac{-\exp\left(\frac{1}{2}h\right) + \exp\left(-h\left(\frac{1+\alpha_{14}}{\alpha_{14}}\frac{\alpha_{14}x_1}{1+\alpha_{14}x_1} - \frac{1}{2}\right)\right)}{\left(1 - \exp\left(\frac{1}{2}h\right)\right)\left(1 + \exp\left(-h\left(\frac{1+\alpha_{14}}{\alpha_{14}}\frac{\alpha_{14}x_1}{1+\alpha_{14}x_1} - \frac{1}{2}\right)\right)\right)} - x_4
\end{aligned} \tag{8.1.3}$$

where we set $\alpha_{12} = \alpha_4 = \alpha_{14} = 1$, $\beta = 10$ and $h = 10$. In Figure 8.1.1, we have the schematic of the network.

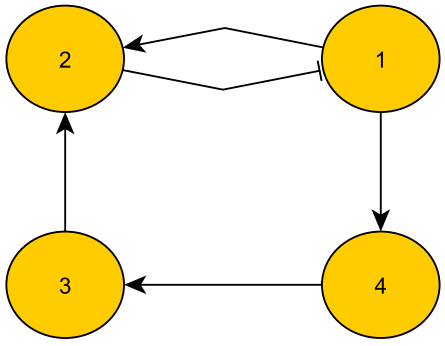

Figure 8.1.1: Schematic of the network (8.1.3).

We use Wolfram Mathematica, namely FindRoot, to find numerically a root of the right hand-side of (8.1.3) which is rounded given by

$$(\bar{x}_1, \bar{x}_2, \bar{x}_3, \bar{x}_4) = (0.196559, 0.13822, 0.0756964, 0.147855)\,. \tag{8.1.4}$$

By Wolfram Mathematica, we calculate the Jacobian of the right hand-side of (8.1.3), evaluate it at $(\bar{x}_1, \bar{x}_2, \bar{x}_3, \bar{x}_4)$ and obtain for its eigenvalues the following rounded values

$$\begin{aligned}&(\lambda_1, \lambda_2, \lambda_3, \lambda_4)\\ &= (-1.6891 + 1.5129\mathrm{i}, -1.6891 - 1.5129\mathrm{i}, -0.3109 + 1.5129\mathrm{i}, -0.3109 - 1.5129\mathrm{i})\,.\end{aligned}$$

Consequently we have an asymptotically stable steady state. In other words, we can say that starting our simulation sufficiently close to the point of rest $(\bar{x}_1, \bar{x}_2, \bar{x}_3, \bar{x}_4)$, the state (x_1, x_2, x_3, x_4) performs a damped oscillation around $(\bar{x}_1, \bar{x}_2, \bar{x}_3, \bar{x}_4)$ converging to the values $(\bar{x}_1, \bar{x}_2, \bar{x}_3, \bar{x}_4)$ when time goes forward. We can see this in Figure 8.1.2 which is calculated with the Mathematica function NDSolve where

$$(x_1(100), x_2(100), x_3(100), x_4(100)) = (0.196559, 0.13822, 0.0756964, 0.147855)$$

and the initial point is $(x_1(0), x_2(0), x_3(0), x_4(0)) = (0, 0, 0, 0)$.

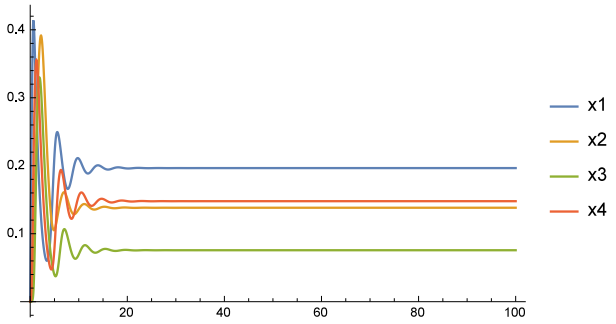

Figure 8.1.2: Plot of the solution to (8.1.3) calculated with NDSolve where the time is on the abscissa.

8.2 Remarks on the numerical treatment of ODEs

If we do not use a solver to find the roots of the right hand-side f but a solver for simulating the network according to (8.1.1) and thus calculate the whole time-dependent course of x, we have to be aware of numerical instabilities in some cases using certain numerical methods for solving (8.1.1). The main issue of these instabilities is that the numerical solution to a system of ordinary differential equation does not reproduce the asymptotic behavior of the analytic solution to the corresponding system. However, the correct asymptotic behavior is crucial to determine the steady states. A subject of this issue are stiff (differential) equations. We illustrate the basic problem with an example. We consider the one dimensional system

$$\begin{cases} \frac{d}{dt}x = \lambda\left(x - \frac{1}{3}\right) \\ x(0) = \frac{4}{3} \end{cases} \tag{8.2.1}$$

with $\lambda \in \mathbb{R}$ which is analytically solved by $x(t) = \exp(\lambda t) + \frac{1}{3}$ whose asymptotic behavior is given by $\lim_{t\to\infty} x(t) = \frac{1}{3}$ if $\lambda < 0$. In order to solve (8.2.1) numerically, we have to discretize its differential equation. There are several possibilities, see for example [13]. We choose the following explicit Euler scheme

$$\frac{x^{l+1} - x^l}{\triangle t} = \lambda\left(x^l - \frac{1}{3}\right) \tag{8.2.2}$$

where x^l is the approximated value of the analytical solution $x(l\triangle t)$ with $\triangle t \in \mathbb{R}^+$ and $l \in \mathbb{N}_0$. From (8.2.2), we can calculate the value x^{l+1} from the known previous time step where $x^0 = \frac{4}{3}$ as follows

$$x^{l+1} = \triangle t\lambda \left(x^l - \frac{1}{3} \right) + x^l$$

which is equivalent to

$$x^{l+1} = (1 + \triangle t\lambda)\, x^l - \frac{1}{3}\triangle t\lambda. \tag{8.2.3}$$

Using (8.2.3), we iteratively obtain

$$\begin{aligned} x^{l+1} &= -\frac{1}{3}\triangle t\lambda \left(\sum_{\ell=0}^{l-1} (1 + \triangle t\lambda)^\ell \right) + (1 + \triangle t\lambda)^l\, x^0 = -\frac{1}{3}\triangle t\lambda \frac{1 - (1 + \triangle t\lambda)^l}{1 - (1 + \triangle t\lambda)} + (1 + \triangle t\lambda)^l\, x^0 \\ &= -\frac{1}{3}\triangle t\lambda \frac{1 - (1 + \triangle t\lambda)^l}{-\triangle t\lambda} + (1 + \triangle t\lambda)^l\, x^0 = \frac{1}{3} - \frac{1}{3}(1 + \triangle t\lambda)^l + (1 + \triangle t\lambda)^l\, x^0 \end{aligned} \tag{8.2.4}$$

where we used the Geometric series [1]. If $|1 + \triangle t\lambda| < 1$, then $\lim_{l\to\infty} x^l = \frac{1}{3}$ and thus the numerical solution to (8.2.1) provides the correct asymptotic behavior. For example, if $\lambda = -4$, then for $\triangle t < \frac{1}{2}$ the scheme (8.2.3) for calculating the numerical solution to (8.2.1) provides the correct asymptotic behavior.

Now, we can also see this stability effects for our system (8.1.3). We solve (8.1.3) for $t \in [0, 100]$ and the initial values $(x_1(0), x_2(0), x_3(0), x_4(0)) = (0, 0, 0, 0)$ with the Mathematica function NDSolve where we set the options StartingStepSize $\to \triangle t$, Method $\to$ {"FixedStep", Method $\to$ "ExplicitEuler"}. This means that we use an explicit Euler scheme with fixed step size such that $x^{l+1} = x^l + \triangle t f\left(x^l\right)$ where f is the right hand-side of (8.1.3). In Figure 8.2.1, we can see the numerical solutions for different step sizes $\triangle t$. The convergence to the steady state can be seen first if the step size $\triangle t$ is sufficiently small. Figure 8.2.1f looks then identically to Figure 8.1.2.

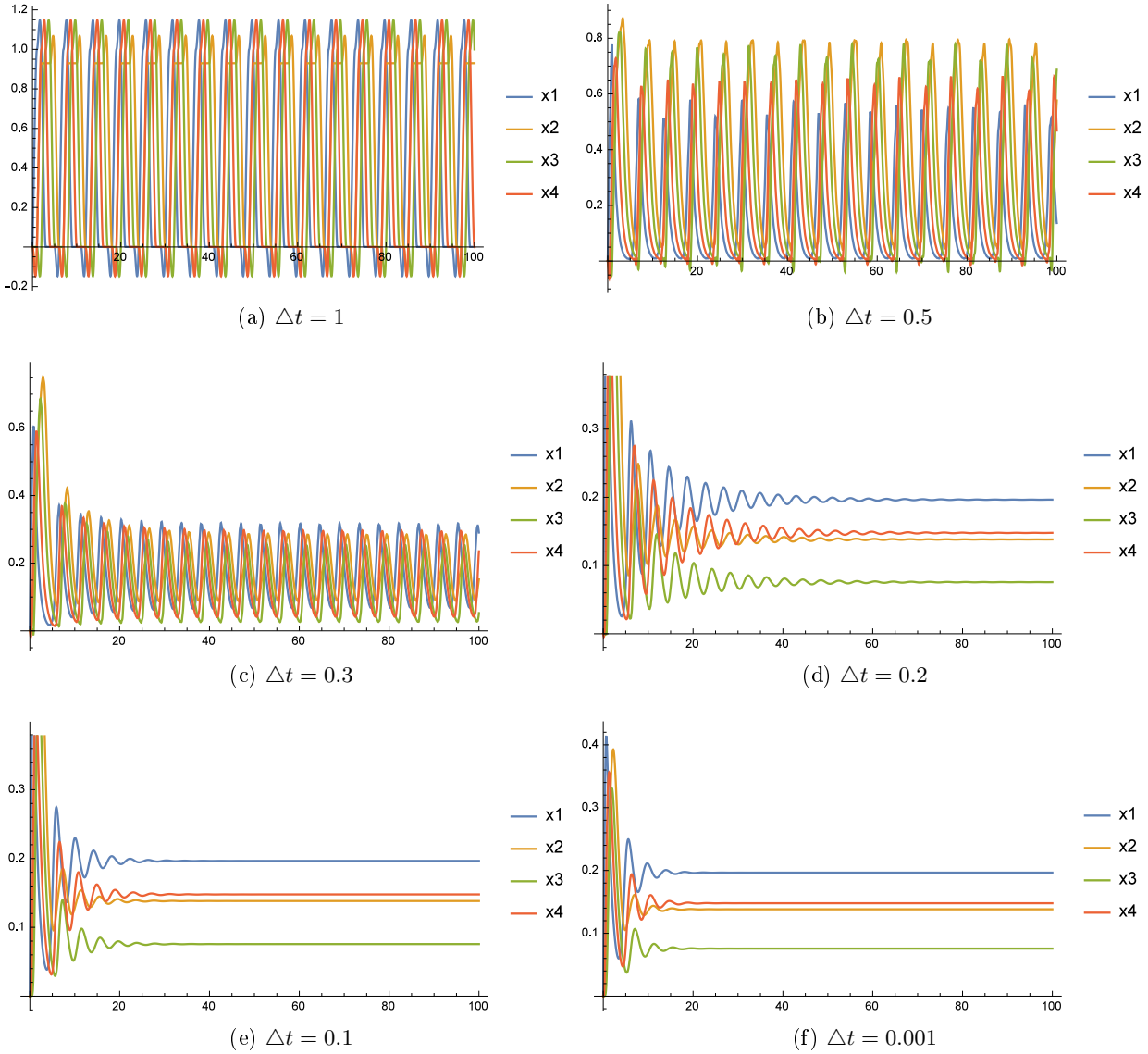

(a) $\triangle t = 1$ (b) $\triangle t = 0.5$

(c) $\triangle t = 0.3$ (d) $\triangle t = 0.2$

(e) $\triangle t = 0.1$ (f) $\triangle t = 0.001$

Figure 8.2.1: Plots of the numerical solution to (8.1.3) for different time steps $\triangle t$ calculated with the explict Euler method. The time is plotted on the abscissa.

Remark 9. Having numerical results like Figure 8.2.1a, Figure 8.2.1b or Figure 8.2.1c for any step size $\triangle t$ and simulation time, that means undampened oscillations, especially then it is worth using an ODE-solver from Matlab like ode45 or NDSolve from Mathematica to solve the system of differential equations belonging to the given network in order to check the numerical results obtained from the tool used to analyze the given network.

Due to the fact that we approximate the time derivatives $\frac{d}{dt}x\left(t\right)$ by their corresponding difference quotients $\frac{x(t+\triangle t)-x(t)}{\triangle t}$ for the numerical solution, we may not expect that the numerical solution equals exactly the analytical solution. As a consequence it is reasonable to give the values of the nodes' activity level of the numerically located points of rest with some error bars. Then, from the numerical perspective, it is reasonable that we distinguish steady states pairwise if and only if there is at least one component of the steady states where the corresponding error bars do not overlap.

Next, we present a procedure how to obtain an idea in what order of magnitude the error bars are. In Table 8.1, we have the values for $\left(x_1\left(100\right), x_2\left(100\right), x_3\left(100\right), x_4\left(100\right)\right)$, which serve as an estimation for the values of the steady state. These values converge to the values for our point of rest calculated by the Mathematica function FindRoot, see (8.1.4) if $\triangle t$ becomes smaller. If we compare the values for $\triangle t = 0.2$ with $\triangle t = 0.1$, we realize that the difference is about $\pm 10^{-5}$. Therefore, if we perform the calculations for (8.1.3) with $\triangle t = 0.1$ and with different initial points in order to find

several points of rest, an error bar in the order of magnitude of $\pm 10^{-5}$ might be reasonable for the identified point of rest with its best values for $\triangle t = 0.1$ in Table 8.1.

$\triangle t$	$x_1\,(100)$	$x_2\,(100)$	$x_3\,(100)$	$x_4\,(100)$
0.21	0.19673	0.13827	0.0757159	0.148116
0.20	0.196604	0.138243	0.0757134	0.147945
0.10	0.196559	0.13822	0.0756964	0.147855

Table 8.1

In general, it is a reasonable procedure to do the simulation for a network with the same initial point but with different step sizes $\triangle t$ and compare the differences in the corresponding values of the nodes' activity level of the points of rest to get an idea for the order of magnitude of their error bars. The step sizes for the calculation for the estimation of the error bar should not be too far from the step size with which the real simulation is performed such that the error bar becomes not too big or too small and the method is still stable.

If we take the absolute value of the difference between the corresponding values of the nodes' activity level of two different steady states starting each from two different initial points from which the network converges to the particular steady state and if this absolute value gets smaller and smaller when we perform the simulation iteratively with decreasing $\triangle t$, then the two different steady states might be the same as in fact the difference comes from the numerical error. But if the absolute value of the difference between the corresponding values of the nodes' activity level of two steady states converges to a fixed number whose absolute value is greater than zero although decreasing $\triangle t$, then the steady states might really be different ones.

Remark 10. The procedure described above is one possibility to estimate the numerical error. In order to compare the numerical results, that means the located steady states, with data from an experiment, we have to be aware of the error bars with which the experimental data is provided. Normally, those error bars are from an order of magnitude of about 10% of the maximum activity level or concentration level, respectively. That means for example in our case where the activity level is between 0 and 1, that the error bar is about ± 0.1 for the experimental data. Thus, in our example, we can neglect our numerical error of about $\pm 10^{-5}$ compared to ± 0.1 and can subsume all the steady states whose values correspond to an experimental steady state within that error bar of ± 0.1 to that one. We can say that they are from an experimental point of view equivalent. In general, if we compare numerical results to experimental data, it is reasonable to compare numerical and experimental error bars and provide the numerical data with the greater one.

Bibliography

[1] Herbert Amann and Joachim Escher. *Analysis I.* Springer, 2005.

[2] Herbert Amann and Joachim Escher. *Analysis II.* Birkhäuser, 2008.

[3] Jürgen Aschoff. Freerunning and entrained circadian rhythms. In *Biological rhythms*, pages 81–93. Springer, 1981.

[4] Jürgen Aschoff. Circadian timing. *Annals of the New York Academy of Sciences*, 423(1):442–468, 1984.

[5] Dimitri P. Bertsekas. *Nonlinear programming.* Athena scientific Belmont, 1999.

[6] Alfio Borzì and Volker Schulz. *Computational optimization of systems governed by partial differential equations.* SIAM, 2011.

[7] Nick Bos, Unni Pulliainen, Liselotte Sundström, and Dalial Freitak. Starvation resistance and tissue-specific gene expression of stress-related genes in a naturally inbred ant population. *Royal Society open science*, 3(4):160062, 2016.

[8] Tim Breitenbach and Alfio Borzì. A sequential quadratic Hamiltonian method for solving parabolic optimal control problems with discontinuous cost functionals. *Journal of Dynamical and Control Systems*, pages 1–33, 2018.

[9] Tim Breitenbach, Charlotte Helfrich-Förster, and Thomas Dandekar. An effective model of endogenous clocks and external stimuli determining circadian rhythms, submitted for publication. 2018.

[10] Tim Breitenbach, Chunguang Liang, Niklas Beyersdorf, and Thomas Dandekar. Analyzing pharmacological intervention points: A method to calculate external stimuli to switch between steady states in regulatory networks, submitted for publication. 2018.

[11] Alexandra Brietz, Kristin Verena Schuch, Gaby Wangorsch, Kristina Lorenz, and Thomas Dandekar. Analyzing ERK 1/2 signalling and targets. *Molecular bioSystems*, 12(8):2436–2446, 2016.

[12] Stéphane Bronner, Henri Monteil, and Gilles Prévost. Regulation of virulence determinants in staphylococcus aureus: complexity and applications. *FEMS microbiology reviews*, 28(2):183–200, 2004.

[13] John Charles Butcher. *Numerical methods for ordinary differential equations.* John Wiley & Sons, 2016.

[14] Hua Cheng, Robert R. Langley, Qiuyu Wu, Wenjuan Wu, Jie Feng, Rachel Tsan, Dominic Fan, and Isaiah J. Fidler. Construction of a novel constitutively active chimeric egfr to identify new targets for therapy. *Neoplasia*, 7(12):1065–1072, 2005.

[15] Matthias Chiquet. Regulation of extracellular matrix gene expression by mechanical stress. *Matrix biology*, 18(5):417–426, 1999.

[16] Francesca Damiola, Nguyet Le Minh, Nicolas Preitner, Benoıt Kornmann, Fabienne Fleury-Olela, and Ueli Schibler. Restricted feeding uncouples circadian oscillators in peripheral tissues from the central pacemaker in the Suprachiasmatic Nucleus. *Genes & development*, 14(23):2950–2961, 2000.

[17] Stephanie Downs-Canner, Sara Berkey, Greg M. Delgoffe, Robert P. Edwards, Tyler Curiel, Kunle Odunsi, David L. Bartlett, and Nataša Obermajer. Suppressive IL-17A+ Foxp3+ and ex-Th17 IL-17A neg Foxp3+ T reg cells are a source of tumour-associated T reg cells. *Nature communications*, 8:14649, 2017.

[18] Wolfgang Engelmann and Karl-Heinz Witte. *How to stop a biological clock: Point of singularity.* Universitätsbibliothek Tübingen, 2016.

[19] Primrose Freestone. Communication between bacteria and their hosts. *Scientifica*, 2013, 2013.

[20] Ping Fu, Xiaohong Jiang, and Murat O. Arcasoy. Constitutively active erythropoietin receptor expression in breast cancer cells promotes cellular proliferation and migration through a map-kinase dependent pathway. *Biochemical and biophysical research communications*, 379(3):696–701, 2009.

[21] Claudia Goettlich, Lena C. Mueller, Meik Kunz, Franziska Schmitt, Heike Walles, Thorsten Walles, Thomas Dandekar, Gudrun Dandekar, and Sarah L. Nietzer. A combined 3D tissue engineered in vitro/in silico lung tumor model for predicting drug effectiveness in specific mutational backgrounds. *Journal of visualized experiments: JoVE*, (110):e53885–e53885, 2016.

[22] Albert Goldbeter. A model for circadian oscillations in the *Drosophila* period protein (per). *Proc. R. Soc. Lond. B*, 261(1362):319–324, 1995.

[23] Donald G. Guiney. Regulation of bacterial virulence gene expression by the host environment. *The Journal of clinical investigation*, 99(4):565–569, 1997.

[24] Michael H. Hastings, Akhilesh B. Reddy, and Elizabeth S. Maywood. A clockwork web: Circadian timing in brain and periphery, in health and disease. *Nature Reviews Neuroscience*, 4(8):649, 2003.

[25] Jana Husse, Gregor Eichele, and Henrik Oster. Synchronization of the mammalian circadian timing system: Light can control peripheral clocks independently of the SCN clock. *Bioessays*, 37(10):1119–1128, 2015.

[26] Aleksandr D. Ioffe and Vladimir M. Tihomirov. *Theory of extremal problems*, volume 6. Elsevier, 2009.

[27] Kazufumi Ito and Karl Kunisch. *Lagrange multiplier approach to variational problems and applications.* SIAM, 2008.

[28] Stefan H.E. Kaufmann and Inge E.A. Flesch. The role of T cell-macrophage interactions in tuberculosis. In *Springer seminars in immunopathology*, volume 10, pages 337–358. Springer, 1988.

[29] Kristen A. Kellar, Matthew V. Lorenzi, Ching Ping Ho, Dan You, Mei-Li Wen, Rolf P. Ryseck, Simone Oppenheimer, Brian E. Fink, Gregory D. Vite, Bruce R. Rowley, et al. Constitutively active receptor tyrosine kinases as oncogenes in preclinical models for cancer therapeutics. *Molecular cancer therapeutics*, 5(6):1571–1576, 2006.

[30] Ronald J. Konopka, Colin Pittendrigh, and Dominic Orr. Reciprocal behaviour associated with altered homeostasis and photosensitivity of *Drosophila* clock mutants. *Journal of neurogenetics*, 6(1):1–10, 1989.

[31] Irina Kratchmarova, Blagoy Blagoev, Mandana Haack-Sorensen, Moustapha Kassem, and Matthias Mann. Mechanism of divergent growth factor effects in mesenchymal stem cell differentiation. *Science*, 308(5727):1472–1477, 2005.

[32] Nicholas D. Lakin and Stephen P. Jackson. Regulation of p53 in response to DNA damage. *Oncogene*, 18(53), 1999.

[33] Wayne Lilyestrom, Michael G. Klein, Rongguang Zhang, Andrzej Joachimiak, and Xiaojiang S. Chen. Crystal structure of SV40 large T-antigen bound to p53: interplay between a viral oncoprotein and a cellular tumor suppressor. *Genes & development*, 20(17):2373–2382, 2006.

[34] Coralia Luna, Guorong Li, Paloma B. Liton, David L. Epstein, and Pedro Gonzalez. Alterations in gene expression induced by cyclic mechanical stress in trabecular meshwork cells. *Molecular vision*, 15:534, 2009.

[35] Shaun Martin, H.K. Lamb, C. Brady, B. Lefkove, M.Y. Bonner, P. Thompson, P.E. Lovat, J.L. Arbiser, A.R. Hawkins, and C.P.F. Redfern. Inducing apoptosis of cancer cells using small-molecule plant compounds that bind to grp78. *British journal of cancer*, 109(2):433–443, 2013.

[36] Luis Mendoza and Fátima Pardo. A robust model to describe the differentiation of T-helper cells. *Theory in biosciences*, 129(4):283–293, 2010.

[37] Luis Mendoza and Ioannis Xenarios. A method for the generation of standardized qualitative dynamical systems of regulatory networks. *Theoretical Biology and Medical Modelling*, 3(1):13, 2006.

[38] Samuel I. Miller, Lucas R. Hoffman, and Sarah Sanowar. Did bacterial sensing of host environments evolve from sensing within microbial communities? *Cell host & microbe*, 1(2):85–87, 2007.

[39] Marcel Mischnik, Stepan Gambaryan, Hariharan Subramanian, Jörg Geiger, Claudia Schütz, Jens Timmer, and Thomas Dandekar. A comparative analysis of the bistability switch for platelet aggregation by logic ODE based dynamical modeling. *Molecular BioSystems*, 10(8):2082–2089, 2014.

[40] Martin C. Moore-Ede, Frank M. Sulzman, and Charles Albert Fuller. *The clocks that time us: physiology of the circadian timing system.* Harvard Univ. Pr., 1982.

[41] Christina Pachel, Denise Mathes, Barbara Bayer, Charlotte Dienesch, Gaby Wangorsch, Wolfram Heitzmann, Isabell Lang, Hossein Ardehali, Georg Ertl, Thomas Dandekar, et al. Exogenous administration of a recombinant variant of TWEAK impairs healing after myocardial infarction by aggravation of inflammation. *PLoS One*, 8(11):e78938, 2013.

[42] Julie S. Pendergast, Rio C. Friday, and Shin Yamazaki. Photic entrainment of period mutant mice is predicted from their phase response curves. *Journal of Neuroscience*, 30(36):12179–12184, 2010.

[43] Colin S. Pittendrigh and Serge Daan. A functional analysis of circadian pacemakers in nocturnal rodents. IV. Entrainment: Pacemaker as clock. *Journal of Comparative Physiology A*, 106(3):291–331, 1976.

[44] Yoshitaka Sato and Tatsuya Tsurumi. Genome guardian p53 and viral infections. *Reviews in medical virology*, 23(4):213–220, 2013.

[45] D.S. Saunders, S.W. Gillanders, and R.D. Lewis. Light-pulse phase response curves for the locomotor activity rhythm in period mutants of *Drosophila melanogaster*. *Journal of Insect Physiology*, 40(11):957–968, 1994.

[46] D.S. Saunders and E.J. Thomson. 'Strong' phase response curve for the circadian rhythm of locomotor activity in a *Cockroach (Nauphoeta cinerea)*. *Nature*, 270(5634):241, 1977.

[47] Maya Schuldiner, Ofra Yanuka, Joseph Itskovitz-Eldor, Douglas A Melton, and Nissim Benvenisty. Effects of eight growth factors on the differentiation of cells derived from human embryonic stem cells. *Proceedings of the National Academy of Sciences*, 97(21):11307–11312, 2000.

[48] Kazuyuki Shimizu. Regulation systems of bacteria such as *Escherichia coli* in response to nutrient limitation and environmental stresses. *Metabolites*, 4(1):1–35, 2013.

[49] Jae-Sik Shin, Seung-Woo Hong, Sae-Lo Oom Lee, Tae-Hee Kim, In-Chul Park, Sung-Kwan An, Won-Keun Lee, Jong-Seok Lim, Keun-Il Kim, Young Yang, et al. Serum starvation induces G1 arrest through suppression of Skp2-CDK2 and CDK4 in SK-OV-3 cells. *International journal of oncology*, 32(2):435–439, 2008.

[50] Thomas C. Sideris. *Ordinary differential equations and dynamical systems*. Springer, 2013.

[51] Sandeep Sreevalsan, Sonia Joseph, Indira Jutooru, Gayathri Chadalapaka, and Stephen H. Safe. Induction of apoptosis by cannabinoids in prostate and colon cancer cells is phosphatase dependent. *Anticancer research*, 31(11):3799–3807, 2011.

[52] Anna T. Stratmann, David Fecher, Gaby Wangorsch, Claudia Göttlich, Thorsten Walles, Heike Walles, Thomas Dandekar, Gudrun Dandekar, and Sarah L. Nietzer. Establishment of a human 3D lung cancer model based on a biological tissue matrix combined with a boolean in silico model. *Molecular oncology*, 8(2):351–365, 2014.

[53] Gerald Teschl. *Ordinary differential equations and dynamical systems*, volume 140. American Mathematical Society Providence, 2012.

[54] Mark S. Thomas and Sivaramesh Wigneshweraraj. Regulation of virulence gene expression. *Virulence*, 5(8):832–834, 2014.

[55] Raja Vukanti, Eric Mintz, and Laura Leff. Changes in gene expression of *E. coli* under conditions of modeled reduced gravity. *Microgravity-Science and Technology*, 20(1):41, 2008.

[56] James H.-C. Wang, Bhavani P. Thampatty, Jeen-Shang Lin, and Hee-Jeong Im. Mechanoregulation of gene expression in fibroblasts. *Gene*, 391(1):1–15, 2007.

[57] Gregor G. Weber, Jens Kortmann, Franz Narberhaus, and Karl E. Klose. RNA thermometer controls temperature-dependent virulence factor expression in vibrio cholerae. *Proceedings of the National Academy of Sciences*, 111(39):14241–14246, 2014.

[58] Klaus Winzer and Paul Williams. Quorum sensing and the regulation of virulence gene expression in pathogenic bacteria. *International Journal of Medical Microbiology*, 291(2):131–143, 2001.

[59] David R. Withers, Matthew R. Hepworth, Xinxin Wang, Emma C. Mackley, Emily E. Halford, Emma E. Dutton, Clare L. Marriott, Verena Brucklacher-Waldert, Marc Veldhoen, Judith Kelsen, et al. Transient inhibition of ROR-γt therapeutically limits intestinal inflammation by reducing T H 17 cells and preserving group 3 innate lymphoid cells. *Nature medicine*, 22(3):319, 2016.

[60] Sheng Xiao, Nir Yosef, Jianfei Yang, Yonghui Wang, Ling Zhou, Chen Zhu, Chuan Wu, Erkan Baloglu, Darby Schmidt, Radha Ramesh, et al. Small-molecule RORγt antagonists inhibit T helper 17 cell transcriptional network by divergent mechanisms. *Immunity*, 40(4):477–489, 2014.

[61] Shun Yamaguchi, Hiromi Isejima, Takuya Matsuo, Ryusuke Okura, Kazuhiro Yagita, Masaki Kobayashi, and Hitoshi Okamura. Synchronization of cellular clocks in the Suprachiasmatic Nucleus. *Science*, 302(5649):1408–1412, 2003.

[62] Shinya Yamanaka and Helen M. Blau. Nuclear reprogramming to a pluripotent state by three approaches. *Nature*, 465(7299):704–712, 2010.

[63] Eun-Kyoung Yim and Jong-Sup Park. The role of HPV E6 and E7 oncoproteins in HPV-associated cervical carcinogenesis. *Cancer research and treatment: official journal of Korean Cancer Association*, 37(6):319, 2005.

Eidesstattliche Erklärungen nach §7 Abs. 2 Satz 3, 4, 5 der Promotionsordnung der Fakultät für Biologie

Eidesstattliche Erklärung

Hiermit erkläre ich an Eides statt, die Dissertation: „**Ein auf mathematischer Optimalkontrolle basierender Ansatz für pharmakologische Modulation mit regulatorischen Netzwerken und externen Stimuli**“, eigenständig, d. h. insbesondere selbständig und ohne Hilfe eines kommerziellen Promotionsberaters, angefertigt und keine anderen, als die von mir angegebenen Quellen und Hilfsmittel verwendet zu haben.

Ich erkläre außerdem, dass die Dissertation weder in gleicher noch in ähnlicher Form bereits in einem anderen Prüfungsverfahren vorgelegen hat.

Weiterhin erkläre ich, dass bei allen Abbildungen und Texten bei denen die Verwertungsrechte (Copyright) nicht bei mir liegen, diese von den Rechtsinhabern eingeholt wurden und die Textstellen bzw. Abbildungen entsprechend den rechtlichen Vorgaben gekennzeichnet sind sowie bei Abbbildungen, die dem Internet entnommen wurden, der entsprechende Hypertextlink angegeben wurde.

Affidavit

I hereby declare that my thesis entitled: „**A mathematical optimal control based approach to pharmacological modulation with regulatory networks and external stimuli**” is the result of my own work. I did not receive any help or support from commercial consultants. All sources and / or materials applied are listed and specified in the thesis.

Furthermore I verify that the thesis has not been submitted as part of another examination process neither in identical nor in similar form.

Besides I declare that if I do not hold the copyright for figures and paragraphs, I obtained it from the rights holder and that paragraphs and figures have been marked according to law or for figures taken from the internet the hyperlink has been added accordingly.

Würzburg, den_____

_____

Signature PhD-student